NOT FOR PUBLICATION

TN951 74-03

Postirradiation Examination

of

GETR-IRT(B)

August, 1974

POWER REACTOR AND NUCLEAR FUEL DEVELOPMENT CORPORATION

〒319-1184　茨城県那珂郡東海村大字村松4番地49
核燃料サイクル開発機構
技術展開部　技術協力課

Inquiries about copyright and reproduction should be addressed to:
Technical Cooperation Section,
Technology Management Division,
Japan Nuclear Cycle Development Institute
4-49 Muramatsu, Tokai-mura, Naka-gun, Ibaraki, 319-1184
Japan

TSN951 74-03
August, 1974

1974.8

AGF

Postirradiation Examination of GETR-1RT (B)

(SN941 73-30 の全訳)

Shigeo Kobayashi,*
Junji Komatsu,*
Shiro Nakayama,*
Koichi Inoue,* and
Koichi Ishikawa*

Period From February, 1972 to April, 1973

Object To study the behavior of fuel for "JOYO", a experimental fast reactor, and various other fuels at the reactor start-up.

Summary The GETR-1RT (B) irradiation was carried out for the purpose of examining the transient behavior of uranium-plutonium oxide fuels for fast reactors at the biginning of irradiation, especially in the course of the rise of power at the start-up of the reactor. The fuels used as samples were different in density, plutonium content and uranium enrichment as well as in fuel form, as the annular pellet and the vibratory compacted fuel. The maximum linear power was 460 - 560 W/cm, the irradiation period was 3 or 24 hours, and the maximum power was reached in 30 min.

The result of postirradiation examination showed that there was no columnar grain growth and no central void in both kinds of pellets having theoretical densities of 84% and 91%, respectively, when irradiated for 3 hours. Changes of structure were greater in fuels having lower density. Especially in the case of vibratory compacted fuels, the structure was changed more rapidly than in pellets and the structure was stabilized in the early stage of irradiation. A vibratory compacted fuel having a plutonium content of 40% showed a change which seemed due to slumping. The cubic shape of lenticular voids was made clear to have a convex lens-shape.

This is the translation of the report, No. SN941 73-30, issued in August, 1973.

* Alpha-Gamma Facility, Ō-arai Engineering Center, Power Reactor and Nuclear Fuel Development Corporation.

In a pellet with a plutonium content of 20%, oxygen tended to increase in the central region of the fuel, but the ratio Pu/Pu+U showed no change. On the other hand, in a pellet with a plutonium content of 40% neither the distribution oxygen nor the ratio Pu/Pu+U showed so great change in the radial direction. Volatile fission products were confirmed to migrate from the fuel to the insulator region.

C O N T E N T S

1. Preface

The GETR-1RT(B) irradiation was a short-term irradiation test for examining the transient behavior of various fuels for fast reactors at the beginning of irradiation, especially in the course of the rise of power at the start-up of the reactor. The fuels used for the test were different in density, plutonium content and uranium enrichment as well in specification for fuel, as the annular pellet and the vibratory compaction. Eight fuel pins were irradiated by using RATC (Radially Adjustable Trail Cable Facility) of GETR in a period from October 28 to December 5, 1969. This was the first capsule irradiation in a series of tests to confirm the integrity and safety of fuels for the purpose of the "development of JOYO's fuel". The irradiated fuel pins were returned to the Alpha-Gamma Facility (AGF), in Oarai Engineering Center, PNC after postirradiation examination in GE-Vallecitos Nuclear Center. In AGF, comparing with the results of the postirradiation examinations in GE, we examined the fuel pins to obtain more detailed data. This paper describes the results of the examinations at AGF.

2. Outline of examination

(1) Fuel pin

The fuel pins used consist of eight kinds of PuO_2-UO_2 fuels contained in cladding tubes of AISI 316 stainless steel, respectively. Each pin was 123mm in total length, 6.3mm in outer diameter and 55mm in effective fuel length. The eight fuel pins were put together in four capsules so that each capsule contained two fuel pins connected with each other lengthwise. Among the eight fuel pins, five contained solid pellets, two were vibratory compacted ones and the other contained annular pellets. The pins were also different from each other in fuel density (91% and 84% of theoritical.), plutonium content (20% and 40%) and uranium enrichment (90%, 20% and natural). The specifications of the fuels, the outline of pins and the combination of pins in the capsules are shown in Table 1, Figs. 1 and 2, respectively.

Each capsule was an instrumented one equippeed with a thermocouple.

(2) Irradiation history and postirradiation examination in GE-VNC

The capsules were irradiated in the pool position Z-9 of GETR by using RATC so as to reach the maximum linear power in about 30 min.

The irradiation was performed at Cycle 111 of GETR in a period from October 28 to November 5, 1969. The maximum linear power was 460 - 560 W/cm and the irradiation period was 3 or 24 hours.

The irradiation history is summarized in Table 2.

The postirradiation examinations carried out in GE-VNC were as follows:

1) Visual inspection
2) Gamma-scanning

3) Neutron radiography

4) Autoradiography

5) Metallography

The results were reported previously.

(3) Examination at AGF

The postirradiation examination at AGF were carried out as follows:

1) As the metallographically observed positions deviated about 4 to 5 mm from the head positions of the thermocouples in the examination carried out in GE, it was necessary to examine the relation between the temperature and restructuring by polishing the specimens, up to the head positions of the thermocouples.

2) The examination in GE showed that damage of the inner surface of the cladding tube was significant in pins E and C. Therefore, we intended to make detailed observations on the phenomenon.

3) Determination of the cubic shape of lenticular voids.

4) Observation of the interaction between the fuel pellet and the insulator UO_2 pellet.

5) Confirmation as to whether slumping is found in fuel pin H or not.

6) Electron probe microanalysis on plutonium, uranium and fission products.

7) Confirmation of the migration of volatile fission products from the fuel region to the insulator region. Samples were sectioned with a diamond wheel cutter (200mmϕ x 1.0 mm^t) by the wet method. The sampling positions are shown in Figs. 2 and 3.

3. Metallography

(1) Method

Resin mounting was performed with a apparatus with a vacuum pump. Each speimen was placed in an mounting tube (31.8mmϕ x 20mm) and resin (a mixture of Epoxy No. R-770 and a curing agent) was poured into it. After pouring the resin, the mounted specimen was kept in a vacuum vessel under a reduced pressure of -50mmHg for 10 min to remove bubbles and then stand under atmospheric pressure for one day.

Polishing was carried out in No.3-2 Box equipped with three remote-controlling autopolishing machines AUTOMET (rough, intermediate and finishing) and a vibromet (final polishing). This box is also provided with such equipment as an inverted microscope for checking polished surfaces, a ultrasonic cleaner, an electrolytic polisher and an apparatus for disposal of liquid waste.

Three specimens were set on the Whilimet polisher at the same time and polished first with No. 240 waterproof emery paper while dropping water, then with Nos. 320, 450 and 600 emery papers in this order for 20

to 30 min, respectively. They were then polished with 6-μm and 1-μm diamond pastes for 40min, respectively.

Finishing polishing was made with the vibromet 1/4-μm for 60 min. Final finishing was carried out with γ -alumina for 30 mins.

Etching was performed chemically with an etching solution (H_2SO_4:H_2O_2:H_2O=1:6:3) at 50°C for 15 to 20 min. This was an etching solution of sulfuric acid and less corrosive for the cladding, but UO_2 was selectively attacked partially in the fuel region near the cladding where the solid solution of plutonium and uranium was not formed.

After polsihing, the surface was observed with a Nikon low magnification microscope (x10) and with a Reichert remote-control metallurgical microscope (x100 and then x400). After etching, observations of the surface were made in the same manner.

The cubic shape of lenticular voids was observed by a special method: A cross section of a matallographic specimen (20202) mounted in GE-VNC was photographed (x10) to obtain a whole surface continuous metallographic photograph (Photograph 1) and an area where lenticular voids were densely distributed was selected by examining the photograph. For the determination of the shape of lenticular voids, it is important that the objective voids lie in parallel with the polished surface. Therefore, the resin mounted was cut off in part, and the sample was re-remounted to make a longitudinal section of it for metallography by the method as shown in Fig. 4. Then polishing and observation of the surface of the section was repeated alternatively while confirming the depth and position of polishing by taking photographs (x10) of it (Photograph 2). As the lenticular void area was located in the narrow region of 300 μm near the central void the surface was finished, to avoid over-polishing, by using only Nos. 400 and 600 waterproof emery papers and diamond paste for a short time after approaching the area.

(2) Results and discussion

1) Restructure

(I) Specimen No. 20102 (Pin A, transverse section) (Photographs 3 and 4). There is a central void about 0.4mm in diameter in central part of fuel, but the center of the void is about 0.6mm deviation from the center of fuel. A columnar grain growth region, 2mm in diameter is present around the central void, but the growth region of columnar grains depends upon the radial directions. An equiaxed grain growth region is observed outside the columnar region.

The size of crystal grains is about 40 μm in the equiaxed grain growth region and about 10μm near the surface of fuel.

There is a crack in the circumferential direction at a distance of about 2mm from the center of fuel, whereas several large cracks are observed along the radial direction.

Lenticular voids are seen in the columnar grain growth region. They also group near the central void. Many small voids as well as large ones about 20μm in maximum size, which are considered to have been formed at the time of fabrication, are observed near the surface of fuel.

Metallic inclusion about 12μm in diameter are present near the voids in the outer margin of the equiaxed grain growth region, but they can not be observed in the structure after etching.

The diametral gap between the fuel and the cladding tube is about 100μm. The interaction between the fuel and the cladding tube is not observed clearly and the structure keeps an integrity, but precipitates are observed up to a depth of about 50μm from the inner surface of the cladding tube.

(II) Specimen No. 20202 (Pin B, transverse section and longitudinal section) (Photographs 1 and 5).

There is a central void about 0.72 mm in diameter in the central part of fuel. The center of fuel is 0.4mm deviated from the thermal center.

No columnar grain growth region is observed. An equiaxed grain growth region about 3.5mm in diameter is present around the central void. The size of crystal grains is 150 to 200μm in the equiaxed grain growth region and about 10μm near the surface of fuel. In the fuel region there are large cracks in the radial direction and many fine cracks in the axial direction. Many lenticular voids are seen in the equiaxed grain growth region. Near the surface of fuel there are many voids, including large ones about 150μm in size, which are regarded as formed at the time of fabrication.

The boundary between the pellets shows evidences of sintering in the central part, but the original stuctur at the time of fabrication is retained in the peripheral part. No metallic inclusion is observed.

The diametral gap between the fuel and the cladding tube is about 90 μm. No interaction is observed between the fuel and the cladding tube, and the structure preserves an integrity.

(III) Specimen No. 20302 (Pin C, transverse section)
(Photographs 6 and 7)

No deviation is observed between the fuel center and the thermal center. There is no central void in the central part

of fuel. No columnar grain growth region is observed. The size of crystal grains is 80 to 90μm in the central part of fuel and 15μm near the surface of it.

There is a crack in the circumferential direction at a distance of about 1.6mm from the center of fuel, and four large cracks are seen in the radial direction.

No lenticular void is observed. Small pores are distributed throughout the fuel and large ones which are about 230μm in diameter and considered to have been formed at the time of fabrication are observed here and there near the surface of fuel.

No metallic inclusion is obseved.

The diametral gap between the fuel and the cladding tube is about 60μm. No interaction is observed between the fuel and the cladding.

(IV) Specimen No.20402 (Pin D, transverse section) (Photographs 8 and 9)

No deviation is observed between the fuel center and the thermal center. No central void is found in the central part of fuel. There is no columnar grain growth. The equiaxed grain growth region is about 3.2mm in diameter. The size of crystal grains is about 130μm in the central part of fuel and 10 to 20 near the surface of fuel.

There are many fine cracks in both radial and circumferential directions.

No lenticular voids are observed. Many small voids as well as large ones, which are about 60μm in size and regarded as formed at the time of fabrication, are distributed throughout the fuel.

No metallic inclusion is found.

The diametral gap between the fuel and the cladding is about 60μm. Damage due to the interaction between the fuel and the cladding is not so significant.

(V) Specimen No.20502 (Pin E, transverse section) (Photographs 10 and 11)

The fuel center is deviated by about 0.4mm from the thermal center. No central void is observed in the central part of fuel. No columnar grain growth is observed. The equiaxed grain growth region is about 3mm in diameter. The size of crystal grains is about 150μm in the central part of fuel and 10 to 20μm near the surface of it.

There are four large cracks in the radial direction of fuel and many fine cracks in both radial and circumferential directions.

In the equiaxed grain growth region there are a comparatively

large number of voids on the grain boundary and 10 to 20μm in size. Large voids 60 to 70μm size are observed near the surface of fuel and considered to have been formed at the time of fabrication.

No metallic inclusion is found.

The diametral gap between the fuel and the cladding is about 30μm. The interaction between the fuel and the cladding is not so significant, but there are structures considered to have been partially lost the some grains along the grain boundary within a depth of about 50μm from the inner surface of the cladding tube after etching.

(VI) Specimen No. 20602 (Pin F, transverse section) (Photographs 12 and 13)

No deviation is observed between the fuel center and the thermal center. There is a central hole about 1.5mm in diameter in the central part of annular pellet.

Columnar grains grow up in a region within a range of about 0.4mm on the high-temperature side of the central hole. The equiaxed grain growth region is about 4.4mm in diameter. A partial breaking off of the edge of the central hole is also observed on this side. There is a structure probably due to the deposit of fuel on the inner edge of the central hole on the low-temperature side. The size of crystal grains is about 30μm in the central region of fuel and about 10μm near the surface of fuel.

There are many fine cracks in both radial and circumferential directions.

Growth of lenticular voids is observed around the central hole. Many small voids are distributed throughout the whole area, and large ones which are about 60μm in size and considered to be formed at the time of fabrication are observed in the peripheral region of fuel.

No metallic inclusion is found.

The diametral gap getween the fuel and the cladding tube is about 60μm. Damage to the inner surface of the cladding tube is not so significant.

(VII) Specimen No. 20702 (Pin G, transverse section) (Photographs 14 and 15)

No deviation is observed between the fuel center and the thermal center. There is a central void about 1.1mm in diameter in the central region of fuel. The columnar grain growth region is about 4.2mm in diameter and there is an equiaxed grain growth region about 5.0mm in diameter around the columnar region. The size of crystal grains is about 50μm in the equiaxed grain growth region, but their size can not be measured near the surface

of fuel because of losing the fuel.

There are several large cracks as well as fine ones in the radial direction. The number of cracks is not so large in the circumferential direction.

Round voids about 10μm in size are distributed around the central void. In the columnar grain growth region small voids are seen in groups along the grain boundary, while in the equiaxed grain growth region they are distributed throughout the whole surface. On the surface of fuel, original fuel particles at the time of vibratory compaction are observed in losing.

No metallic inclusion is found.

The gap between the fuel and the cladding tube is not measured, because fuel has been lost. The inner surface of the cladding is seen to have had an interaction with the fuel within a depth of about 10μm; the surface is uneven and a reaction layer is observed in the fuel.

(VIII) Specimen No. 20802 (Pin H, transverse section) (Photographs 16 and 17)

The center of fuel is deviated by about 0.2mm from the thermal center. A central void about 2mm in diameter is seen in the central region of fuel. The columnar grain growth region is about 4.9mm in diameter, being surrounded by an equiaxed grain growth region about 5.1mm in diameter. The columnar grain growth region is remarkable in growth and contains large crystal grains. The size of crystal grains is about 30μm in the equiaxed grain growth region.

There are several large and many fine cracks in the radial direction. Cracks are not observed in the circumferential direction.

Voids are small, several 10μm in size, around the central hole and a little larger on the grain boundary in the columnar grain growth region, while fine ones are scattered in the other region. On the surface of fuel, vibratory compaction particles are seen in losing off.

No metallic inclusion is found.

The gap between the fuel and the cladding is not clear owing to losing the fuel. Damage to the inner surface of the cladding tube is little, though the surface is uneven.

(IX) Specimen No. 20803 (Pin H, longitudinal section, boundary between the UO_2 upper insulator pellet and the fuel pellet) (Photograph 18)

There is a central void. The range of columnar grain growth region is about 5mm, becoming smaller toward the UO_2 insulator. The central hole disappears in a position about 9mm inward from

the fuel-UO_2 insulator boundary in the axial direction.

There are several large cracks together with many fine ones in the radial direction, while they are not abserved in the circumferential direction.

Voids are seen in groups on the grain boundary in the columnar grain region, while fine ones are distributed in the whole area.

In a range of about 13mm from the UO_2 insulator pellet boundary in the axial direction there is a secondary strucure in a range of about 2mm in the central hole which seems to have formed by restructuring of the center of fuel. This restructuring may be due to the slumping of fuel and shows abnormality in the profile of gamma-scanning. The peripheral region of fuel retains the original structure at the time of fabrication.

No metallic inclusion is found.

The UO_2 insulator-pellet boundary is observed to have disappeared in a range of about 3.6mm in diameter owing to sintering, and structure change reaches a position about 0.6mm inward the UO_2 in the central region.

The gap between the fuel and the cladding is not clear because of the losing vibratory-compaction fuel particles. Damage to the inner surface of the cladding tube is not so signicicant.

(X) Specimen No. 20805 (Pin H, longitudinal section, lower UO_2 insulator-pellet boundary) (Photograph 19)

No central hole is observed in the central region of fuel. Cracks are observed in both longitudinal and transverse direction. Voids are distributed in the whole area.

The fuel-UO_2 insulator boundary is found to have disappeared in a range of about 3.1mm in diameter owing to sintering. Restructuring due to an influence of heating is observed up to a place of about 0.4mm inward the UO_2 in the central region. A gray secondary phase is present in the boundary region. The peripheral region of fuel retains the primary structure at the time of fabrication.

No metallic inclusion is observed.

The inner surface of the cladding near the boundary region between the fuel and the UO_2 insulator has a cavity within a range of about 7mm along the axial direction, showing an evidence of mechanical interaction.

A comparison of the restructure observed in the head position of thermocouple in AGF and that observed in GE-VNC in a point 4 to 5mm distant from the head position is indicated in Table 3.

2) Shape of lenticular void

It has been reported that lenticular void contributes to the formation of columnar grain, but there is no detailed report except that the voids have a shape of lens. Therefore, observations of the shape were performed in a specimen (20202, Pin B) which is remarkable in the growth of lenticular voids.

In the observations two points were taken into consideration. One is the shape of voids which were not in parallel with polished surface and the other is the shape of crystal grains in the area observed. Photographs 20 and 21 show metallographic photographs of the longitudinal section. The voids observed in the objective area are not lenticular but a little polygonal, while lenticular ones are seen outside the area. The crystal grains also are not slender but a little polygonal in the objective area, while a little slender ones are seen outsides the area.

Photograph 22 shows a stereogram of the specimen.

From the above-mentioned observations a cubic model of a lenticular void is considered to be shown as in Fig. 5. In the figure the Z axis coincides with the axial direction of the fuel pin and the Y axis corresponds with the radial direction.

The void is convex lens-shaped and has a symmetrical plane in plane XZ. It moves from the lower temperature side to the higher temperature side in the radial direction to form a columnar grain. Accordingly, when observed in plane XY (transverse section), the void appears lenticular and the columnar grain has a slender appearance, while both of them look polygonal when observed in plane XZ (longitudinal section).

3) Slumping of fuel

The gamma-scanning carried out in GE-VNC showed abnormal profiles of Pin H, as a decrease of gamma-ray intensity in the central part and an increase of it on the gas plenum side which was located in the bottom in the reactor (Fig. 6). A large central hole is observed in a transverse section of a central part of this fuel pin. (Specimen No. 20802, Photographs 16 and 17). In the longitudinal section of the part including the boundary between the UO_2 insulator and the fuel at the gas plenum side which was located in the bottom in the reactor, the central hole seems to be blocked with the upper part of fuel which was melted and fell into it and is seen to be wedgeshaped. Growth of dendrite structure which seems to have been formed during solidification is also seen (Specimen No. 20803, Photograph 18).

4) Damage on the inner surface of the cladding tube

Damage on the inner surface of the cladding tube are remarkable in Pins E (Specimen No.20502) and G (Specimen No.20702). As shown in Photograph 23, damage on the inner surface of the cladding tube reaches a depth of about 50μm and shows the structure losing some grain along the grain boundary in Pin E which contains pellet fuel having a plutonium content of 40%. Damage on the inner surface of the cladding tube corresponds to concaves, probably voids, on the surface of the fuel and shows the evidence of a mechanical interaction between them (Photograph 24).

In Pin G which contains vibratory compacted fuel having a plutonium content of 20% the inner surface of the cladding tube shows unevenness within a depth of about 20μm.

In Pin A (Specimen No.20102), damage is observed along the grain boundary within a depth of about 50μm from the inner surface of the cladding tube.

5) Comparison by irradiation parameters

(i) Irradiation period

To evaluate the effect of irradiation period on structure changes, a comparison of two fuels irradiated for 3 and 24 hours, respectively, was made between Pins A and C both of which were 91% in pellet density and between Pins B and D both of which had a pellet density of 84%:

a) Pellet having 91% of theoretical density

Irradiation period	24 hours	3 hours
Specimen No.	20102 (Pin A)	20302 (Pin C)
Structure change	o A central hole is present	o No central hole
	o Lenticular voids are present	o No lenticular void
	o Columnar grain has grown	o Only equiaxed grain growth region is observed
	o Many cracks	o A few cracks
	o The center of fuel deviates from the thermal center	o No deviation between both centers
	o The grain boundary is damaged on the inner surface of the cladding tube (50μm in depth)	o No damage

b) Pellets having 84% of theoretical density

Irradiation period	24 hours	3 hours
Specimen No.	20202 (Pin B)	20402 (Pin D)
Structure change	o A central hole is present	o No central hole
	o The columnar grain growth region is present.	o No columnar grain growth region
		o Equiaxed grain growth region had developed.
	o A center of fuel deviates from the thermal center	o No deviation between both centers
	o No damage on inner surface of cladding tube	o No damage on inner surface of clading tube
	o Large cracks are present	o Many fine cracks are present

In the case of 3 hours irradiation the central hole is not formed, lenticular voids are not developed and no columnar grain growth region is observed.

(ii) Fuel density

A comparion of two pelletized fuels having theoretical density of 91% and 84%, respectively, was made after irradiation between Pin A (Specimen No. 20102, 91% T.D.) and Pin B (Specimen No. 20202, 84% T.D.) and between Pin C (Specimen No. 20302, 91% T.D.) and Pin D (Specimen No. 20402, 84% T.D.):

a) 24 hours irradiation

Fuel density	91%	84%
Specimen No.	20102 (Pin A)	20202 (Pin B)
Structure change	o The central hole is 0.4mm in diameter	o The central hole is 1.2mm in diameter
	o The columnar grain growth region is narrow	o The columnar grain growth region is wider
	o Lenticular voids are smaller in number than in the case of 84% T.D.	o Lenticular voids are large
	o Large voids are small in number	o Large voids are large in number
	o Cracks are a little fewer than in the case of 84% T.D.	o Cracks are a little large in number

b) 3 hours' irradiation

Fuel density	91% T.D.	84% T.D.
Specimen No.	20302 (Pin C)	20402 (Pin D)
Structure change	o No central hole	o No central hole
	o No columnar grain growth region	o No columnar grain growth region
	o The equiaxed grain growth region is narrower than in the case of 84% T.D.	o The equiaxed grain growth region is wider than in the case of 91% T.D.
	o Crystal grains are about 90μm in size in the central part of fuel	o Crystal grains are about 130μm in size in the central part of fuel
	o Large voids are small in number	o Large voids are large in number
	o Cracks are smaller in number than in the case of 84% T.D.	o Fine cracks are large in number

Changes of structure are generally greater in pellets having a lower density of 84% T.D. In the case of 24 hours' irradiation the central hole is larger in diameter, lenticular voids are larger in number and the columnar grain growth region is wider in the pellets having the density of 84% T.D. (1.2mmϕ) than in those having the density of 91% T.D. (0.4mmϕ). In the case of 3 hours' irradiation the central hole is not formed in both kinds of pellets and the size of crystal grains in the central part of fuel is larger in the pellets having lower density.

(iii) Plutonium content

To evalnate the effect of plutonium centent, a comparision of two fuels which are different in the plutonium content (20% and 40%) was made between Pin A (Specimen No. 20102, 20% Pu, 90% U^{235} and Pin E (Specimen No. 20502, 40%, Pu, 20% U^{235}) both of which contain pellet fuel and between Pin G (Speciman No. 20702, 20% Pu, Nat. U) and Pin H (Specimen No. 20802, 40% Pu, Nat. U) both of which contain vibratory compacted fuel:

a) Pellet fuel

Plutonium content (enrichment of uranium)	20% (90% U^{235})	40% (20% U^{235})
Specimen No.	20102 (Pin A)	20502 (pin E)
Structure change	o The central hole is about 0.4mm in diamter	o Almost no central hole

	o The columnar grain growth region is present	o No columnar grain growth region
	o Lenticular voids are present	o No lenticular void
	o Cracks are large in number	o Many small round voids are observed in the central part of fuel
	o Damage to the grain boundary reaches a depth of about 50μm on the inner surface of the cladding tube	o Layer losing grains reaches about 50μm in depth on the inner surface of cladding tube
		o The beta-gamma autoradiographic sensitive part is larger in size than in the case of 20% Pu

b) Vibratory compacted fuel

Plutonium content	20%	40%
(enrichment of uranium)	(Nat. U)	(Nat. U)
Specimen No.	20702 (Pin G)	20802 (Pin H)
Structure change	o The central hole is 1.1mm in diameter	o The central hole is 2.0mm in diameter
	o The columnar grain growth region is smaller in size than in the case of 40% Pu	o The columnar grain growth region is larger in size than in the case of 20% Pu
	o Cracks are a little larger in number	
	o The beta-gamma autoradiographic sensitive part is larger in size than in the case of 40% Pu	

In case of the pellet fuels, changes of structure are less in degree at 40% plutonium content than at 20%.
But in the case of vibratory-compacted fuels, changes of structure are, on the contrary, greater at 40%.

(iv) Annular pellet and solid pellet

A comparison of Pin E (Specimen No. 20502, solid pellet) and Pin F (Speciment No. 20602, annular pellet) was made as to the change of structure:

	Solid pellet	Annular pellet
Specimen No.	20502 (pin E)	20602 (Pin F)
Structure change	o No central hole o No columnar grain growth region o Small round voids group in the central part of fuel o Damage to the grain boundary is observed within a depth of 50μm on the inner surface of the cladding tube	o A little development of columnar grain around the central hole o Lenticular voids are observed

Changes of structure are a little greater in the annular pellets.

(v) Pellet fuel and vibratory-compaction fuel

Comparisons of Pin B and Pin G which are 20% in plutonium content, and of Pin E and Pin H which are 40% in plutonium content, respectively, were made:

a) 20% Plutonium content

	Pellet fuel	Vibratory-compaction fuel
Specimen No.	20202 (Pin B)	20702 (Pin G)
Structure change	o The central hole columnar grain region and lenticular voids, etc. are observed. The structure is observed to be in the course of change	o The central hole and columnar grain growth region are larger in size. No lenticular void. The structure is obseved in final and complete change

b) 40% plutonium content

	Pellet fuel	Vibratory-compaction fuel
Specimen No.	20502 (Pin E)	20802 (Pin H)
Structure change	o No central hole and no columnar grain growth region. Only the equiaxed grain growth region is observed. Small voids of about 10μm in size group in the central part. Damage to the grain boundary is observed within a depth of 50μm on the inner surface of the cladding tube.	o The central hole and columnar grain growth region are greater in development. Cracks also are large in size.

When the pellet is compared with the vibratory-compaction fuel, changes of structure are greater in the latter, and the restructuring under irradiation seems to be finished and stabilized earlier in the latter.

4. Electron probe microanalysis

(1) Method

Measurements were carried out in specimens 20102 and 20502. The locations where point analysis, line analysis and plane analysis were made are shown in Figs. 7 and 8. The samples (after chemical etching treatment) were coated with carbon in a vacuum evaporator and given electric conductivity with silver paste.

(i) Point analysis (qualitative analysis)

The locations for analysis were selected by comparing metallographic photographs with the back scattered electron images, and analysis was performed by focusing a electron beam on the selected locations. The number of the locations selected was three in the fuel region (the equiaxed grain growth region, or as fabricated region, the columnar grain growth region and the central region of fuel) and two in the cladding tube (the outer and the inner surface of the cladding tube).

(ii) Line analysis (measurement of the intensity of characteristic X-rays)

Changes of the intensity of characteristic X-ray were measured for uranium, pulutonium, and oxygen in a range from the surface to the center of fuel, and for chromium, iron, nickel, and molybdenum from the outer surface to the inner surface of the cladding tube.

(iii) Plane analysis (X-ray display)

Plane analysis was performed for iron, nickel, chromium, molybdenum, uranium and pulutonium in the center of fuel and the gap between the fuel and the cladding tube as well as on the outer surface of the tube.

(iv) Back scattered electron image

Back scattered electron image were obtained from the locations where the point, plane and line analysis had been carried out. And the results were used for the selection of measuring locations, comparison with the metallographic photographs and understanding of the state of the locations.

(v) Measurement of background

The effect of radiation from the irradiated sample itself as background on the electron beam is measurement was examined by the following two methods: (1) Electron beam is stopped, the specimen is fixed and only the analyzing crystal is moved; (2) Electronbeam is stopped in the same way as above, the analyzing crystal is fixed and the specimen is moved. The results of measurement are shown in Figs. 9 and 10. As shown in the figures, the background seems to have nearly no effect.

(2) Results and discussion

(i) Point analysis

Plutonium, uranium, oxygen, silicon, palladium and praseodymium were detected by point analysis in the fuel region of both specimens 20102 and 20502. These elements were detected in every region selected for measurement. As for the fission products, measurements were carried out to intend to detect each element of Rb, Sr, Y, Zr, Nb, Mo, Tc, Ru, Rh, Pd, Ba, La, Ce, Pr, Mo, Pm, Sm, and Cs, but none of them was detected.

In the cladding tube iron, nickel, chromium, molybdenum, manganese, and silicon were detected. The presence of silicon seems due to the remaining of silicon contained in abrasive materials used. No fission products were detected.

(ii) Line analysis of cladding tube

Fig. 11 shows changes of the characteristic X-rays of Fe-Mo in the cladding tube of Specimen 20102. The first peak of iron was detected at a position of 3.3μm inward from the outer surface of the cladding. No such a peak was detected for molybdenum. No peak of iron and molybdenum is seen on the inner surface of the cladding. Whether the decrease of iron observed only in both ends of the cladding is due to an inattentive preparation of the sample or to leaching is not clear. Molybdenum does not show such a phenomenon in either end of the cladding. Neither iron nor molybdenum show diffusion into the gap between the fuel and the cladding. The characteristic X-rays of iron and molybdenum are uniform in intensity except both ends. Fig. 12 shows changes in the intensity of the characteristic X-rays of nickel and chromium measured in the same place as shown in Fig. 11. The first peak of nickel is detected in the vicinity of the outer surface of the cladding as in the case of iron. Such a peak is barely observed for chromium. As seen from the profile of specimen current, these peaks are observed within the cladding tube wall thickness of 0.35mm. The diffusion of chromium into the gap between the fuel and the cladding is observed. Nickel shows a decrease in the intensity of characteristic X-rays in both ends of the cladding as in the case of iron. Chromium does not show such a steep decrease of characteristic X-rays. Nickel and chromium are uniform in characteristic X-ray intensity except both ends of the cladding. The characteristic X-ray intensity of iron resembles that of nickel.

Fig. 13 shows changes of the characteristic X-rays of iron and molybdenum in the cladding tube of specimen 20502. The first peak of iron is detected in the vicinity of the outer surface of the cladding

as in the case of Specimen 20102. Such a peak can not be seen in the vicinity of the inner surface.

Iron and molybdenum show no diffusion into the gap between the fuel and the cladding. The content of iron is the highest around the center of the cladding and decreases twards both ends, while molybdenum is distributed almost uniformly. Fig. 14 indicates changes of the characteristic X-rays of nickel and chromium in the same place as shown in Fig. 13. The first peak of nickel is detected in the vicinity of the outer surface of the cladding as in the case of iron. As seen from the profile of specimen current, these peaks are observed within the cladding tube wall thickness of 0.34mm. Such a peak cannot be seen in the vicinity of the inner surface of the cladding. Chromium shows a little decrease on the outer surface of the cladding. No diffusion of nickel is observed in the gap between the fuel and the cladding.

(iii) Line analysis of the fuel region

Fig. 15 shows changes of the characteristic X-rays of uranium, pulutonium, and oxygen in the fuel region of Specimen 20102. Changes of specimen current are remarkable, because many voids are contained in this specimen as shown in the metallographbic photograph (Photograph 4). The region as fabricated, the equiaxed grain growth region, the columnar grain growth region and the central void can be distinguished clearly by the change of specimen current. Uranium, pulutonium, and oxygen show similar decreases in the area of void.

The characteristic X-rays of uranium, pulutonium, and oxygen change nearly in the same manner.

Fig. 16 shows changes of the characteristic X-rays of uranium, pulutonium and oxygen in the fuel region of Specimen 20502. Changes of specimen current are a little in contrast to the above-mentioned, because voids are small in number as seen from the metallographic photograph (Photograph 11). The region as fabricated, the equiaxed grain growth region, the columnar grain growth region and the central void can not be distinguished by the change of specimen current. No development of the central void and columnar grain growth also observed from the metallographic photograph. In the metallographic photograph, crystal grains are observed to be different in tone, but no significant quantitative difference of uranium, pulutonium, and oxygen is observed among these grains.

In two areas near the surface of the fuel, increases of uranium and corresponding decreases of plutonium are observed (pointed with arrows in the figure). This is considered due to uneven distribution of plutonium and uranium at the time of fabrication.

There was also a place where uranium and oxygen decreased and plutonium increased around the center of the fuel region.

The intensity of the characteristic X-ray of oxygen and the relative intensities of Pu/PU+U and O/Pu+U at various points of the fuel region are plotted in Figs. 17 and 18. In Fig. 17 it is seen that oxygen tends to increase in the center of the fuel of Specimen No. 20102 which contains 20% PuO_2-UO_2 (90% in enrichment). Such a change is not observed in plutonium.

The distribution of oxygen and plutonium is noted to be nearly uniform in Specimen 20502 which contains 40% PuO_2-UO_2 (20% in enrichment) as shown in Fig. 18.

(iv) Plane analysis

X-ray displays of various elements obtained in the gap region between the fuel and the cladding tube, on the outer surface of the cladding and in the central part of fuel of Specimen 20102 are shown in Figs. 25, 26 and 27, respectively. In the gap the distribution of iron, nickel, chromium, molybdenum, uranium and plutonium agrees with the result of the line analysis.

The distribution of iron, chromium, nickel, and molybdenum also agrees with the result of the line analysis on the outer surface of the cladding tube. The concentrations of uranium and plutonium are observed in decrease along the grain boundary in the X-ray display taken in the central part of fuel.

X-ray displays of various elements obtained in the gap region between the fuel and the cladding tube, on the outer surface of the cladding and in the central part of fuel of Specimen 20502 are shown in Photographs 28, 29 and 30, respectively. In the line analysis diffusion of elements could not be observed in the gap region between the fuel and the cladding tube. In the X-ray display the boundary is not clear partly owing to the fact that the inside of cladding tube is attached and some grains are fallen off. (Fig. 28).

Every element on the outer surface of the cladding tube is observed to show changes of the intensity of characteristic X-rays which agree with the result of line analysis.

In the central part of fuel, no qualitative difference of uranium and plutonium was found among the crystal grains which were different in tone. This is corresponding to the result of line analysis.

(v) Back scattered electron image

The unevenness of the surface of samples was observed by the use of back scattered electron image. Fig. 30 shows the position corresponding to the part where crystal grains are seen to be different in

tone in the metallographic photograph of Specimen 20502. Such difference of tone of crystal grains is not found in Specimen 20102. The same difference is seen in a metellographic photograph of Pin H (Photograph 18).

All these samples were 40% in plutonium content. The difference of results seems due the difference of crystal plane. The crystal plane is rough and concave, as shown in Photograph 34, in the case where the grains show the difference in tone.

Considerable unevenness due to the presence of voids is seen in the vicinity of the surface of the fuel of Specimen 20102, while the unevenness is little in the corresponding part of Specimen 20502, showing a difference of crystal plane between two samples.

5. Confirmation of the migration of volatile fission products

(1) Method

An insulator (Specimen No. 20106) and a fuel regions (Specimen No. 20104) were immersed in nitric acid (1+1) in a chemical cell to dissolve nuclear materials and, after that the cladding tube was washed sufficiently. After leaching, the solution was adjusted to 200 ml, and 200 $\mu\ell$ of it was taken for the sample of gamma-spectrum measurment with a Ge (Li) detector and quantitative determination of nuclides.

(2) Results and discussion

Three nuclides, Ce-144, Rh-106 and Cs-137, were detected. The results of quantitative determination are shown in Table 4. The values given in the table are those of radioactivity in the solution after leaching. The total amount of volatile nuclides adhering to the sample is unknown, because the leaching ratio can not be determined correctly. Therefore, as an indication for estimating the migration of these volatile nuclides, the relative intensity of the radiation of each nuclide is also shown in the table. Fig. 19 shows how these relative intensities increase in the insulator region. In the figure the ordinate represents the increasing rate of relative intensity in the insulator region on the basis of the relative intensity in the fuel region. Cerum is generally present as a solid solution and said to be small in deviation of distribution. Accordingly, the increase of the ratio of Cs-137 to Ce-144 in the insulator region means that cesium migrates from the fuel region as a volatile fission product. In the same way, the relative increase of Rh-106 is considered to show that Ru-106 migrates to both insulator and plenum regions as a volatile fission product. The Ce-144 detected in the insulator region is estimated to have been derived from the sectioning surface of the pin which got into the insulator region.

From the above-mentioned results, cesium and ruthenium are observed to have accumulated actually in the insulator region of the fuel pin, but it is difficult to believe that the amount is sufficient enough to cause the abnormal steep activity of the peaks as shown in the profile of gamma-scanning.

6. Conclusion

The following items have been made clear as a result of the present examination:

(1) In the case of 3 hours' irradiation, no central void and no columnar grain growth were observed in both of the fuels having a 91% of theoretical density and 84%, respectively.

(2) When a pellet fuel having a 84% of theoretical density is compared with that having a 91% of theoretical, changes of structure are greater and the diameter of the central void is larger in the former.

(3) When a pellet fuel is compared with a vibratory-compaction fuel, changes of structure are greater in the latter, and the structure changes are completed and stabilized earilier than in the former.

(4) In a vibratory-compaction fuel having a plutonium content of 40% (Pin H), a structure change suggested slumping of fuel, but the fuel pin was intact and damage to the inner surface of the cladding tube was little.

Sintering occurred in the central part of the boundary between the fuel and the UO_2 insulator pellet and no gap was observed there.

(5) A lenticular void appears to be lenticular in a transverse cross section and looks polygonal in a longitudinal section, so it has stereographically convex lens-shape.

(6) In a pellet fuel having a plutonium content of 40% (Pin E), damage was found within a depth of about 50μm inside surface of the cladding tube and some grains were lost along the grain boundary. In a vibratory-compaction fuel having a plutonium content of 20% (Pin G), damage was observed within a depth of 20μm.

(7) As for the distribution of plutonium, uranium, and oxygen in the fuel of Specimen 20102 (Pin A) containing 20% PuO_2-UO_2, oxygen tended to increase in the central part of the fuel. The ratio Pu/Pu+U showed no changes. In Specimen 20502 (Pin E) containing 40% PuO_2-UO_2, changes of both oxygen and Pu/Pu+U were not so great.

(8) Palladium and praseodymium were detected in addition to uranium, plutonium, oxygen, and silicone in various region of the fuel.

(9) A local increase of uranium accompanied by a decrease of plutonium was found on the surface of the fuel of Specimen 20502. This is considered to be due to uneven distribution of plutonium and uranium at the time of fabrication.

(10) Crystal grains were observed to be different in tone in metallographic photographs of Specimen 20502 containing 40% PuO_2-UO_2, and the surface of them was found to be different in roughness in the back scattered electron images of the sample, but the concentrations of uranium, plutonium, and oxygen were independent of the difference of the tone.

(11) Changes of the concentrations of iron and chronium were detected on the outer surface of the cladding tube.

(12) No other element except the components was detected in the cladding tube.

(13) Cesium and ruthenium, which are volatile fission products, were confirmed to migrate from the fuel region to the insulator region.

Table 1. Specifications of GETR-1RT(B) fuel pin

Capsule No.	1		2		3		4	
Fuel pin No.	A	B	C	D	E	F	G	H
Fuel form	Pellet	Pellet	Pellet	Pellet	Pellet	Annular pellet	Vibratory compaction	Vibratory compaction
Pu content (%)	20.19	20.32	20.19	20.32	39.47	40.67	19.7	39.5
Uranium enrichment (%)	89.89	89.89	89.89	89.89	19.91	19.91	Nat	Nat
Pellet density	10.09(g/cc) 91.31 (%)	9.32(g/cc) 84.30 (%)	10.09(g/cc) 91.31 (%)	9.32(g/cc) 84.30 (%)	10.05(g/cc) 90.97 (%)	9.94(g/cc) 89.95 (%)		
Smear density (%)	88.0	81.30	88.0	81.3	87.7	86.6	75.8	75.4
Pellet diameter (mm)	5.5 ± 0.01	5.5 ± 0.01	5.5 ± 0.01	5.5 ± 0.01	5.5 ± 0.01	OD 5.5±0.01 ID 1.5		
Cladding tube, inside diameter (mm)	5.6 ± 0.025	5.6 ± 0.025	5.6 ± 0.025	5.6 ± 0.025	5.6 ± 0.025	5.6 ± 0.025	5.6 ± 0.025	5.6 ± 0.025
Diametral gap (mm)	0.1 ± 0.075	0.1 ± 0.075	0.1 ± 0.075	0.1 ± 0.075	0.1 ± 0.075	0.1 ± 0.075		
Fuel pin, total length (mm)	122.0	123.75	122.20	123.80	122.00	123.75	122.15	123.80
Effective fuel, length (mm)	54.3	55.0	55.2	55.1	55.1	55.6	55.3	55.6
Plenum length (mm)	13.0	12.5	12.3	12.4	12.2	11.7	11.9	12.0
Fuel pin, total weight (g)	29.70	29.13	29.66	29.35	29.93	29.44	28.55	29.14
PuO_2-UO_2 weight (g)	13.1	12.0	13.1	12.2	13.3	12.2	12.0	12.0
Pu weight (g)	2.33	2.15	2.33	2.18	4.63	4.37	2.09	4.18
E.U weight (g)	9.20	8.41	9.20	8.55	7.09	6.38	Nat. U 8.49	Nat. U 6.40
U-235 weight (g)	8.27	7.56	8.27	7.69	1.41	1.27		
Nat-UO_2 weight (g)	4.86	4.74	4.80	4.74	4.80	4.83	4.80	4.74
ZrO_2 weight (g)	0.52	0.55	0.49	0.49	0.55	0.54	0.54	0.50
Spring weight (g)	0.30	0.31	0.30	0.30	0.30	0.30	0.27	0.30
Stainless steel weight (g)	10.92	11.53	10.97	11.62	10.98	11.57	10.94	11.60
Fuel O/M ratio	1.987	1.986	1.987	1.986	1.982	1.984	1.991	1.989
Cladding tube, quality of material	AISI 316	"	"	"	"	"	"	"
Cladding tube, inside diameter (mm)	5.6 ± 0.025	"	"	"	"	"	"	"
Cladding tube, outside diameter (mm)	6.3 ± 0.003	"	"	"	"	"	"	"
Cladding tube supplier	K Co.	"	"	""	"	"	"	"
Cladding tube No.	Suitably cut from Nos. 506, 508, 510, 570 and 581							

Table 2. Irradiation history

(Irradiation cycle 111)

Pin No.	Average linear power (W/cm)	Maximum linear power (W/cm)	Irradiation period (hr)	Burn-up (MWD/T)
A	490	510	24	204.4
B	515	520	24	232.6
C	530	560	3	27.6
D	450	460	3	25.4
E	505	520	24	211.1
F	505	515	24	231.0
G	450	470	24	218.0
H	532	545	24	250.0

Table 3. Observations of structure changes

Fuel pin (Specimen No.)	Deviation of thermal center (mm)	Central void diameter (mm)	Columnar grain growth region (mm)	Equiaxed grain growth region (mm)	Crystal grain size (μm)			Inclusions or precipitates	Diametral gap between fuel and cladding tube (μm)	Remarks
					Equiaxed grain growth region		Fuel surface			
					Inside	Outside				
A (20102)	0.6 (0.5)	0.4 (0.4)	2.0 (1.5)	N.A (3.9)	~ 40 (50 ~ 60)	N.A (20)	~ 10 (N.A)	+ (+)	~ 100 (~ 80)	
B (20202)	0.4 (0.5)	N.A (1.2)	N.A (3.3)	N.A (4.0)	N.A (~ 40)	N.A (~ 20)	N.A (6 ~ 10)	- (+)	N.A (~ 40)	
C (20302)	0 (0)	0 (0)	0 (0)	N.A (3.5)	80 ~ 90 (70 ~ 90)	N.A (~ 20)	~ 15 (~ 10)	- (-)	~ 60 (~ 60)	
D (20402)	0 (0)	0 (0)	0 (0)	3.2 (3.2)	~ 130 (~ 100)	N.A (~ 25)	10~20 (~ 8)	- (-)	~ 60 (~ 70)	
E (20502)	0.4 (0.3)	0 (0.1)	0 (0)	3.0 (3.9)	100 (~ 80)	N.A (20)	10~20 N.A	- (+)	~ 30 (~ 20)	
F (20602)	0 (0.1)	1.5 (1.4)	2.3 (2.2)	4.4 (4.4)	~ 30 (40)	N.A (20)	~ 10 (10)	- (+)	~ 60 (~ 50)	
G (20702)	0 (0)	1.1 (1.1)	4.2 (4.6)	5.0 (5.1)	~ 50 (40)	N.A (20)	N.A (N.A)	- (-)	N.A (N.A)	
H (20802)	0.2 (0.3)	2.0 (2.2)	4.9 (5.1)	5.1 (5.1)	~ 30 (20)	N.A (10)	N.A (N.A)	- (+)	N.A (N.A)	

( ): GE data. N.A: not measured

Table 4. Quantitative determination of fission products

Location	Specimen No.	Radioactivity in leaching solution (μCi)			Relative intensity				
		Ce-144	Rh-106	Cs-137	Ce/total %	Rh/total %	Cs/total %	Rh/Ce	Cs/Ce
Fuel region	20104	127.3	58.1	334.8	24.5	11.2	64.4	0.456	2.6
Insulator region	20106	77.5	37.8	233.8	22.2	10.8	66.9	0.488	3.0

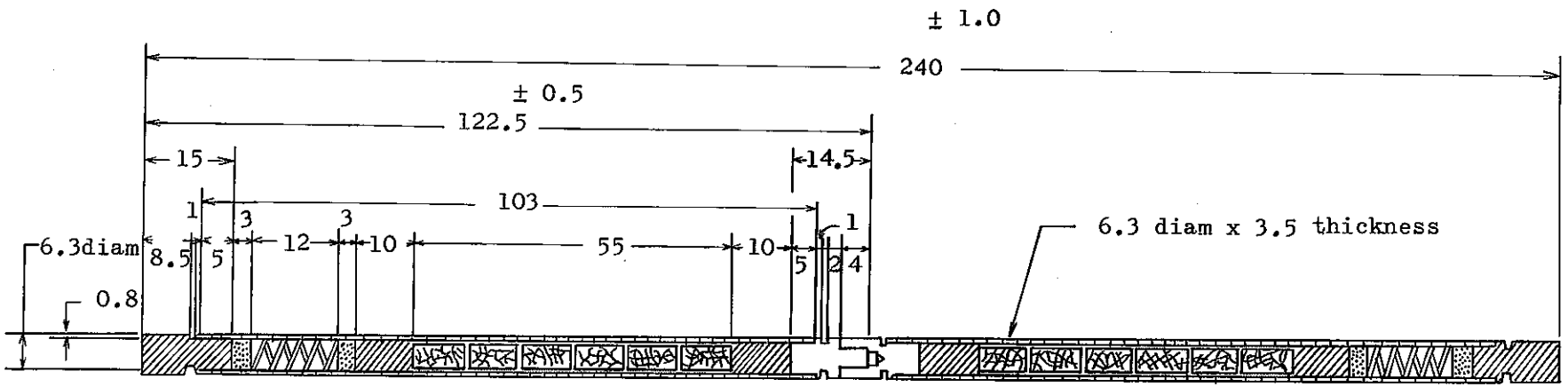

Fig. 1. Fuel pin

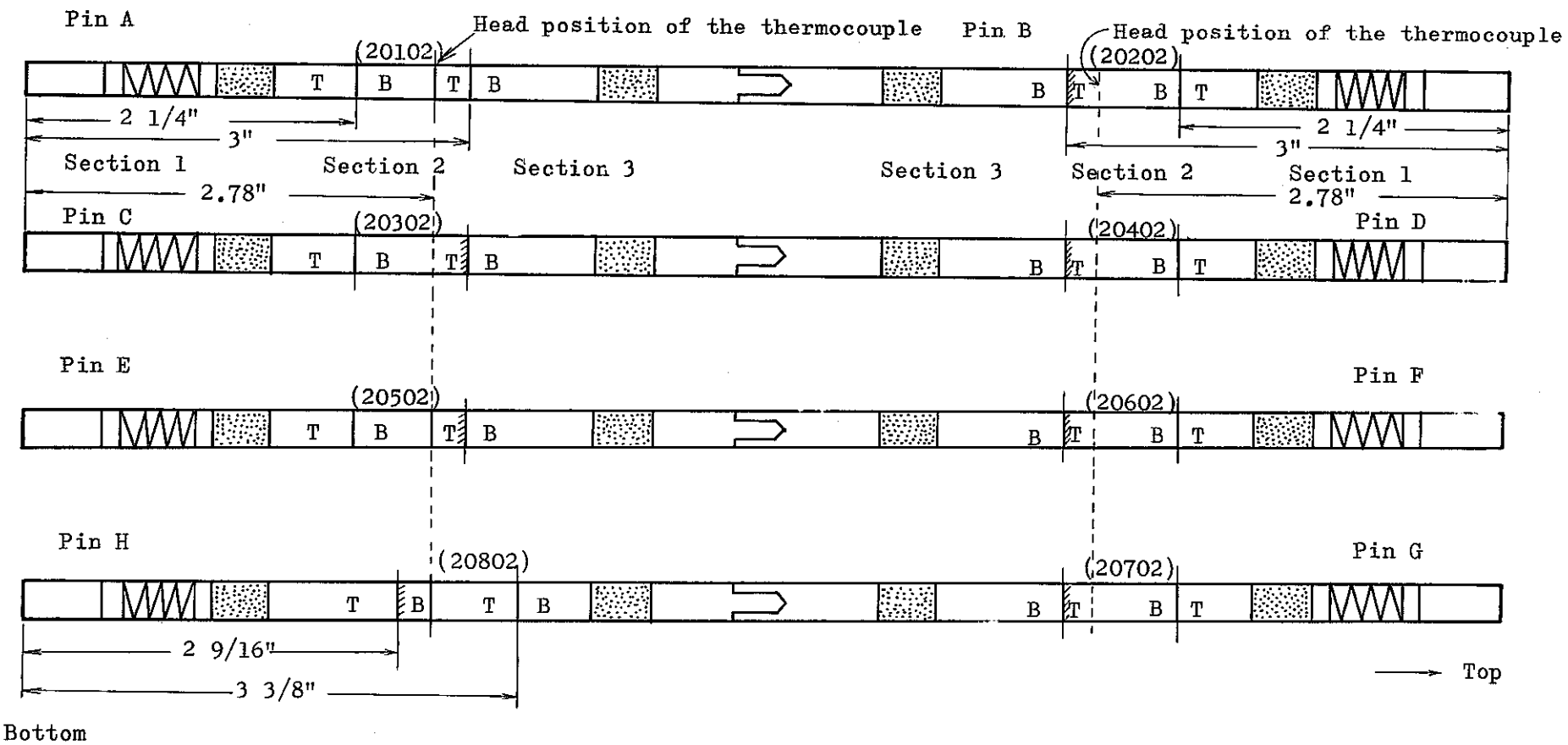

Fig. 2. Combination of fuel pins in capsules

( ) : Specimen No.

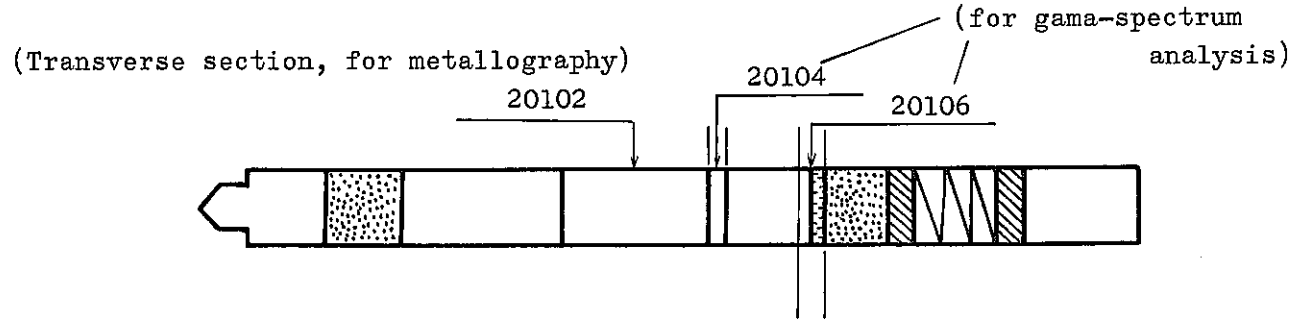

Pin A

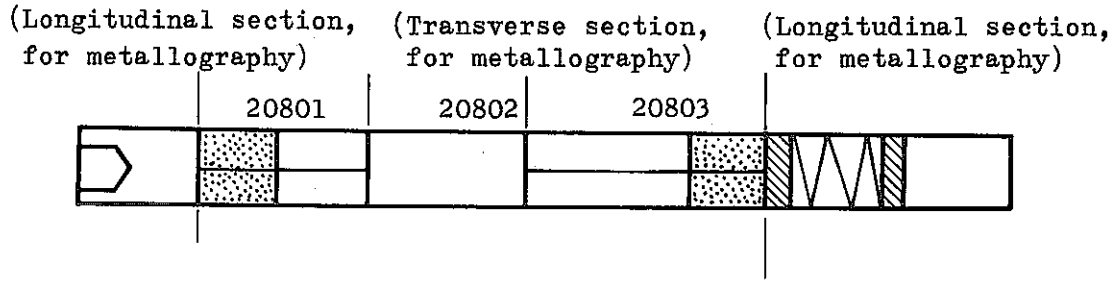

Pin H

Fig. 3 Sectioning diagram of Pin A and Pin H

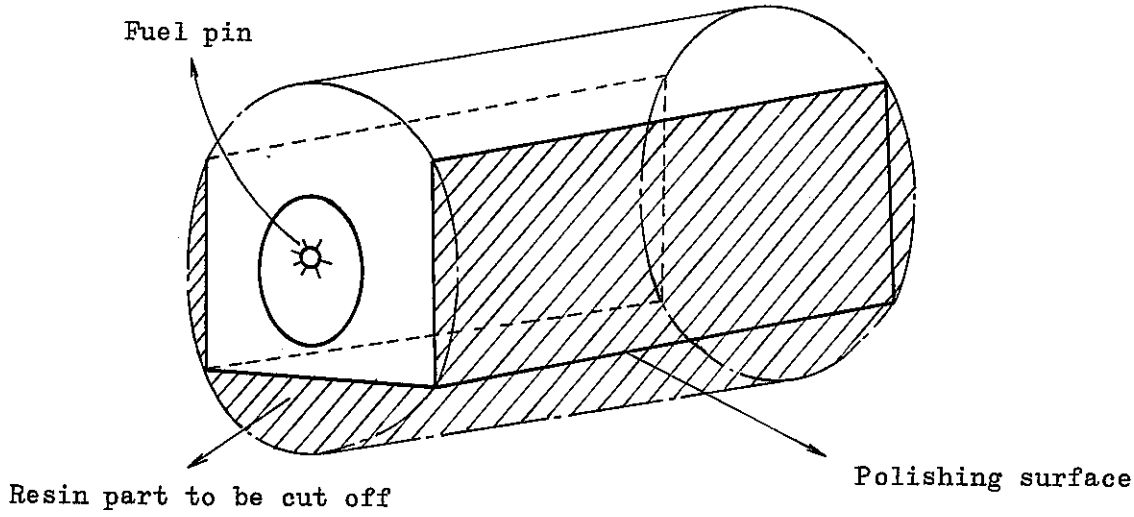

Sectioning plan of Pin B (20202)

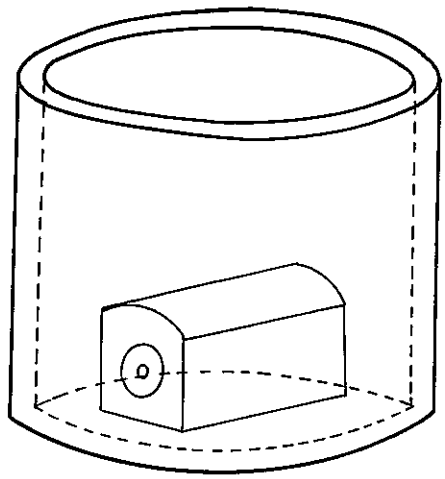

Mounting of Pin B (20202)

Fig. 4. Sectioning and mounting of specimen 20202 for observations of lenticular voids

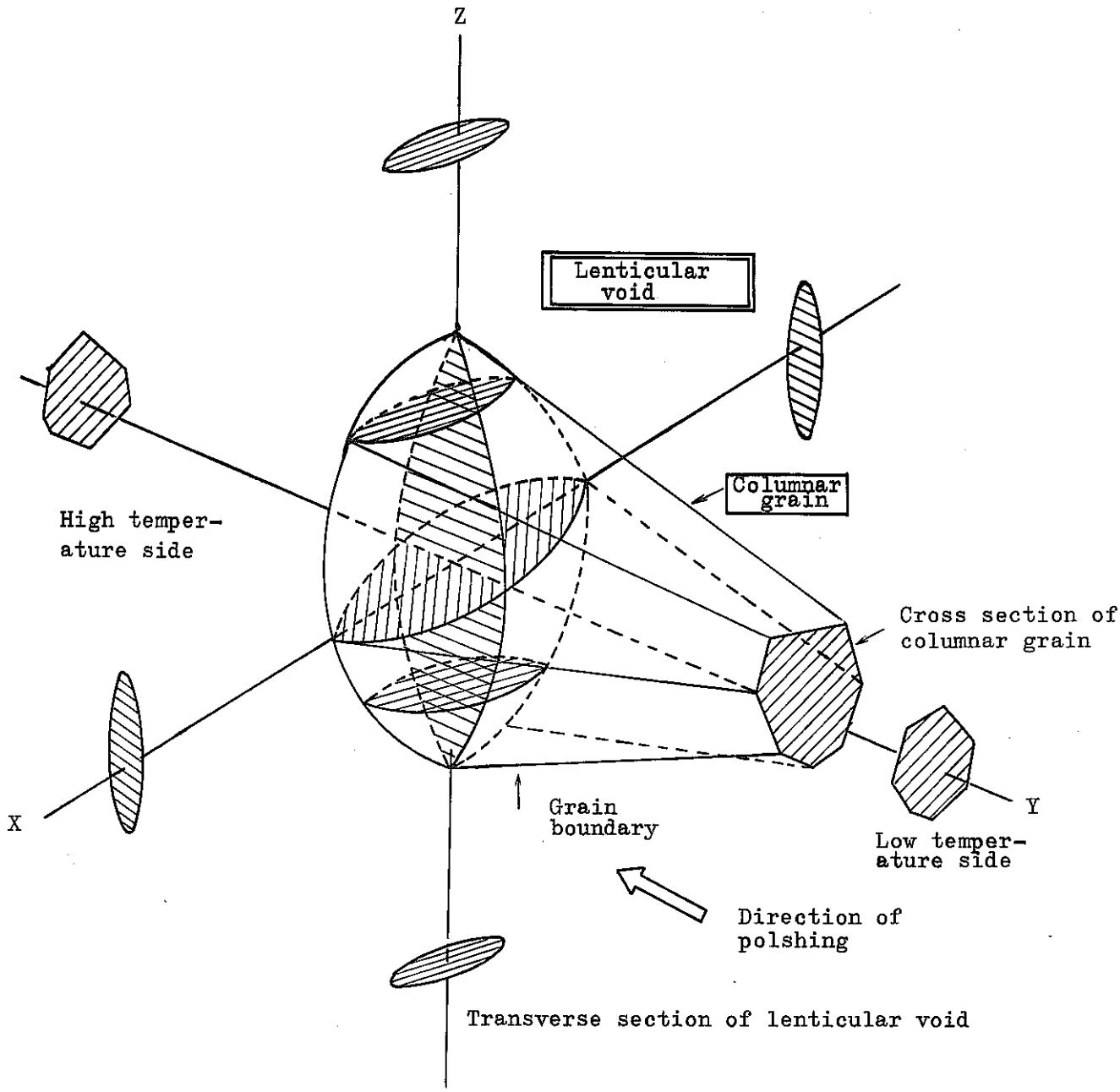

Fig. 5. Shape of lenticular void

(Lenticular void accompanied with columnar grain)

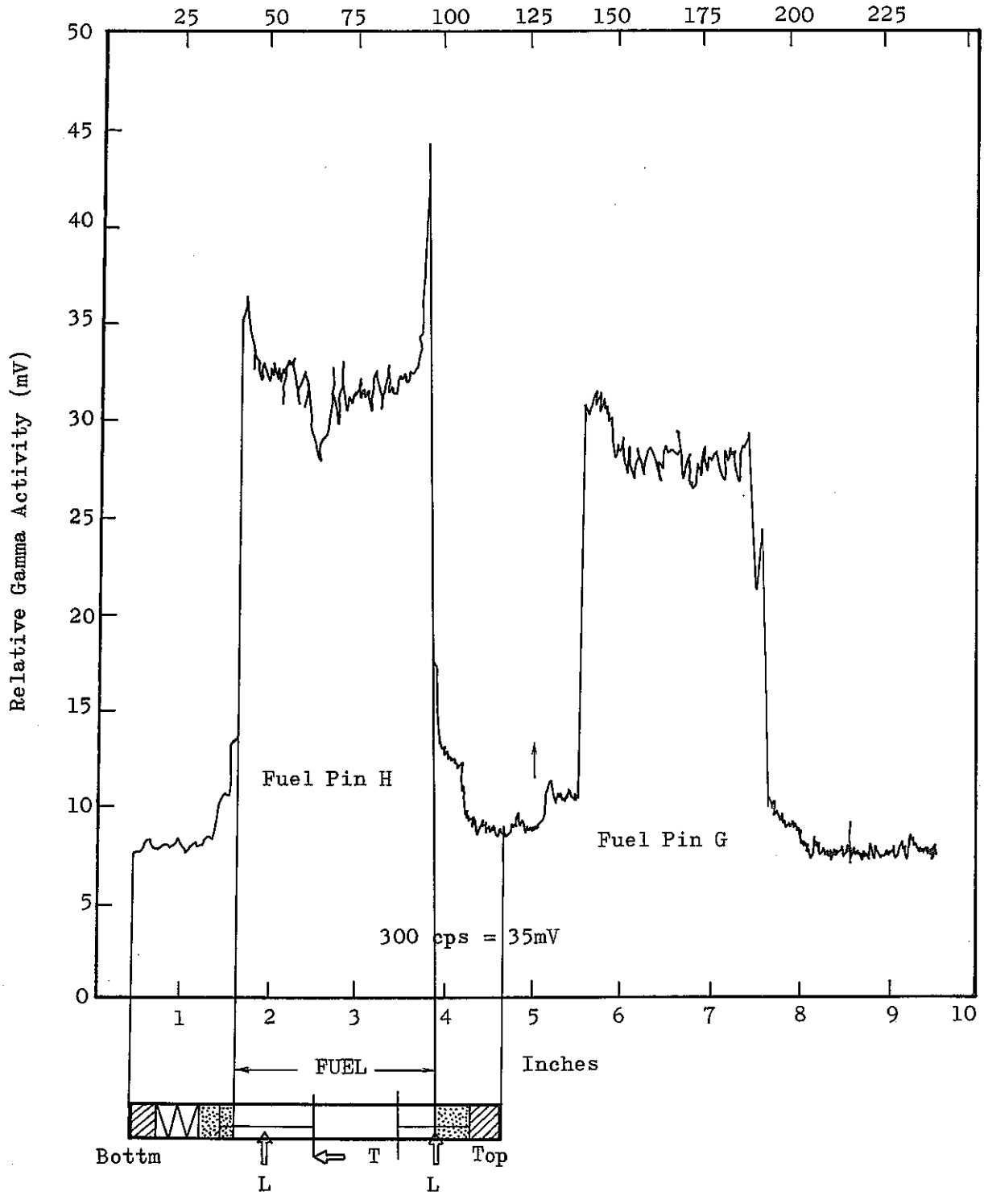

Fig. 6 Gamma - scanning of Pin H

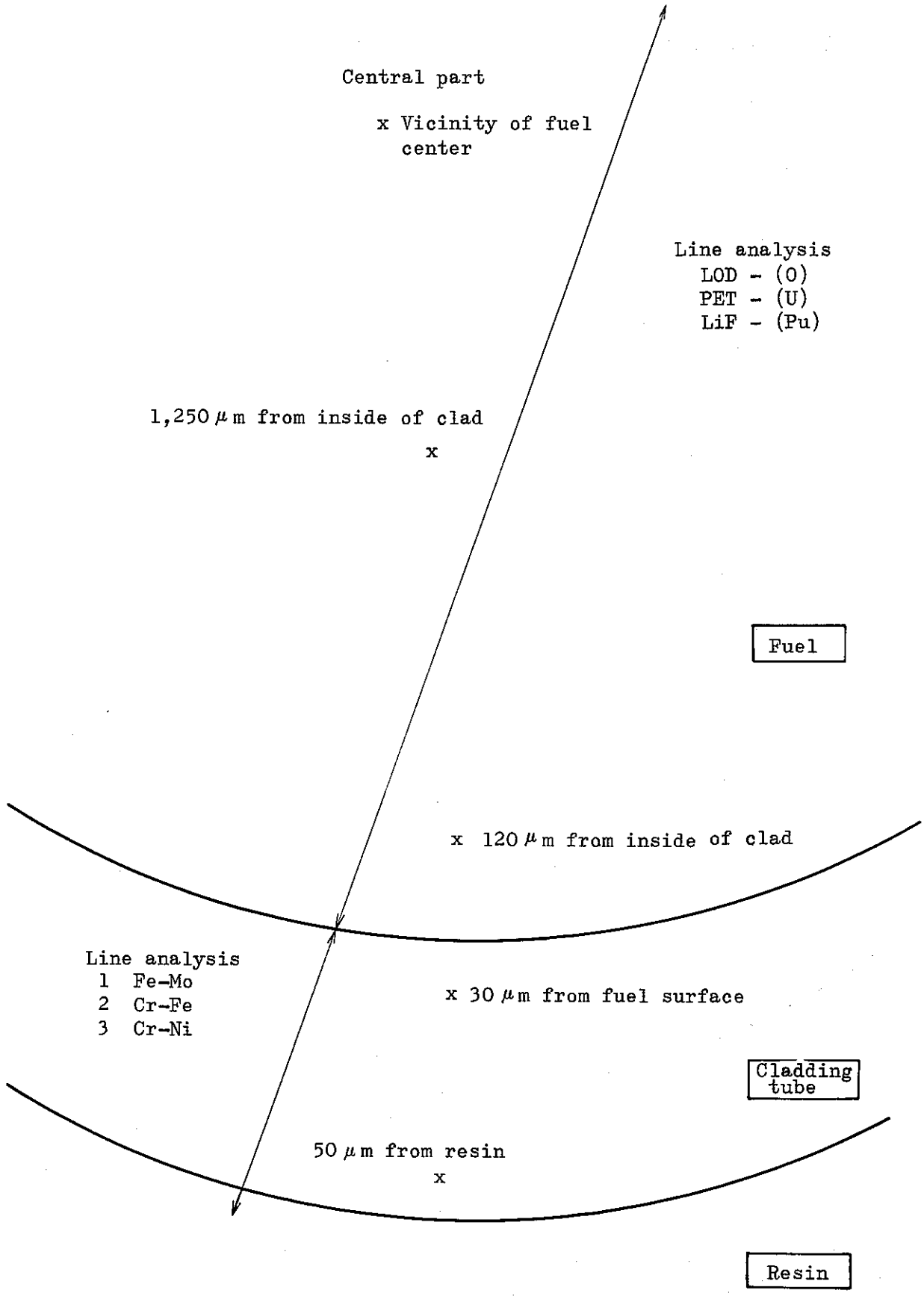

Fig. 7. Measuring location of electron probe microanalysis (Pin A, No. 20102)

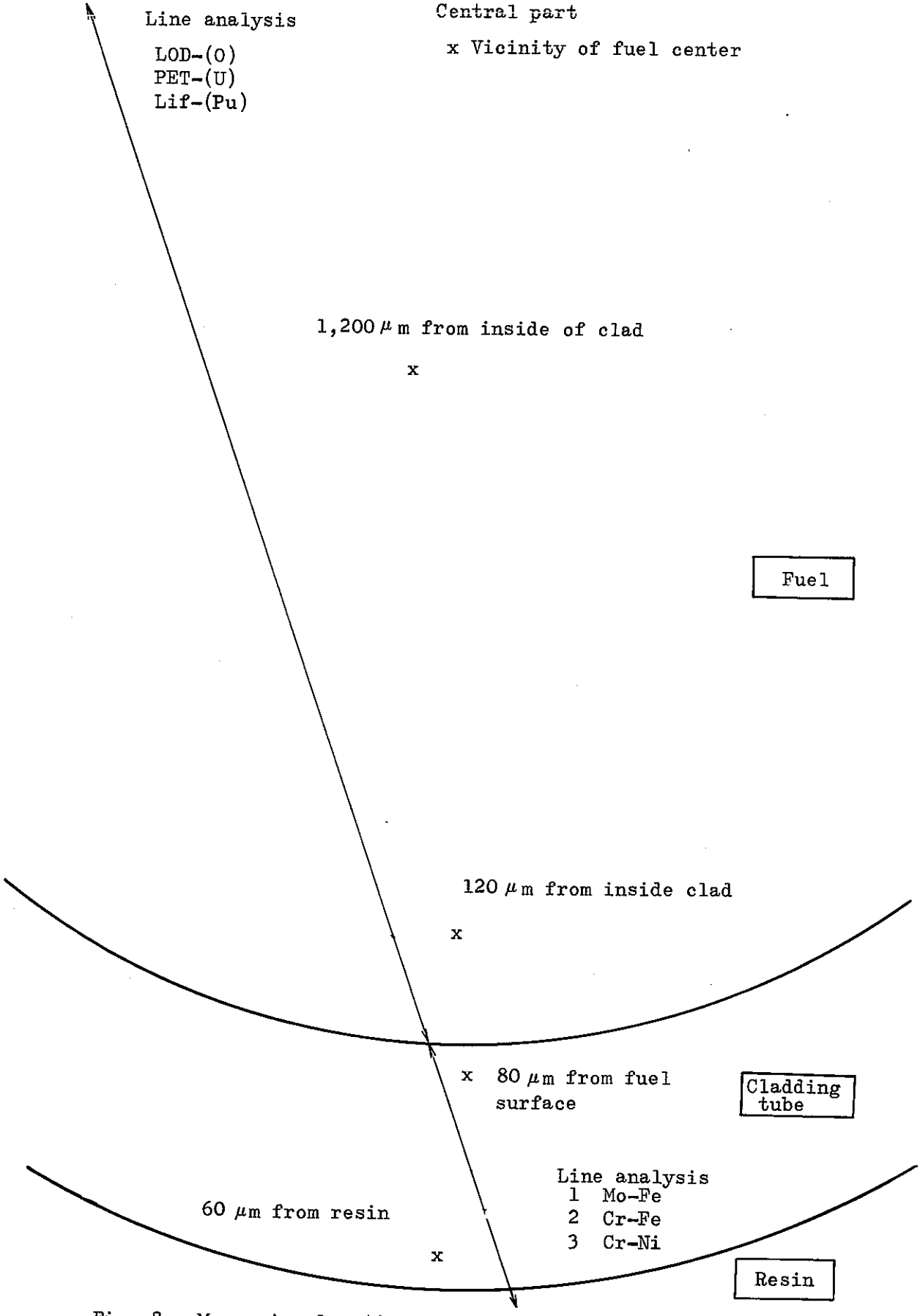

Fig. 8. Measuring location of electron probe microanalysis (Pin E, No. 20502)

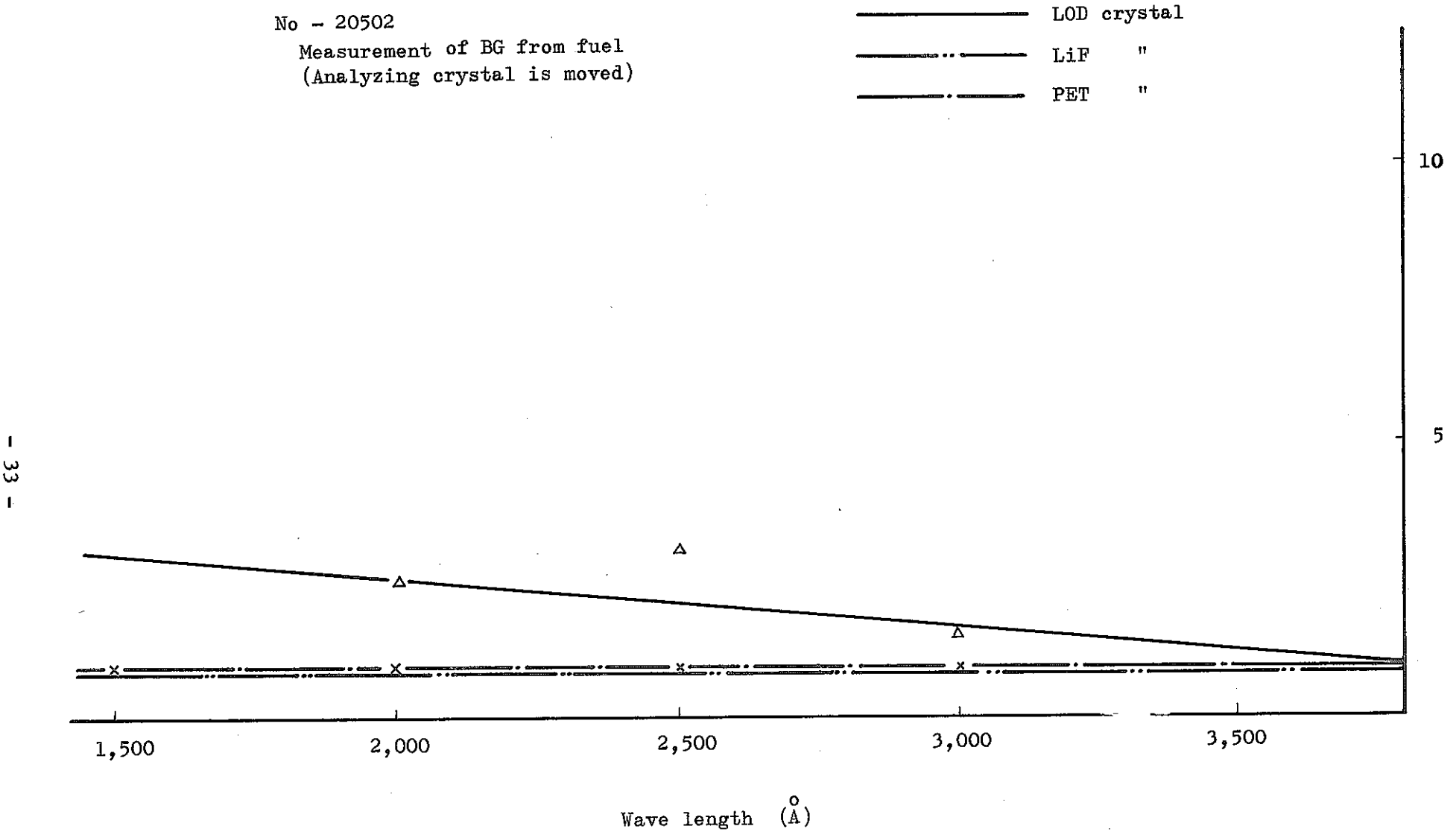

Fig. 9. Result of the measurement of background

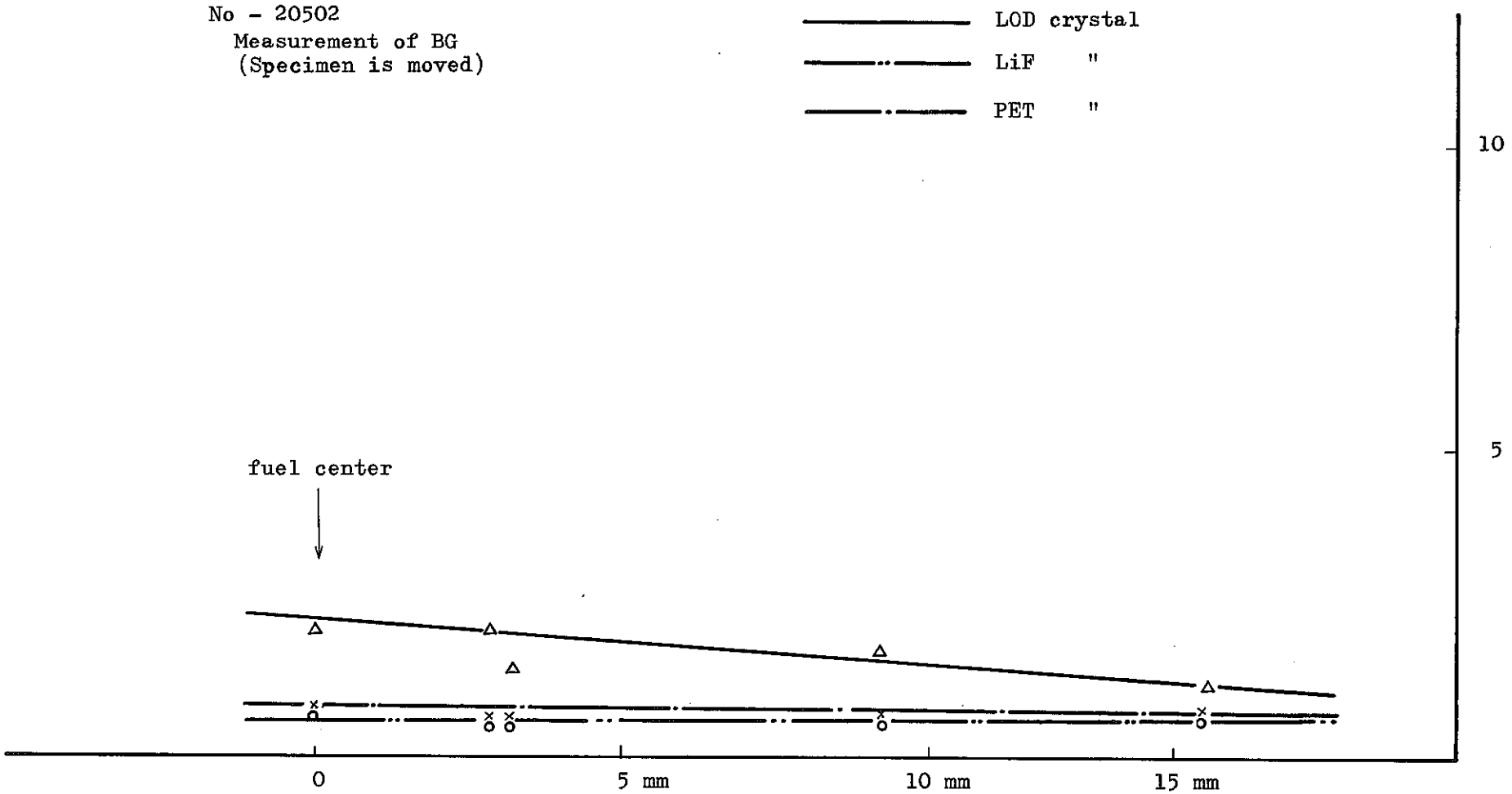

Fig. 10. Result of the measurement of background

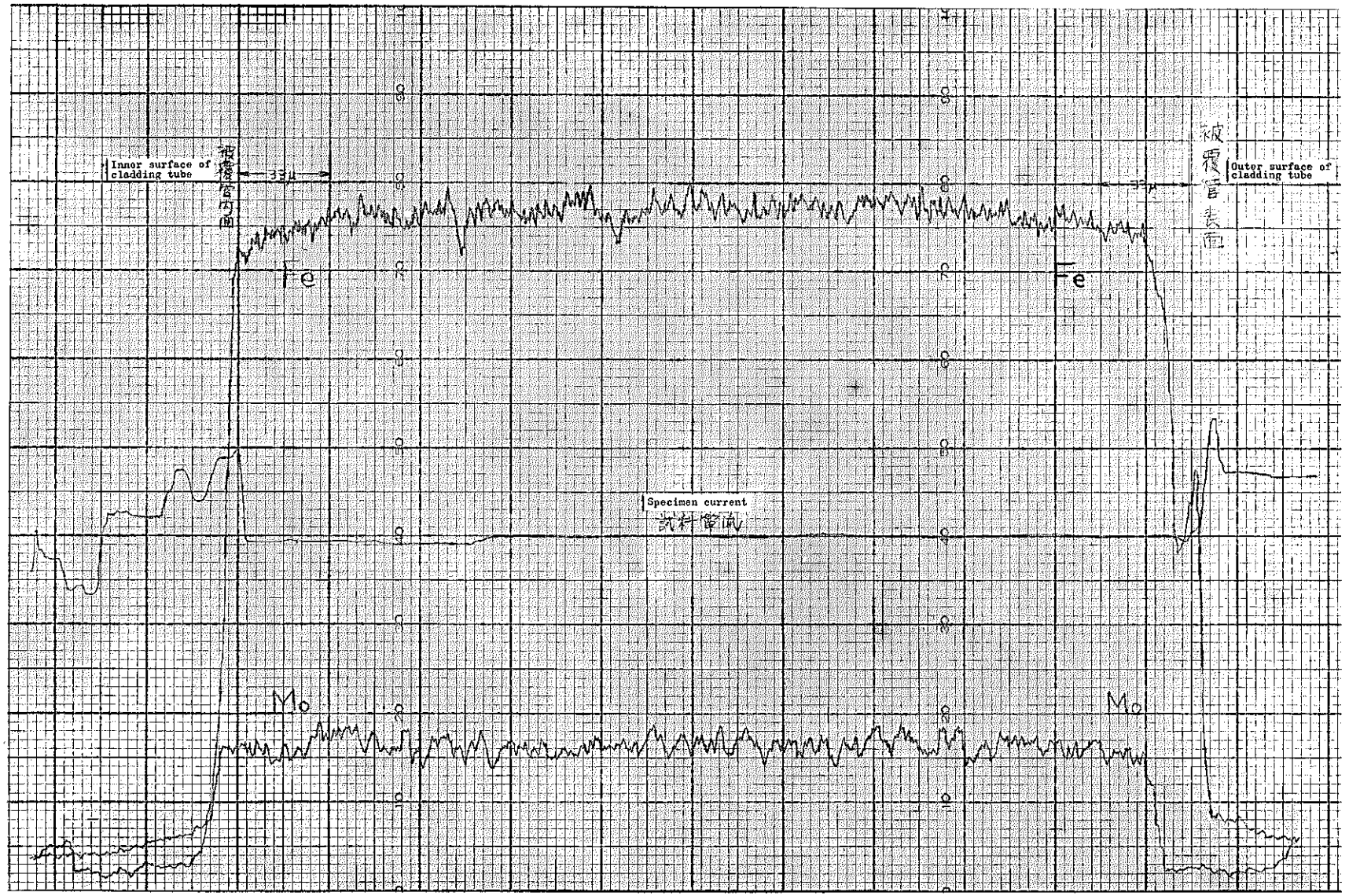

Fig. 11. Line analysis of cladding tube, specimen 20102

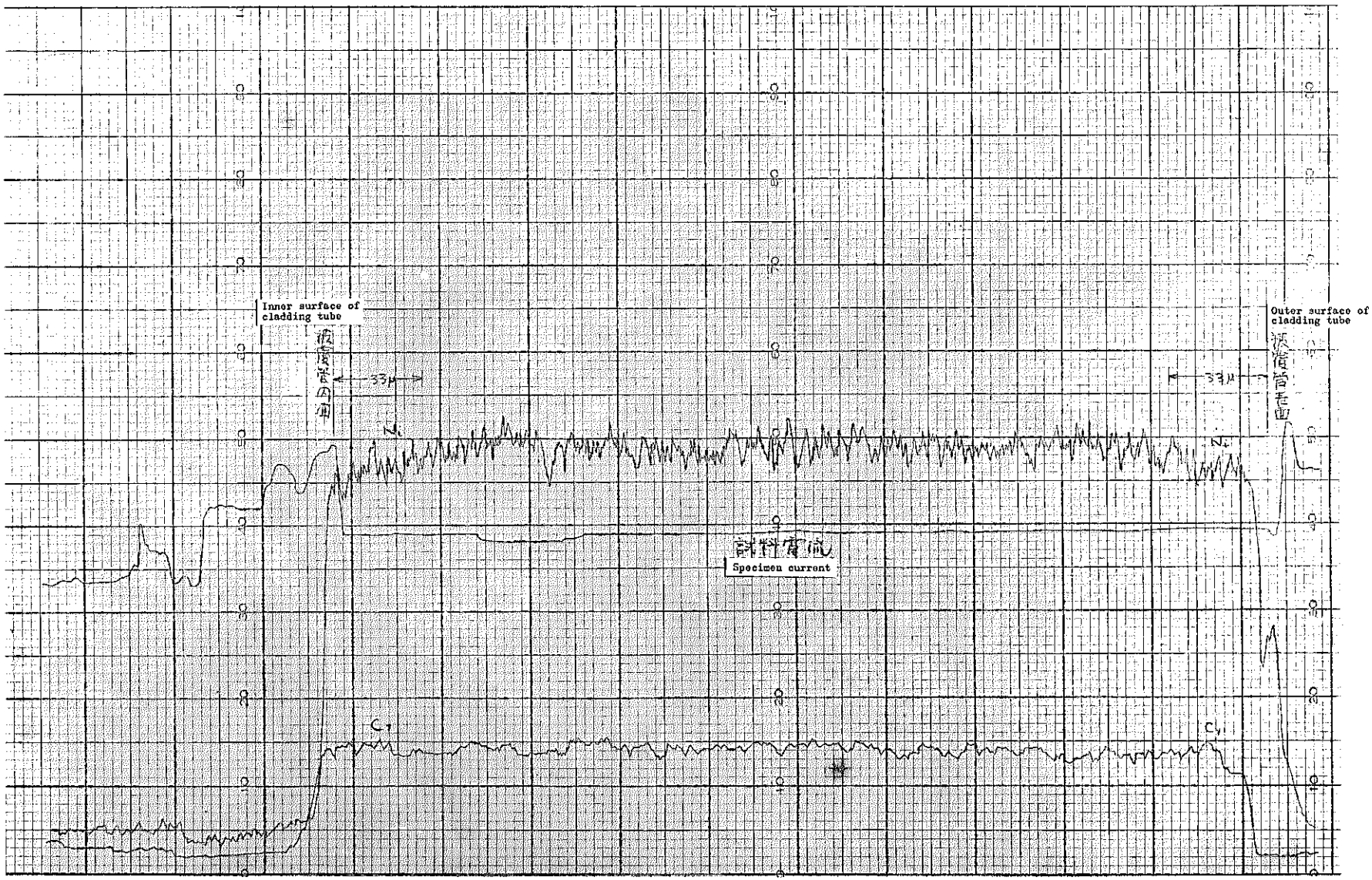

Fig. 12. Line analysis of cladding tube, specimen 20102

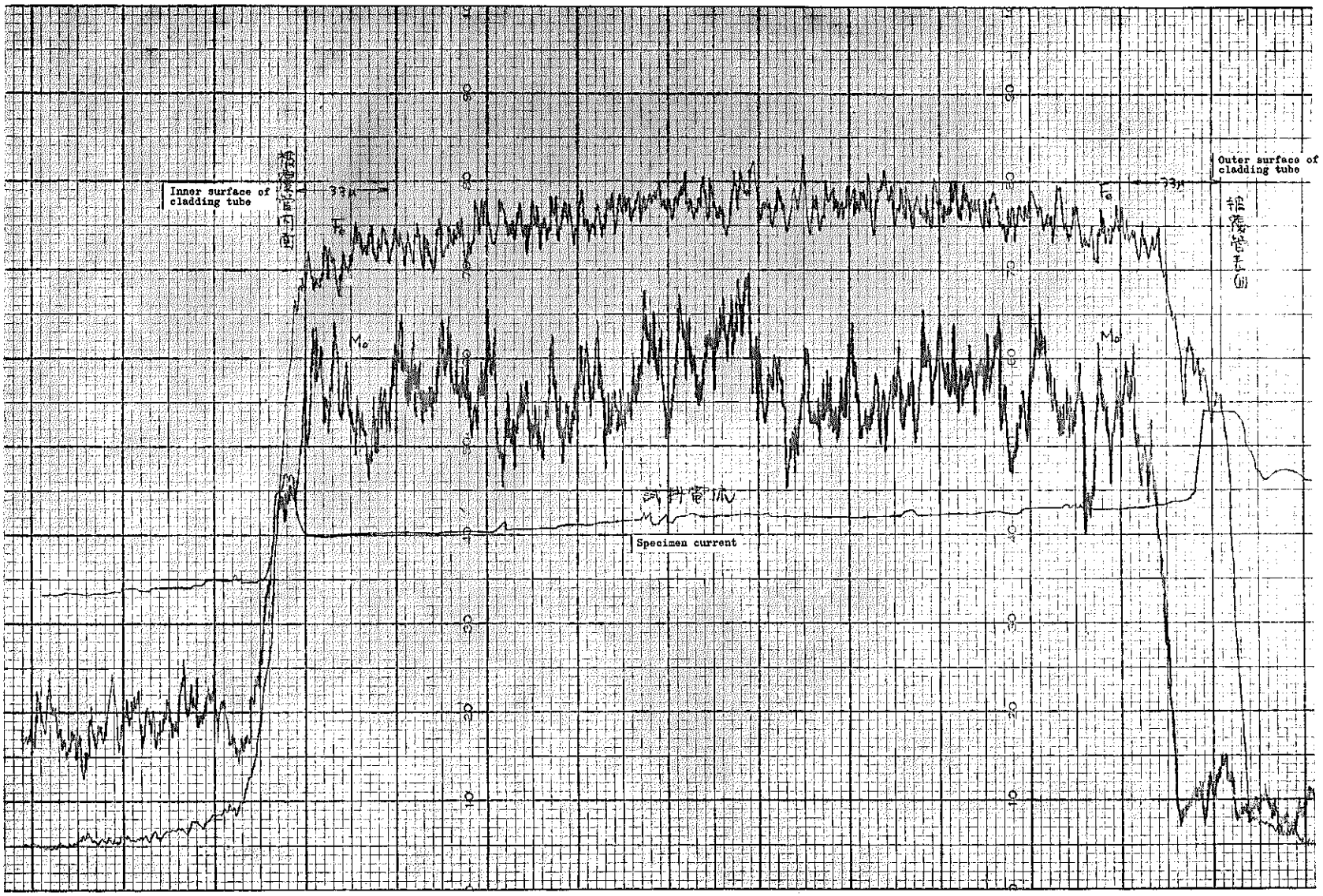

Fig. 13. Line analysis of cladding tube, Specimen 20502

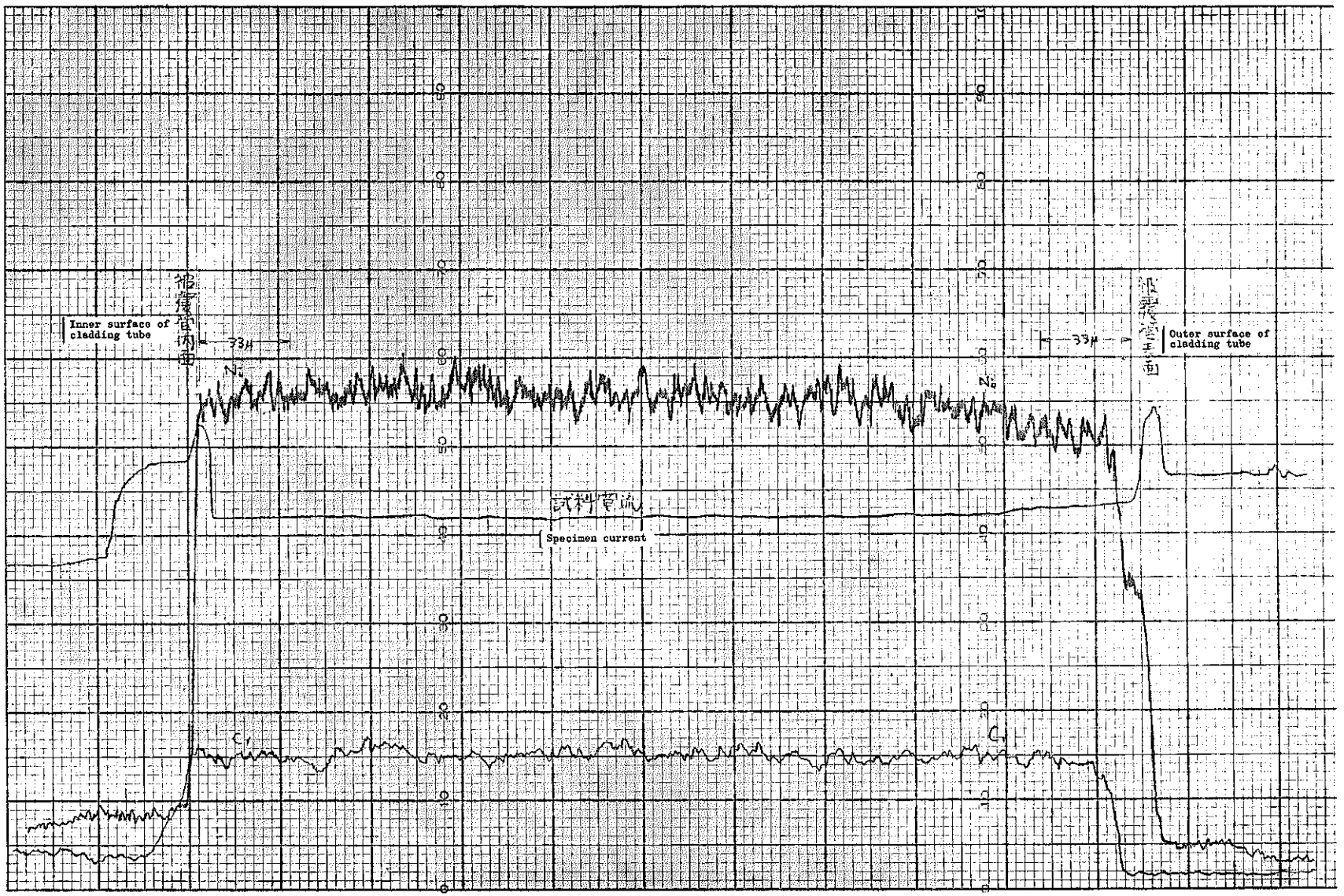

Fig. 14. Line analysis of cladding tube, Specimen 20502

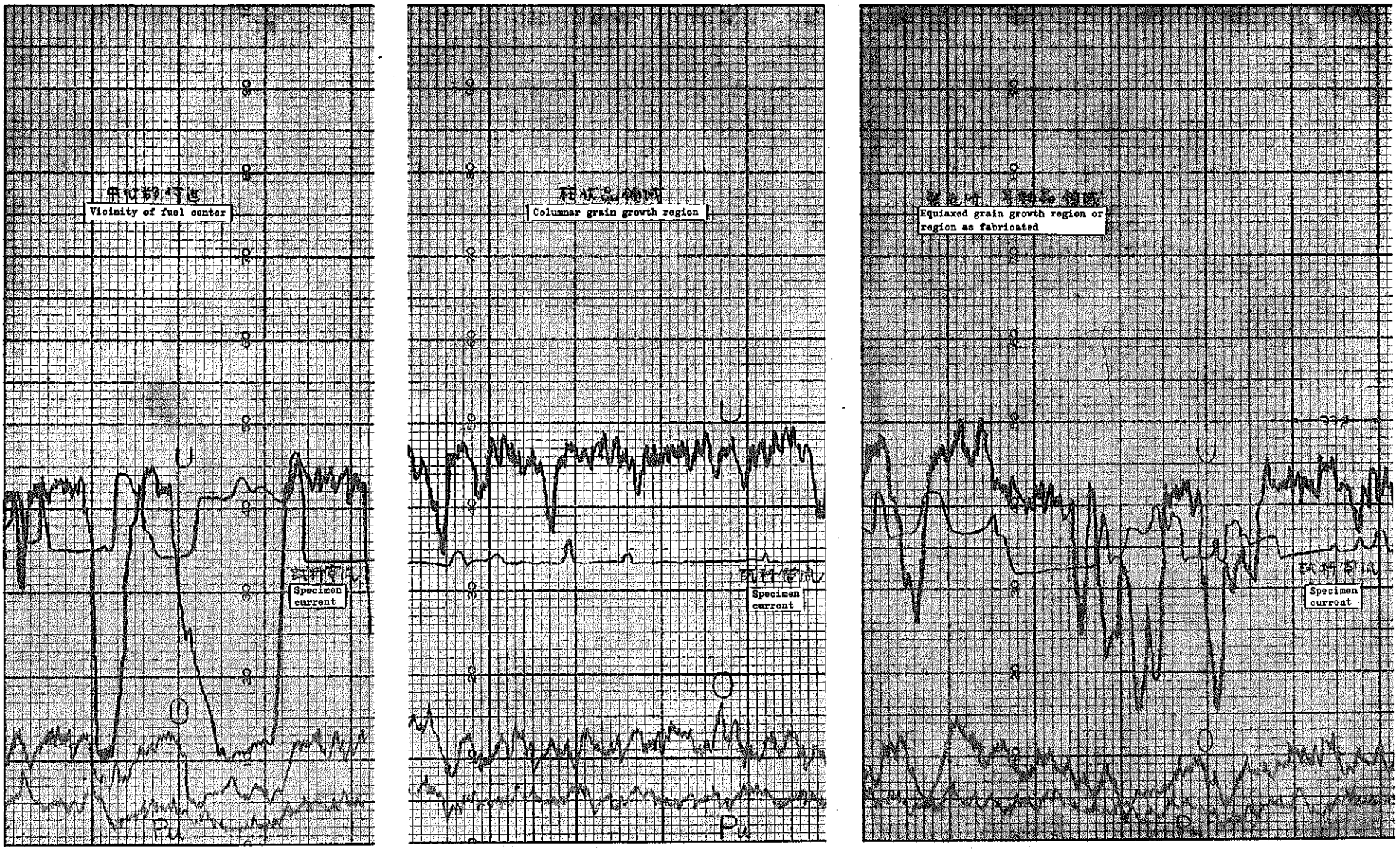

Fig. 15. Line analysis of fuel region Specimen 20102

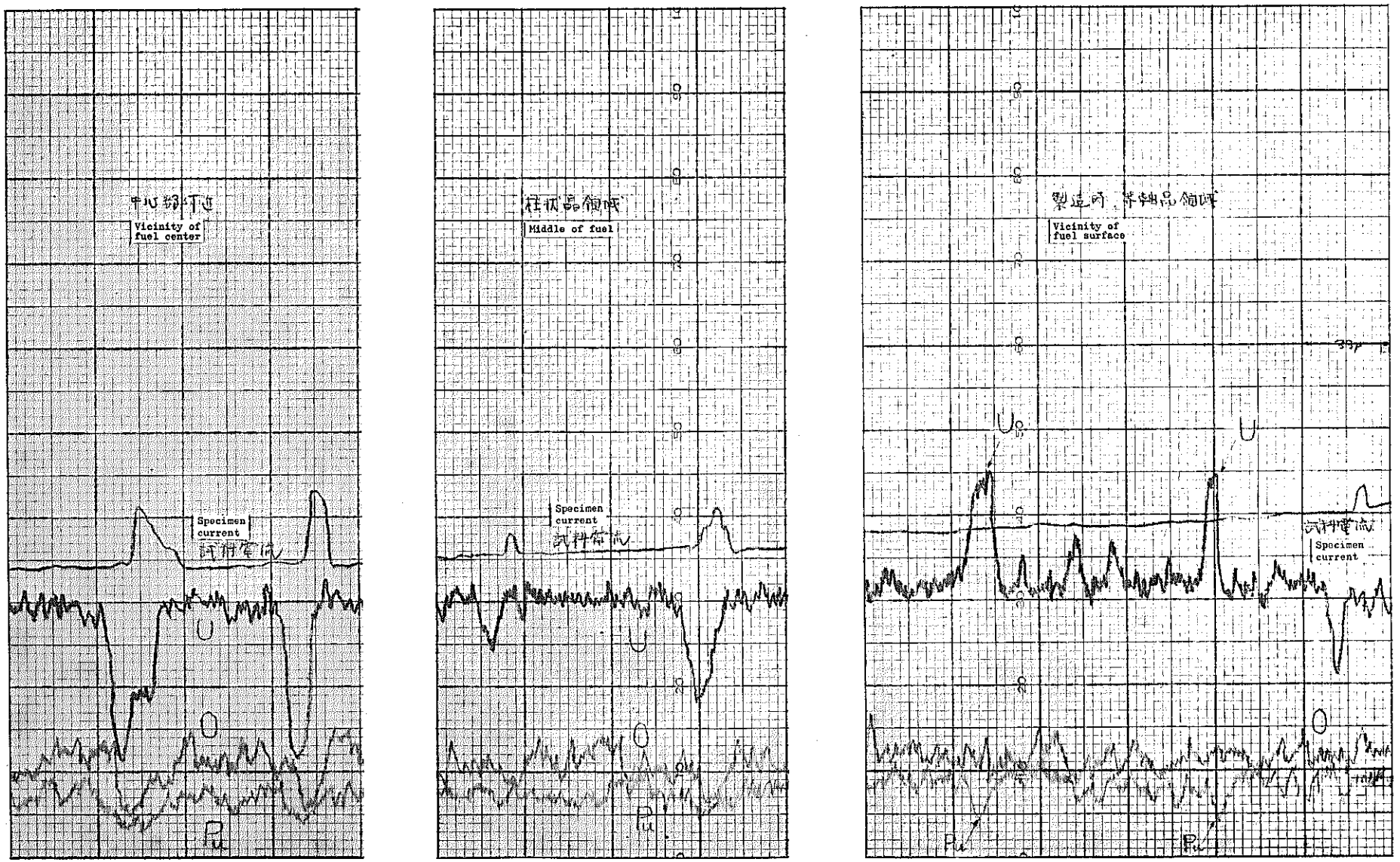

Fig. 16. Line analysis of fuel region specimen 20502

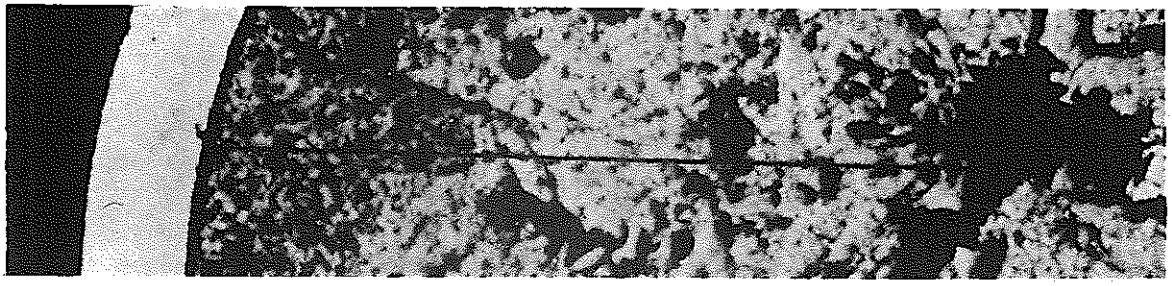

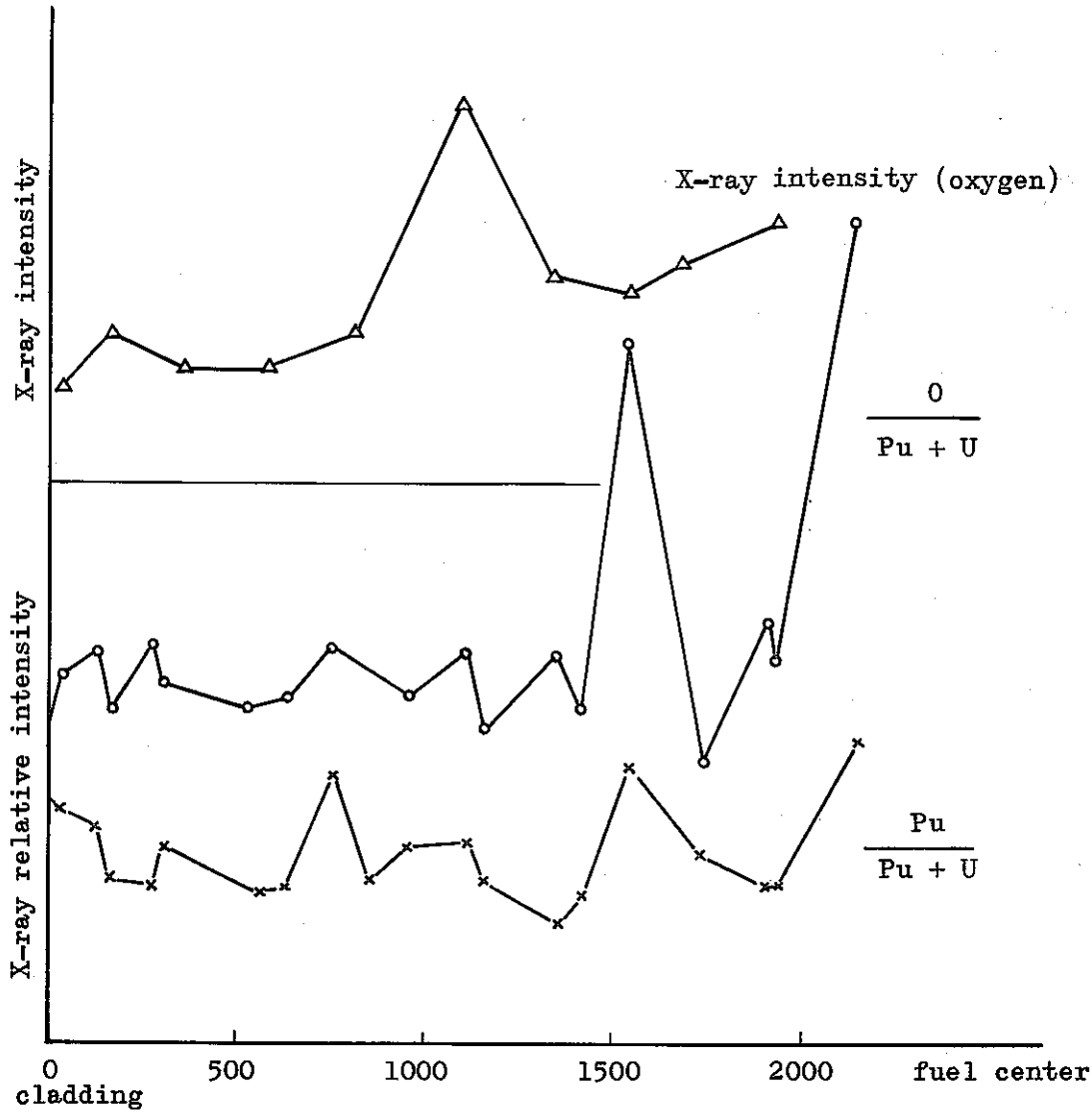

Fig. 17. Changes of X-ray intensity (oxygen) and X-ray relative intensity ($\frac{O}{Pu + U}$, $\frac{Pu}{Pu + U}$), specimen 20102

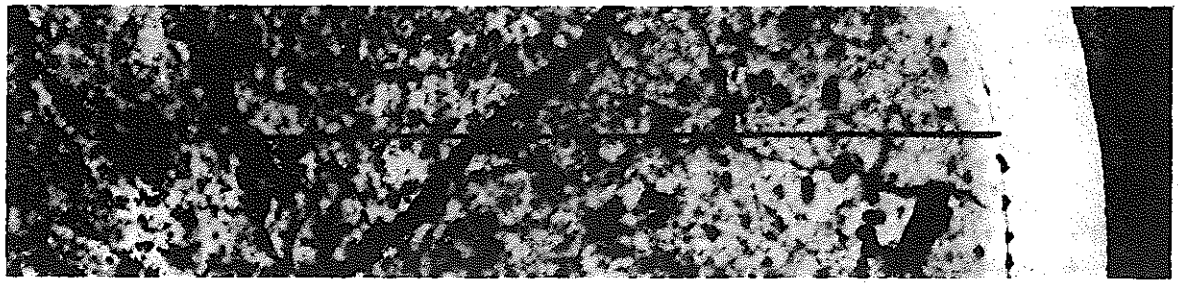

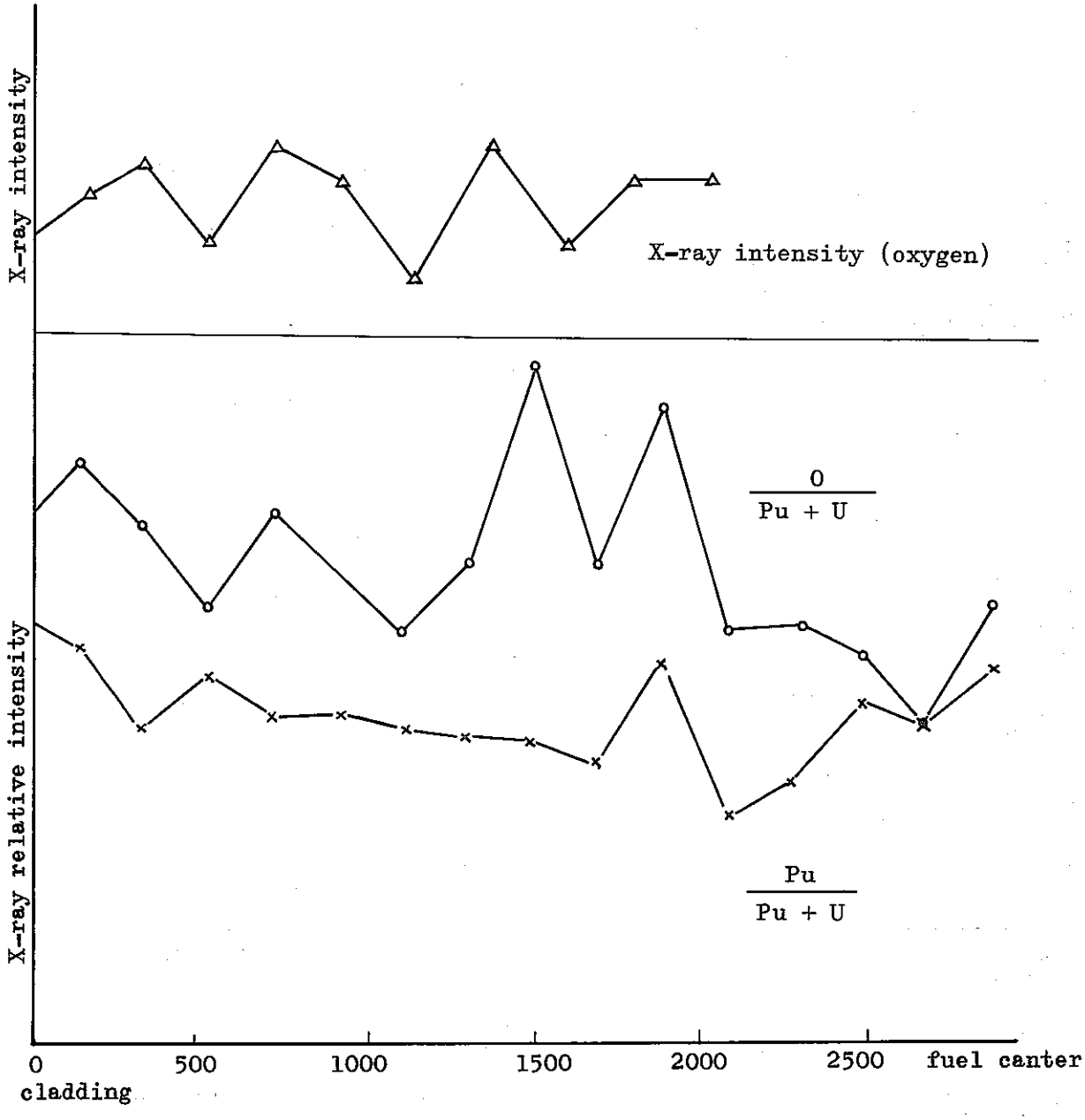

Fig. 18. Changes of X-ray intensity (oxygen) and X-ray relative intensity ($\frac{O}{Pu + U}$, $\frac{Pu}{Pu + U}$), specimen 20502

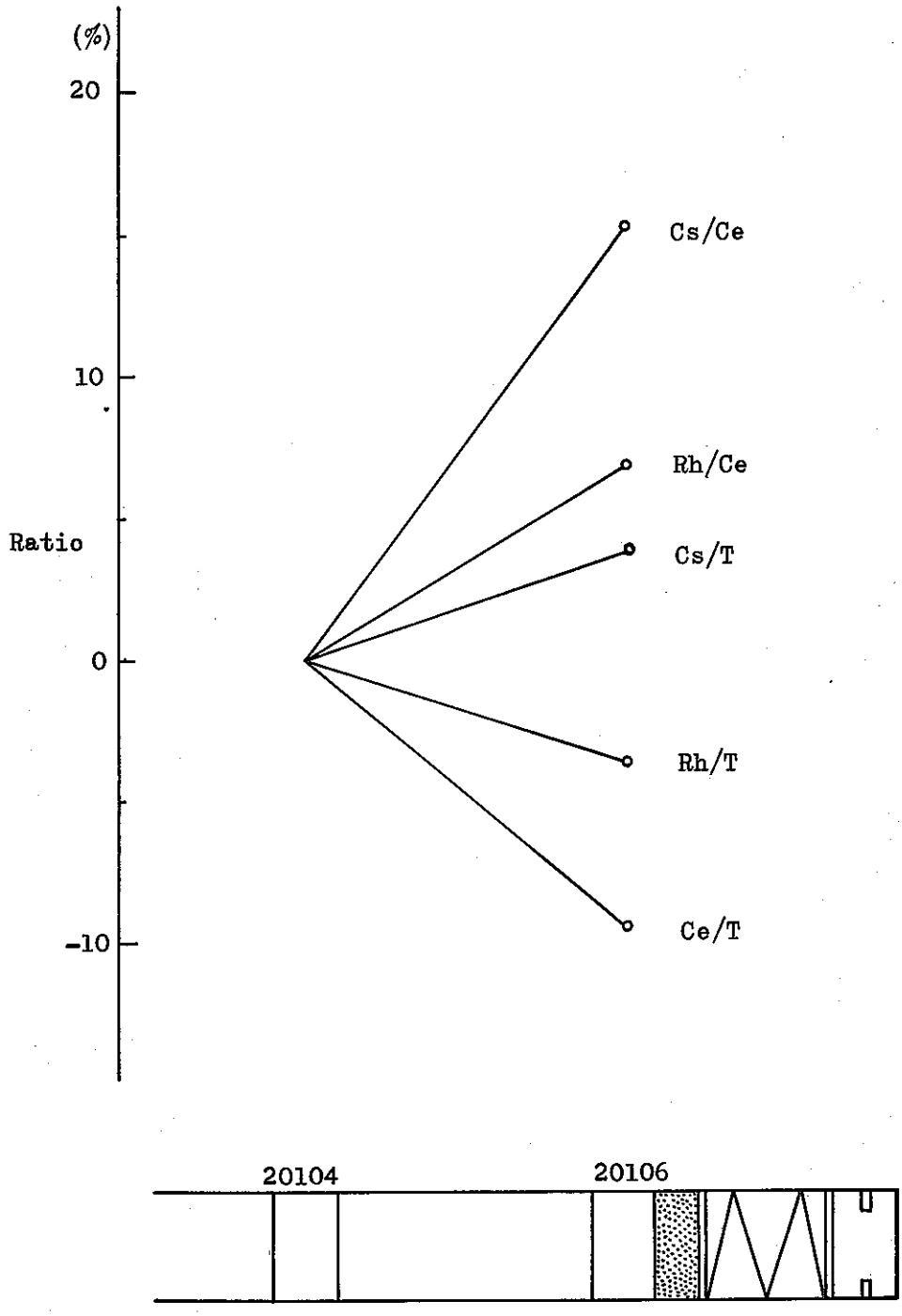

Fig. 19. Ratios of the radioactivity from nuclides detected in insulator region to those in fuel region

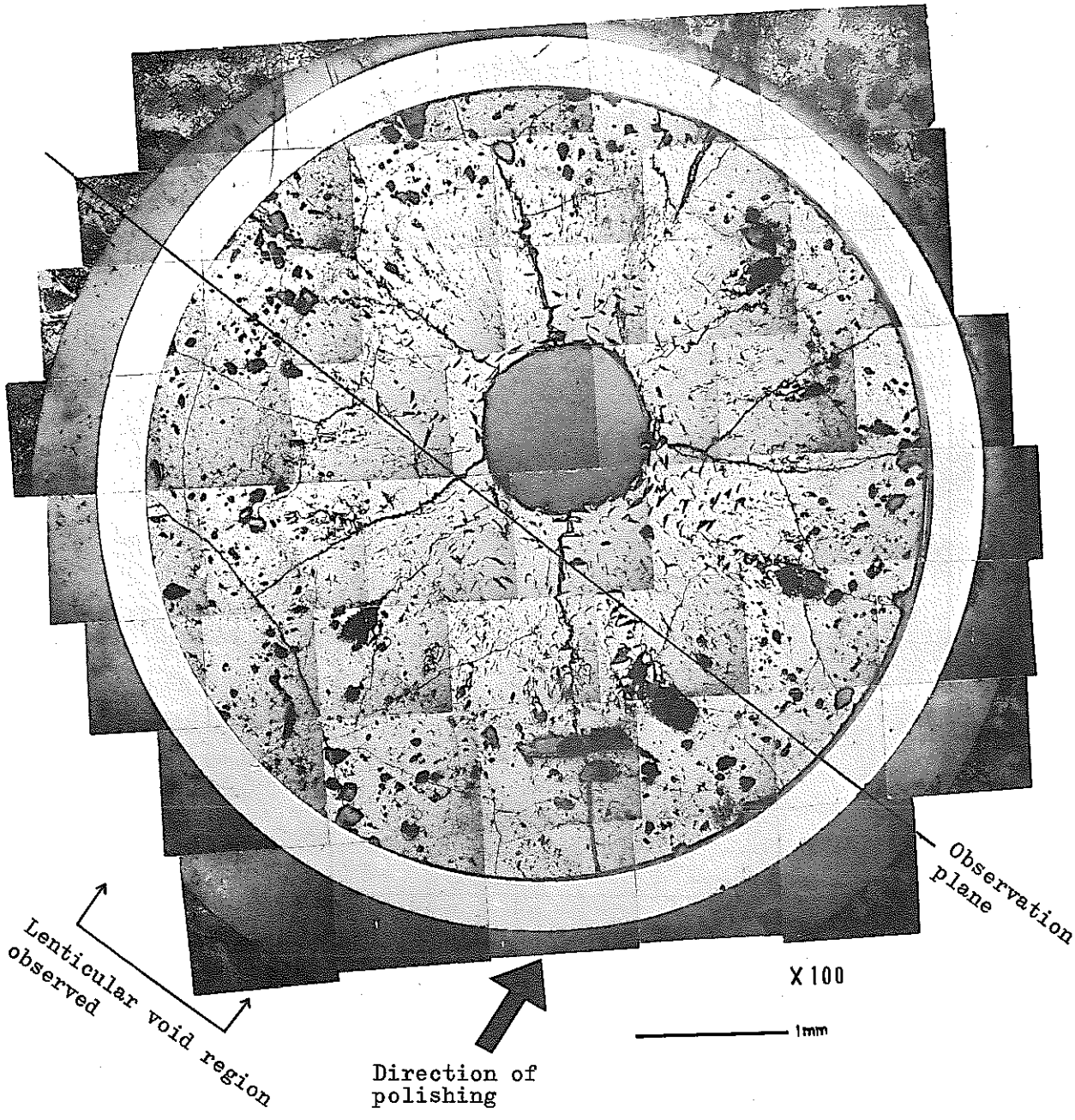

Photograph 1. Metallographic photograph of transverse cross section specimen 20202

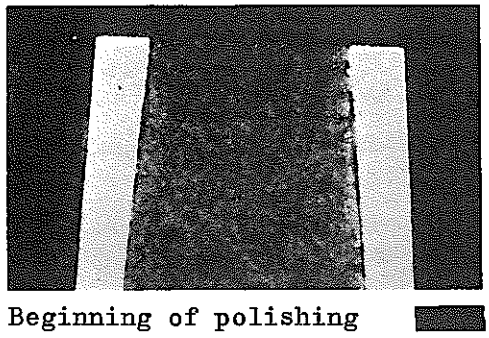

Depth of grinding
(0.3 mm)

Beginning of polishing

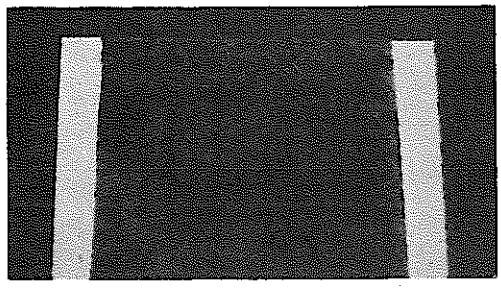

(0.7 mm)

Middle stage of polishing × 10

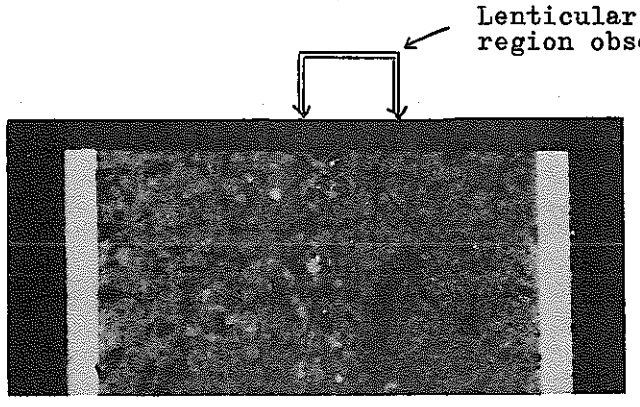

Lenticular void region observed

(2.3 mm)

Latter stage of polishing × 10

Polishing method:
Waterproof polishing paper
No. 320, step-polishing

Photograph 2. Photographs of longitudinal cross section in process of grinding

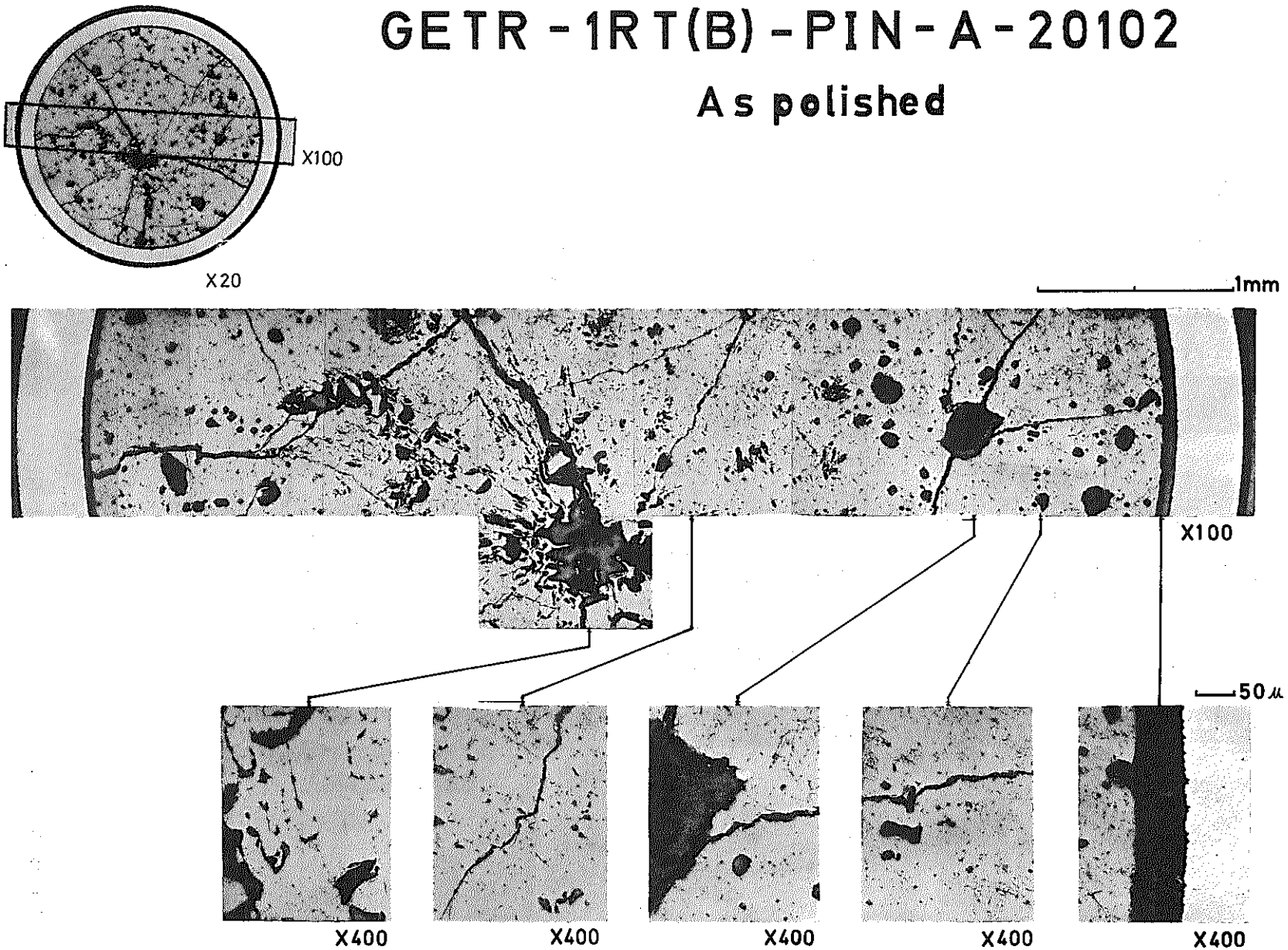

Photograph 3. Metallographic photograph, Specimen 20102

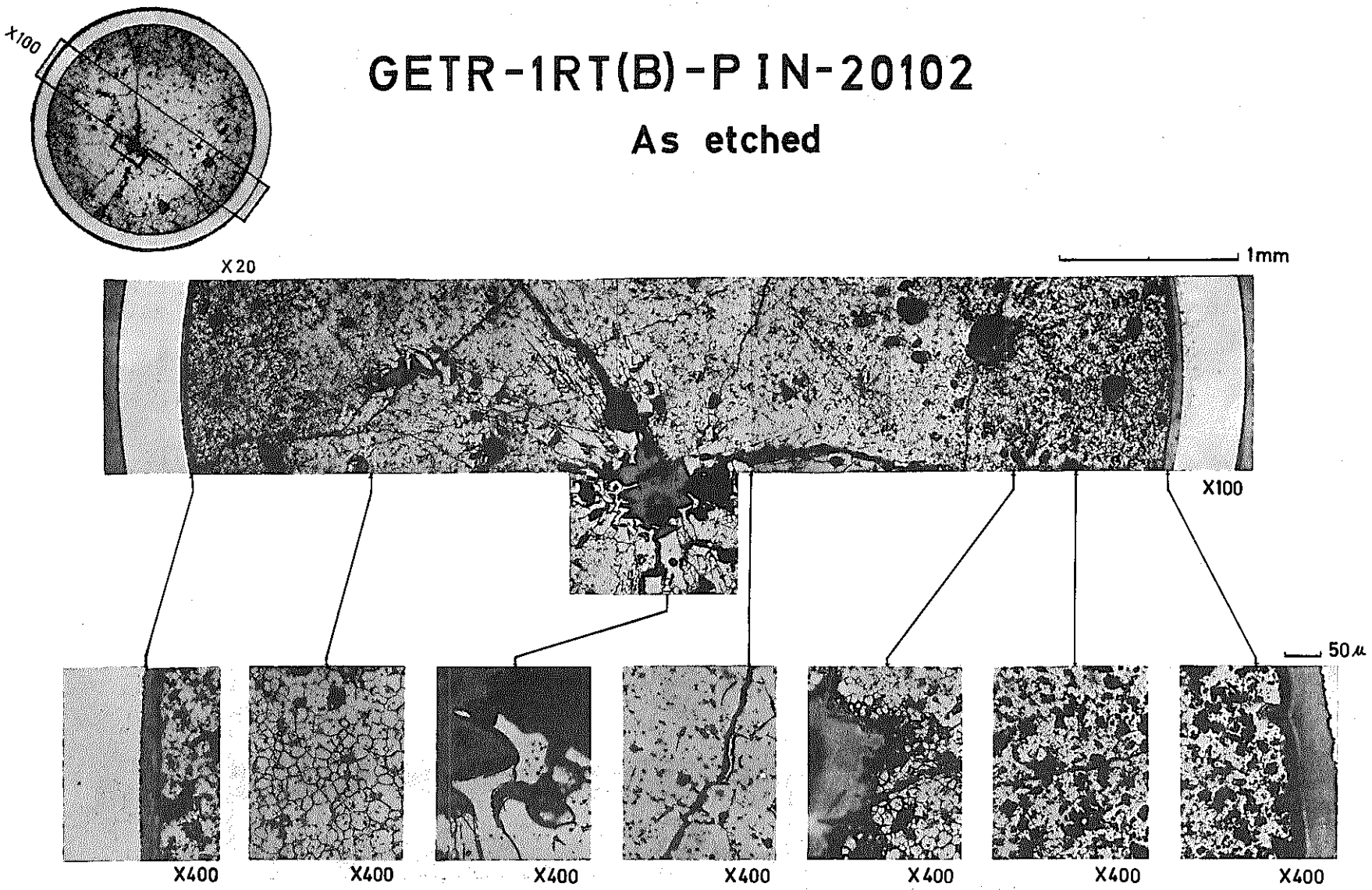

Photograph 4. Metallographic photograph, Specimen 20102

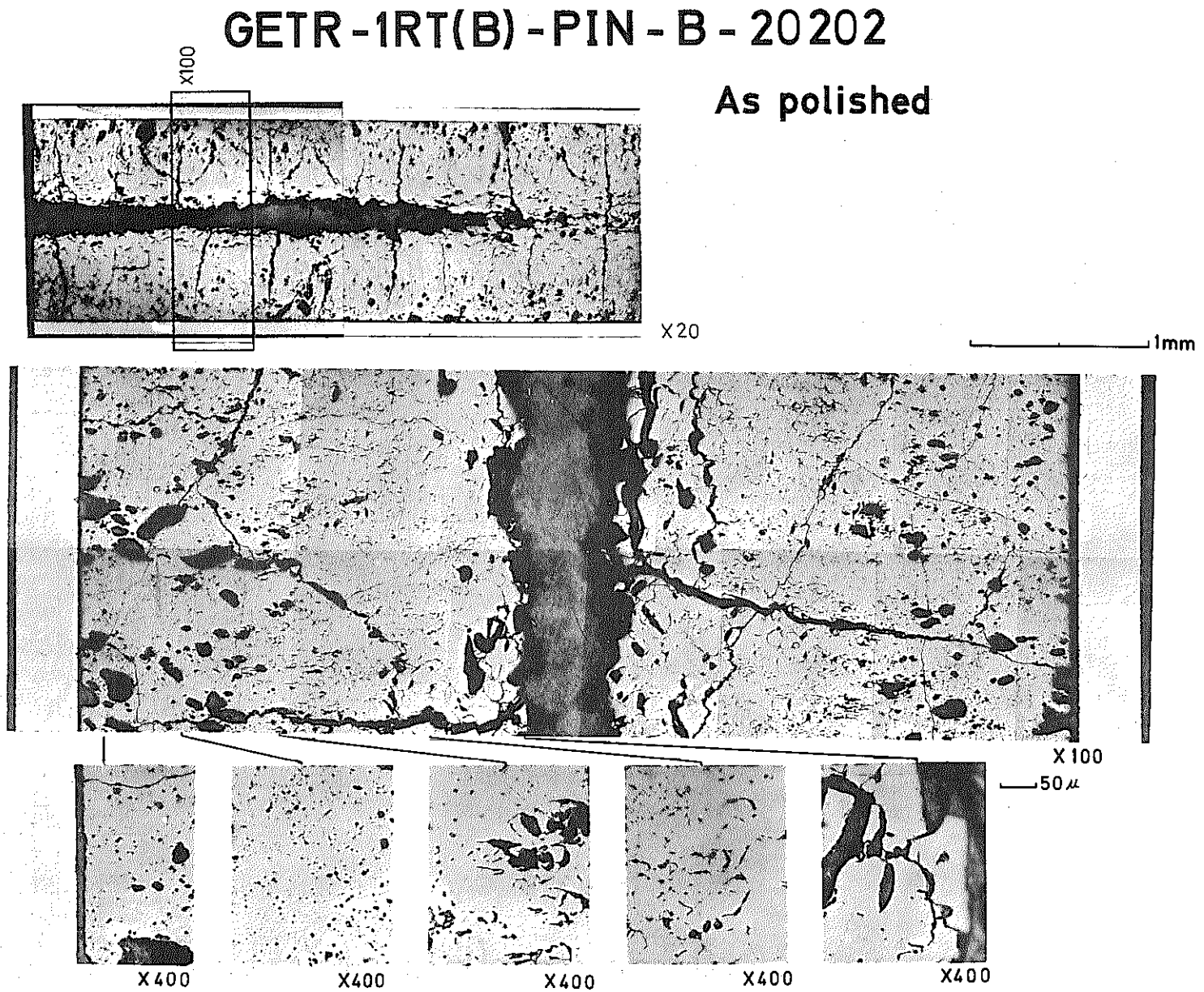

Photograph 5. Metallographic photograph, Specimen 20202

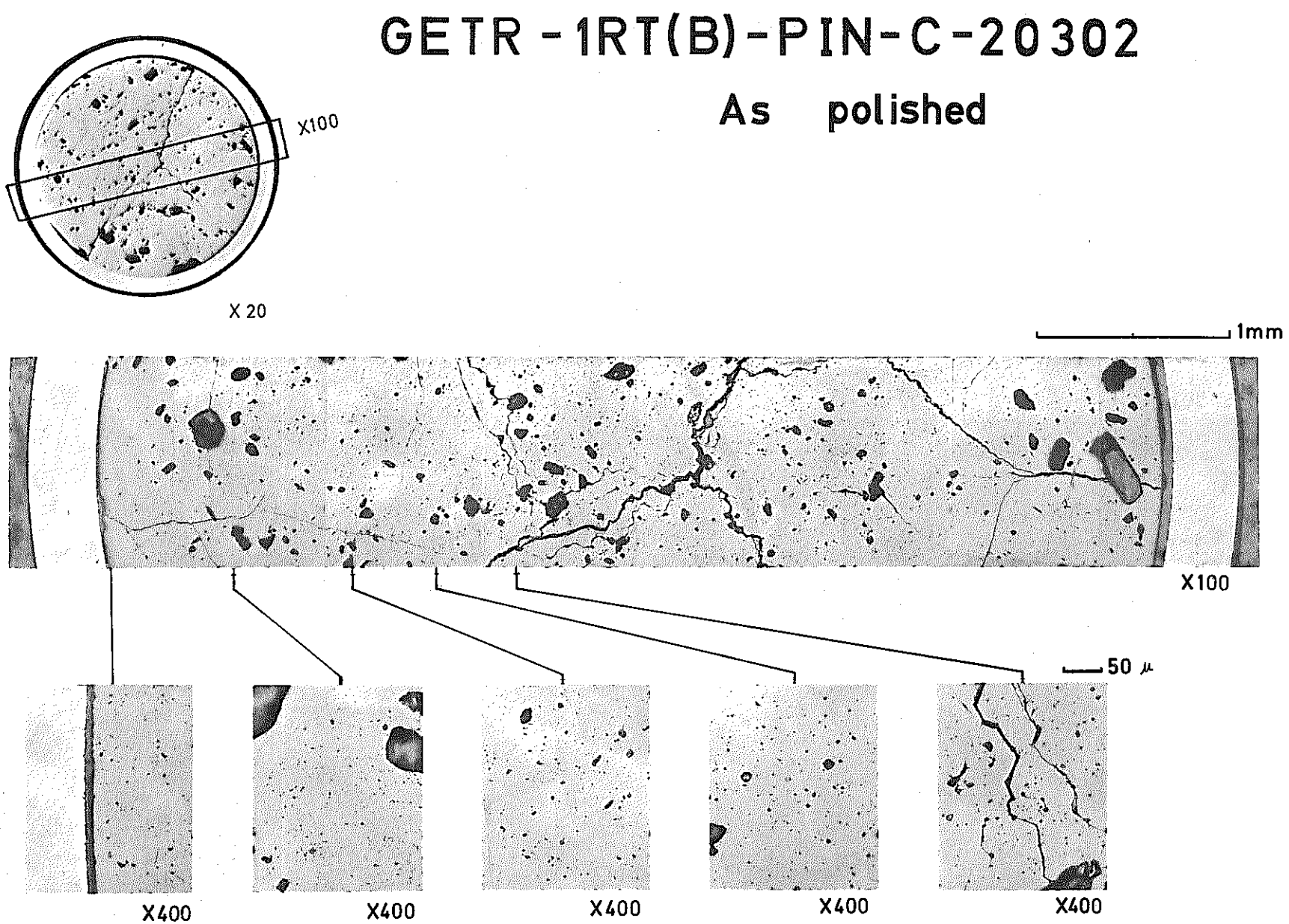

Photograph 6. Metallographic photograph, Specimen 20302

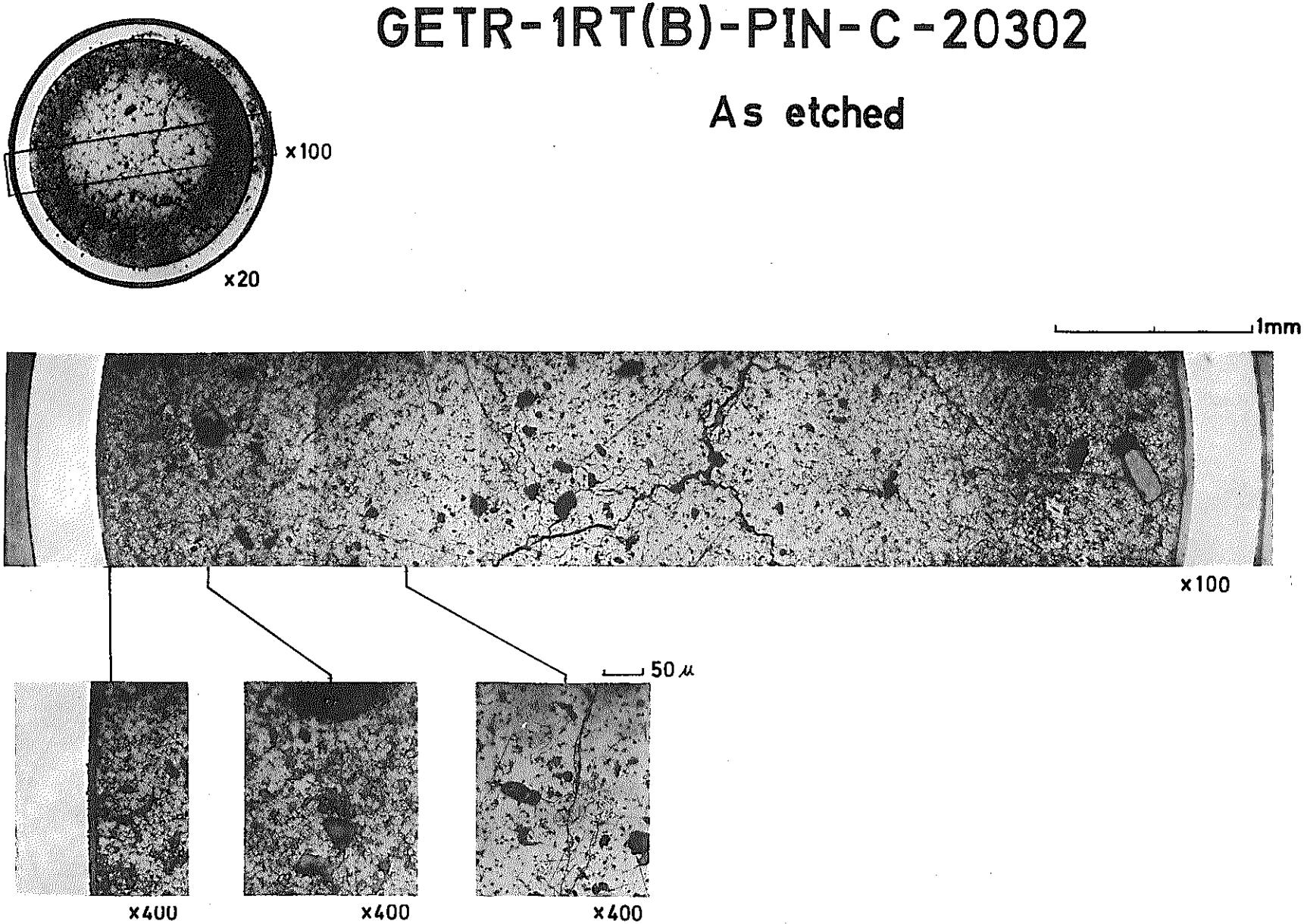

Photograph 7. Metallographic photograph, Specimen 20302

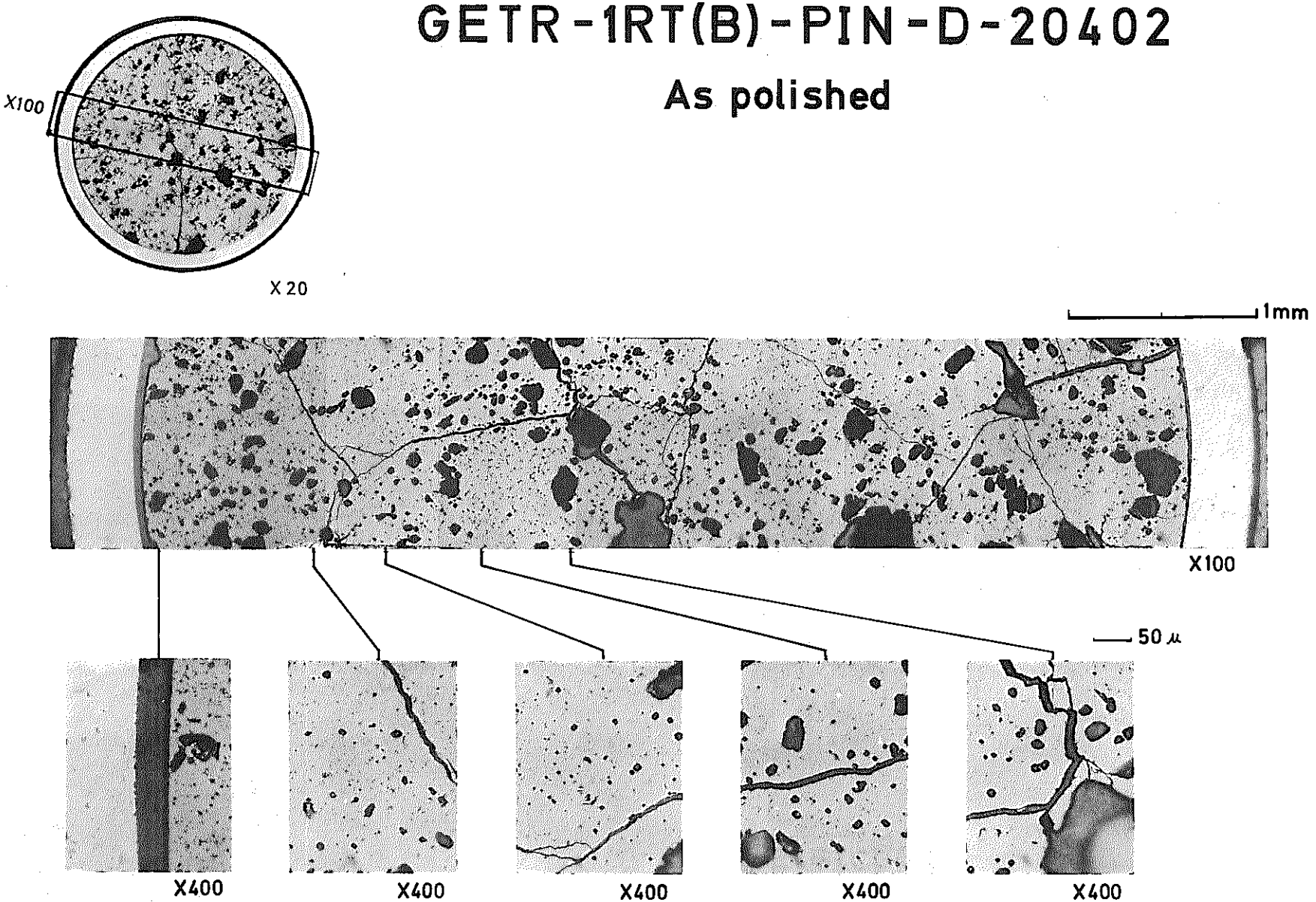

Photograph 8. Metallographic photograph, Specimen 20402

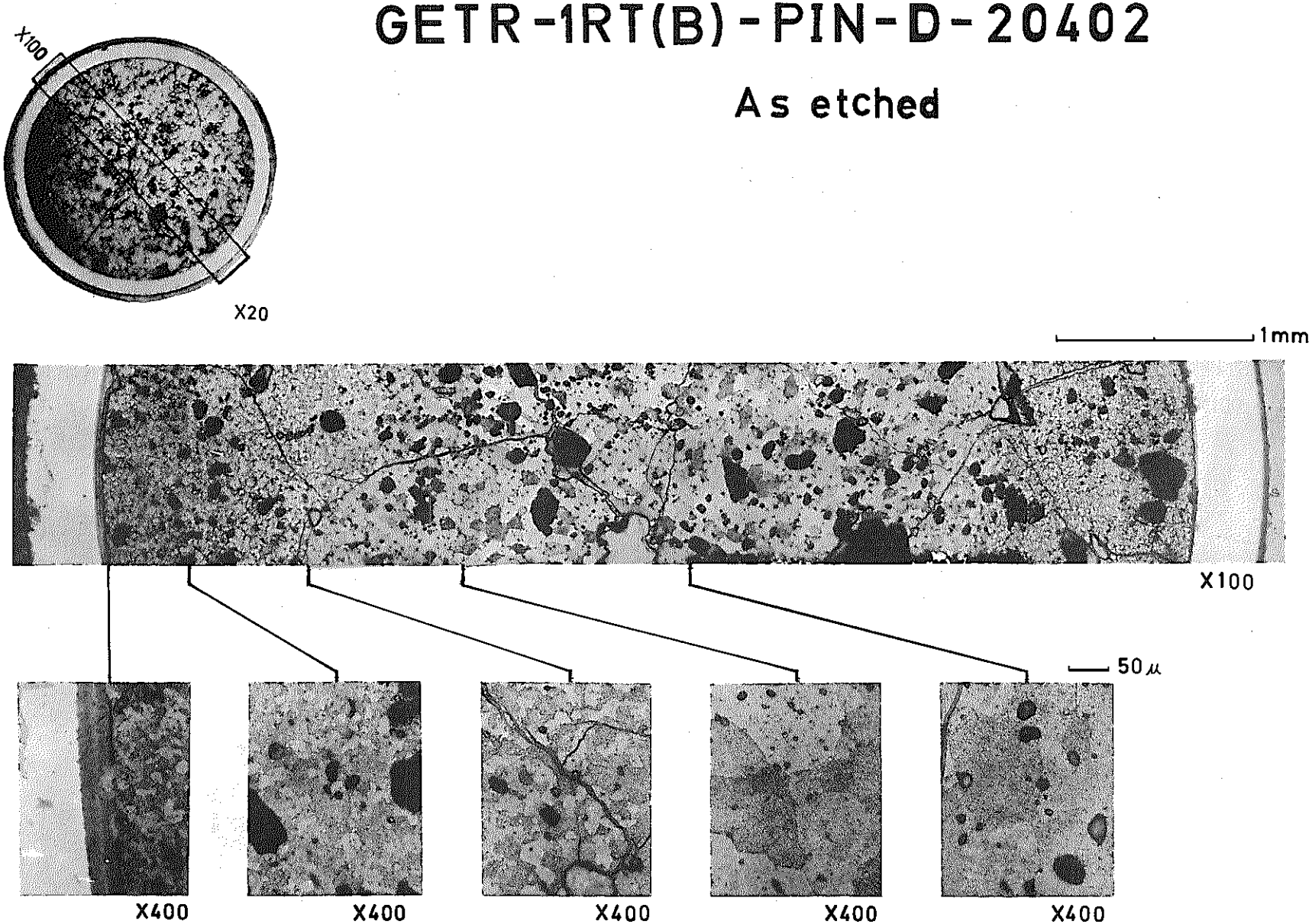

Photograph 9. Metallographic photograph, Specimen 20402

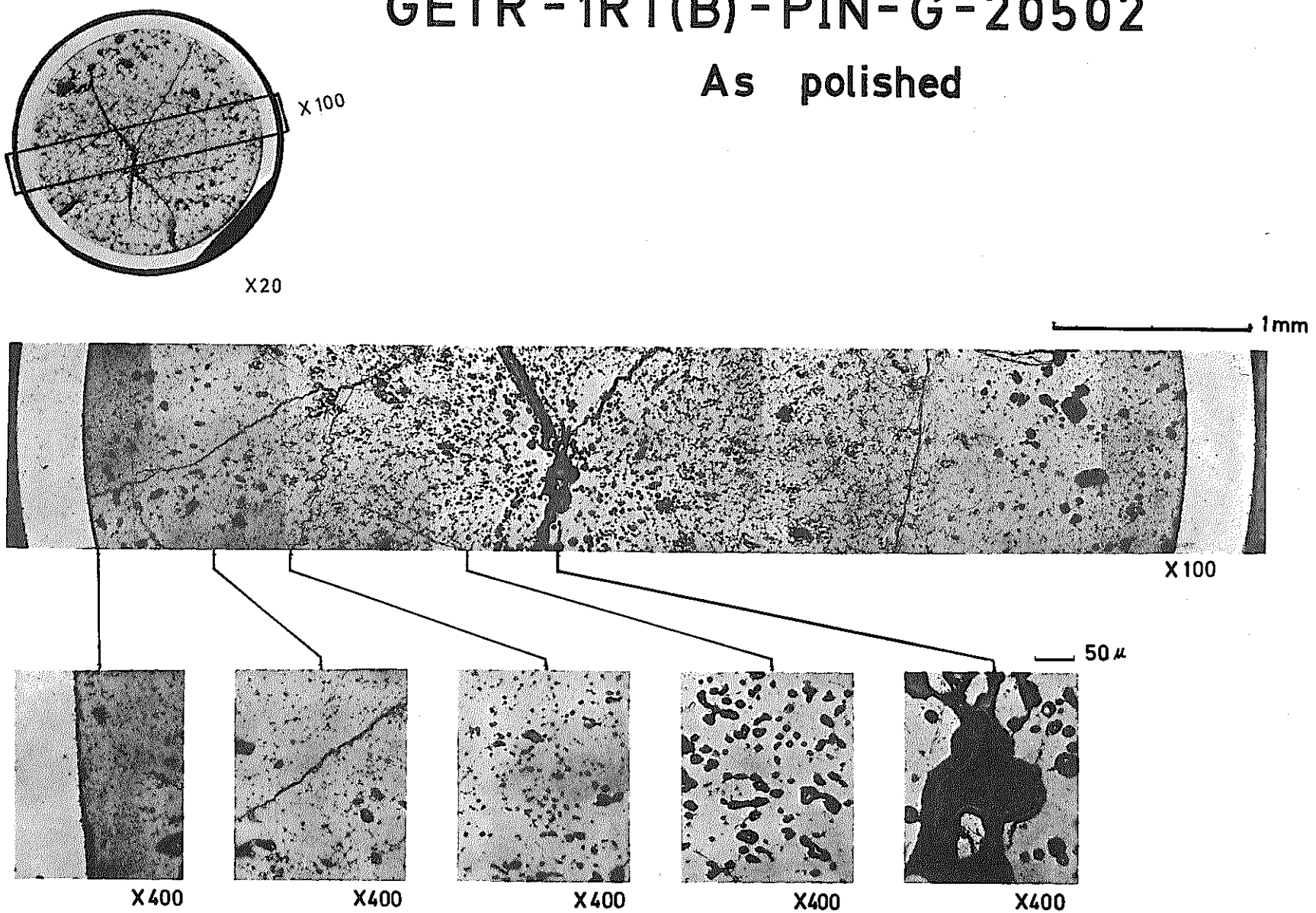

Photograph 10. Metallographic photograph, Specimen 20502

GETR-1RT(B)-PIN-E-20502

As etched

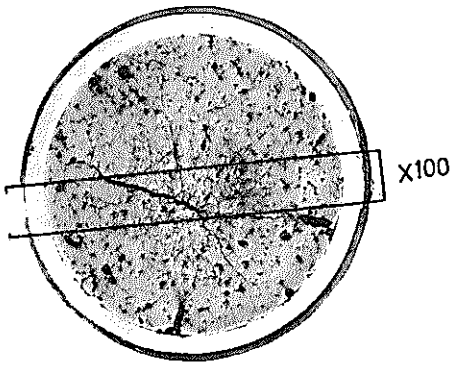

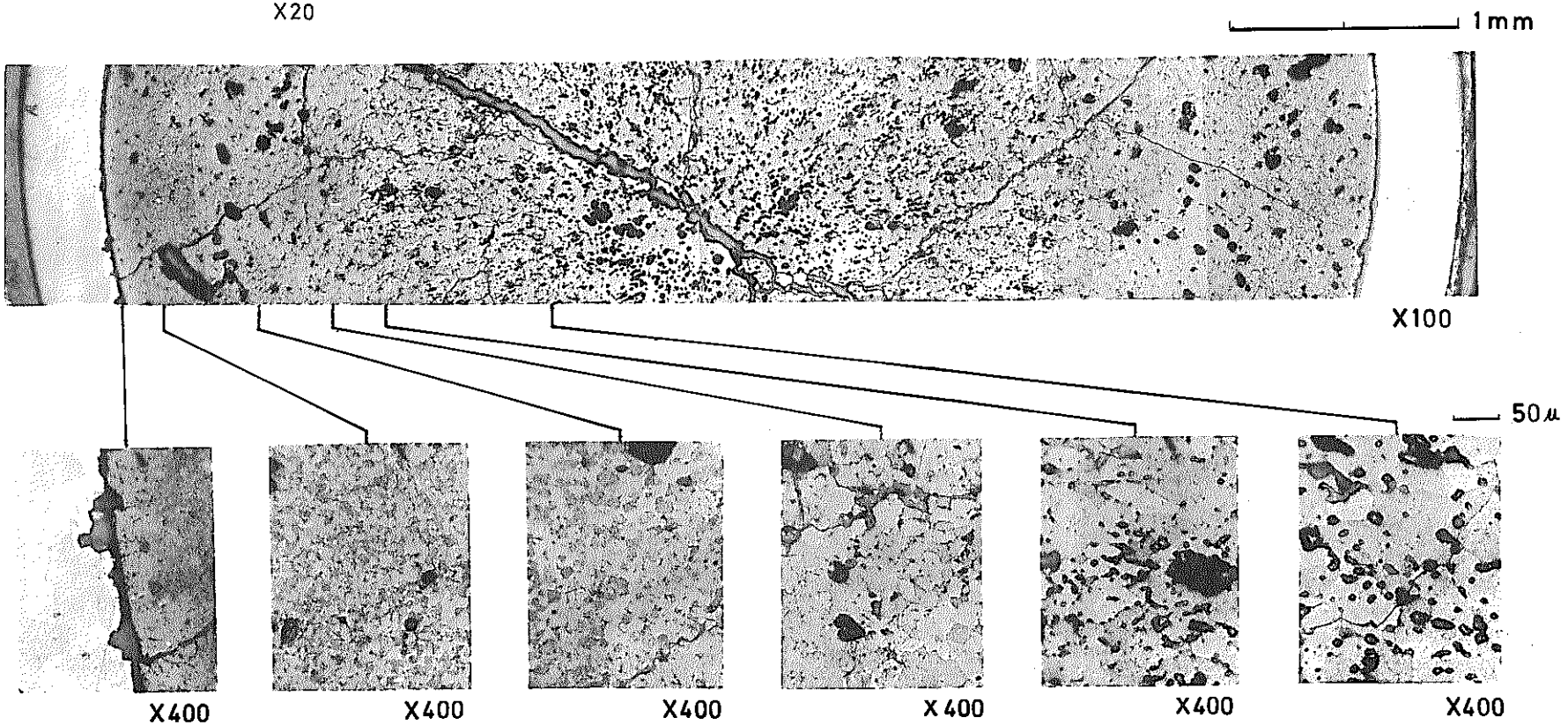

Photograph 11. Metallographic photograph, Specimen 20502

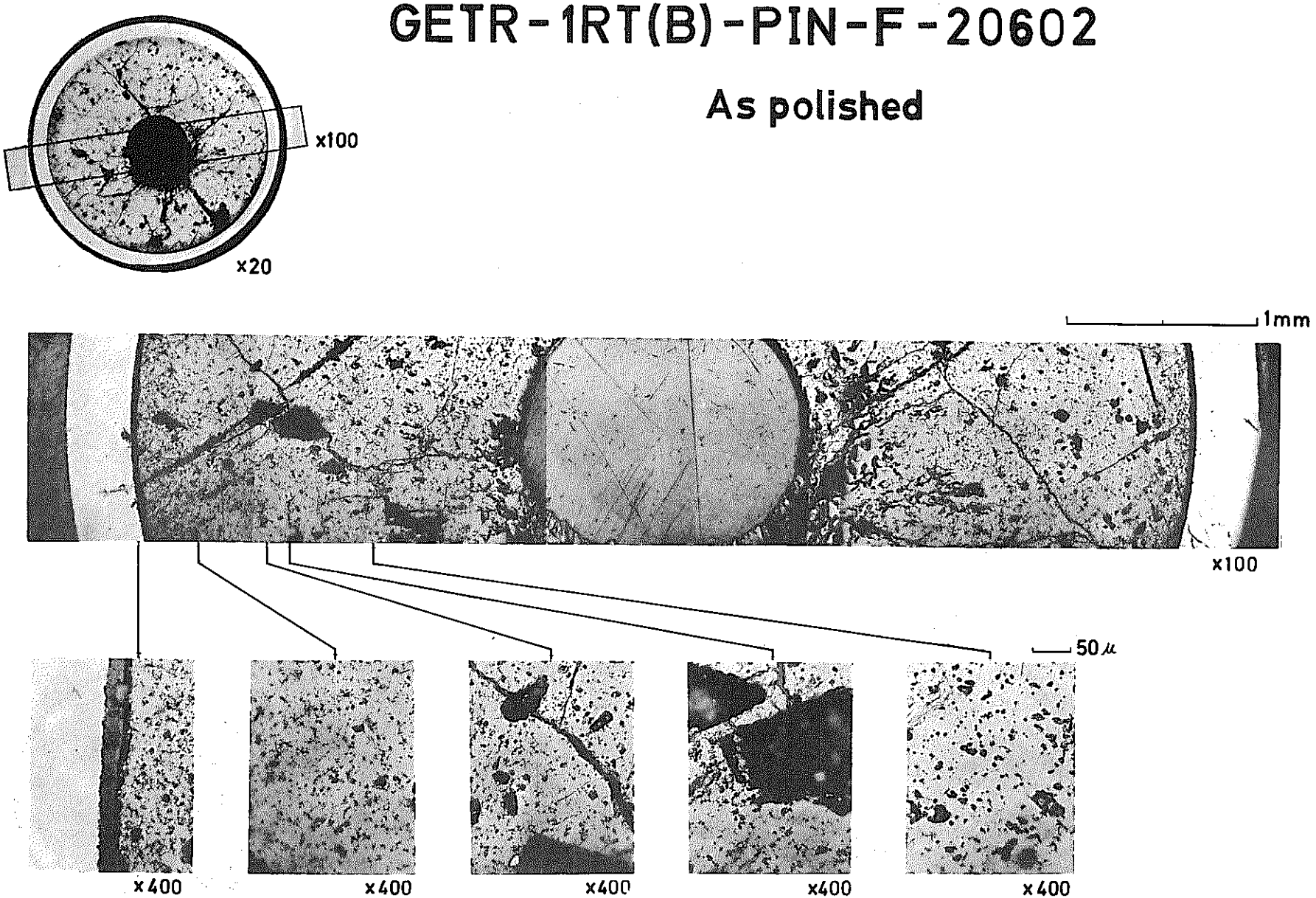

Photograph 12. Metallographic photograph, Specimen 20602

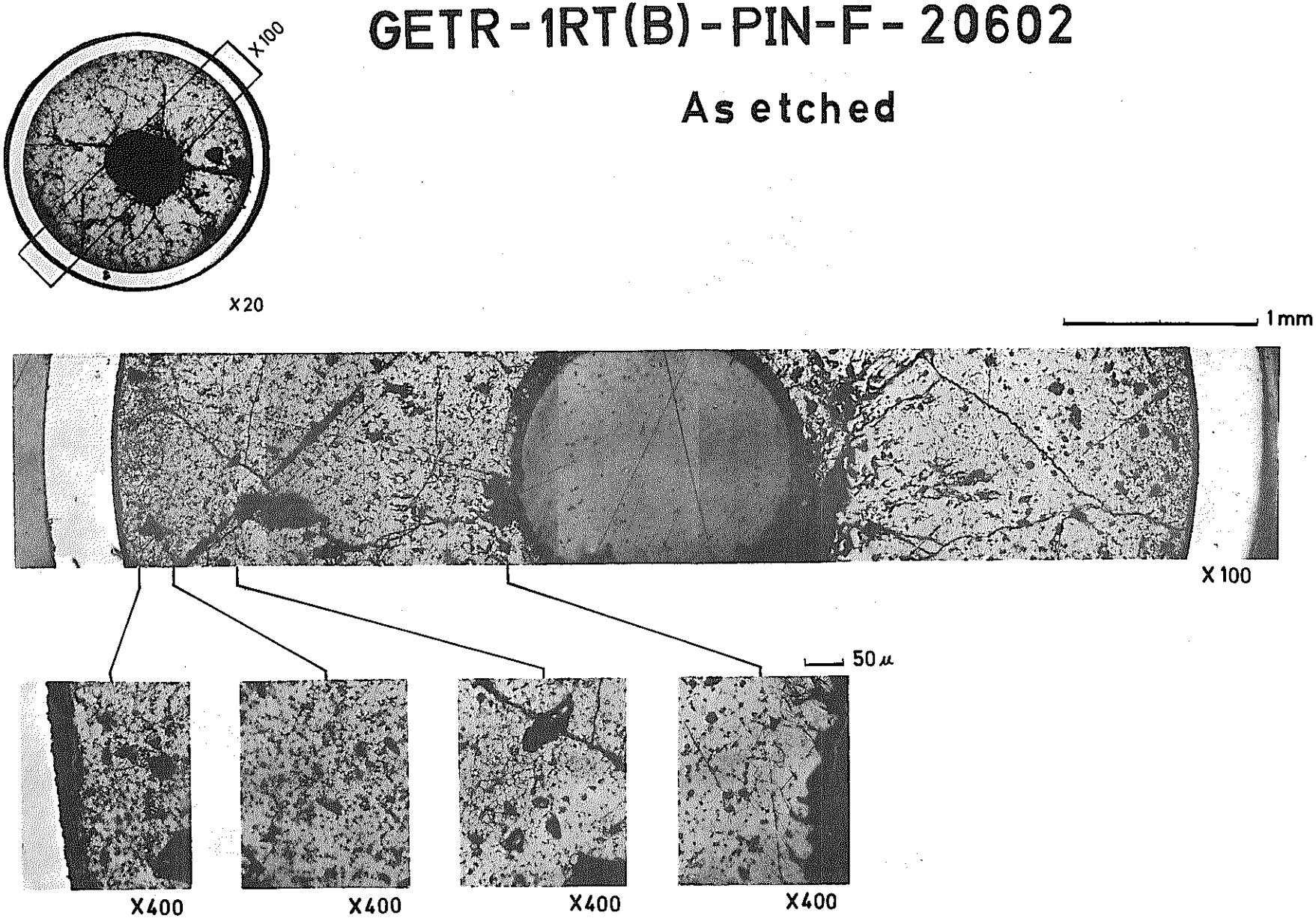

Photograph 13. Metallographic photograph, Specimen 20602

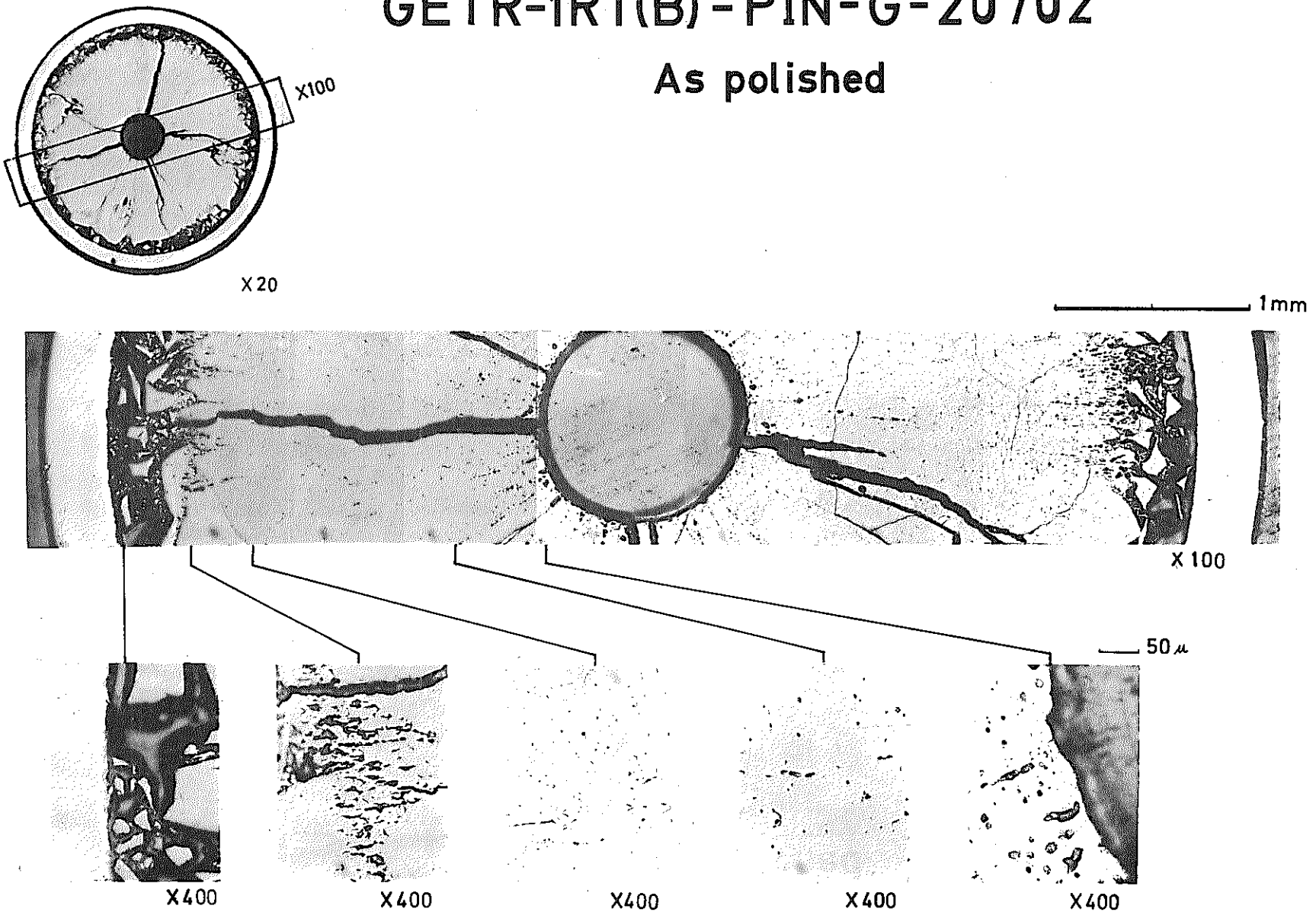

Photograph 14. Metallographic photograph, Specimen 20702

GETR-1RT(B)-PIN-20702

As etched

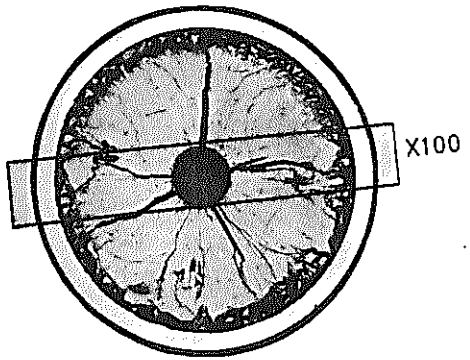

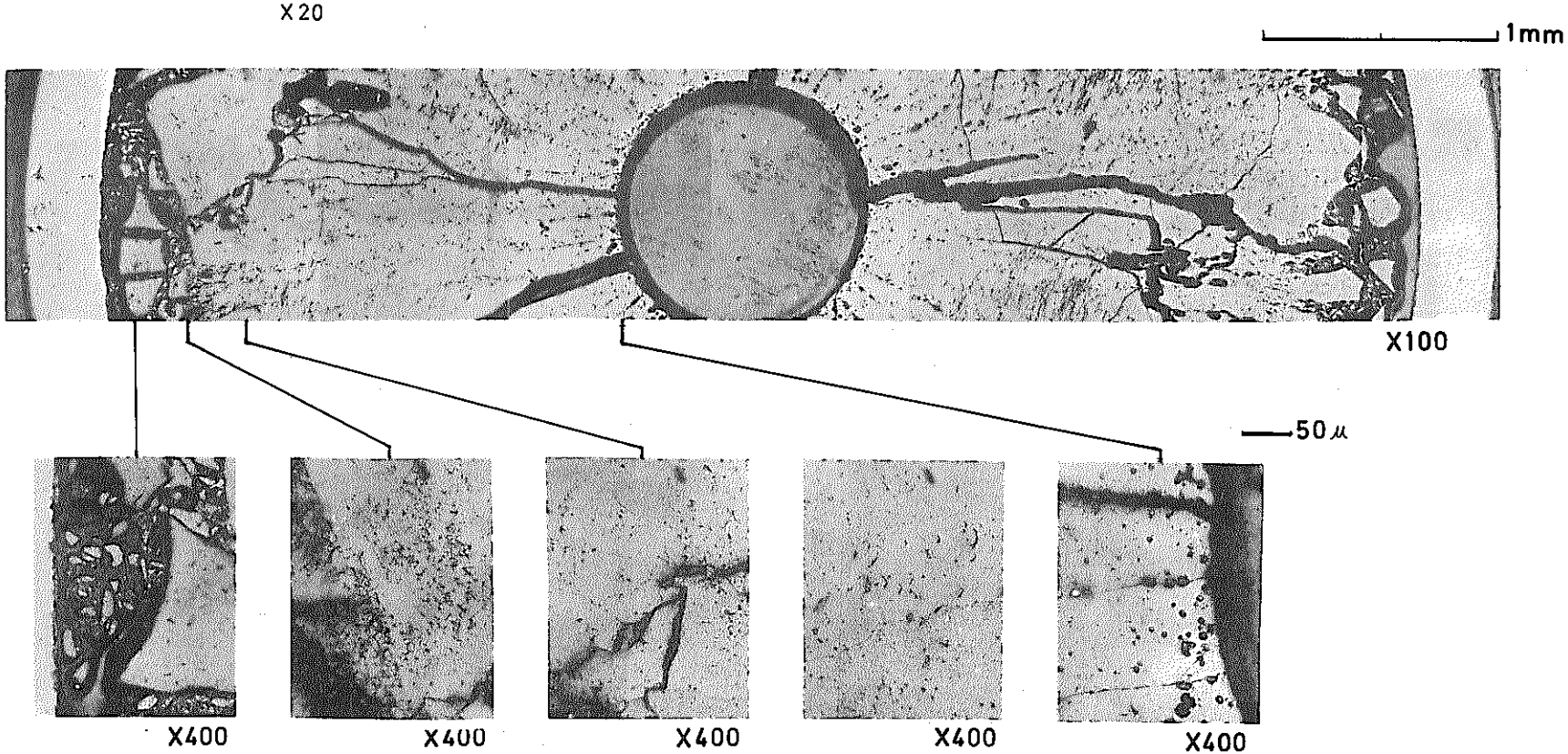

Photograph 15. Metallographic photograph, Specimen 20702

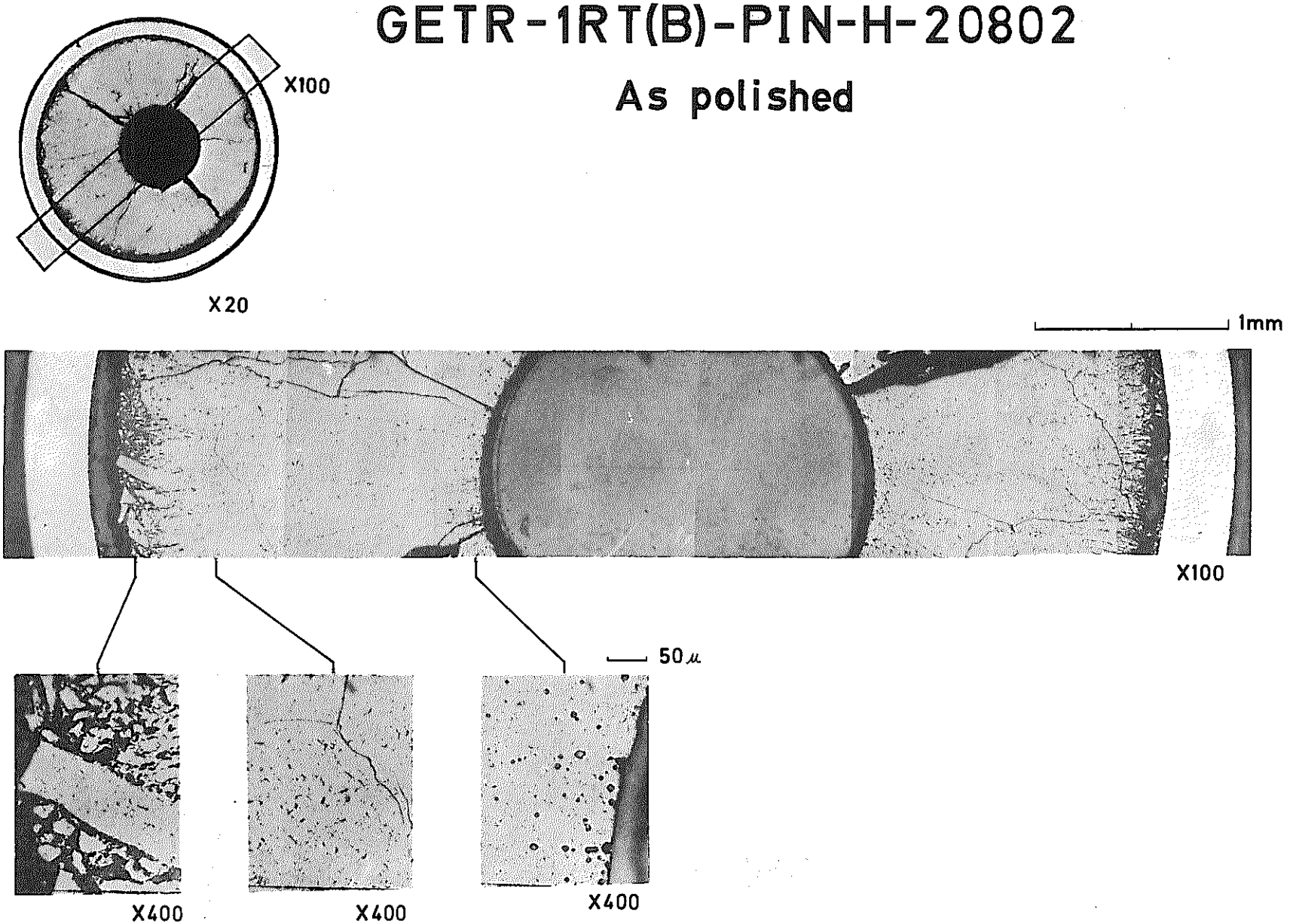

Photograph 16. Metallographic photograph, Specimen 20802

GETR-1RT(B)-PIN-20802

As etched

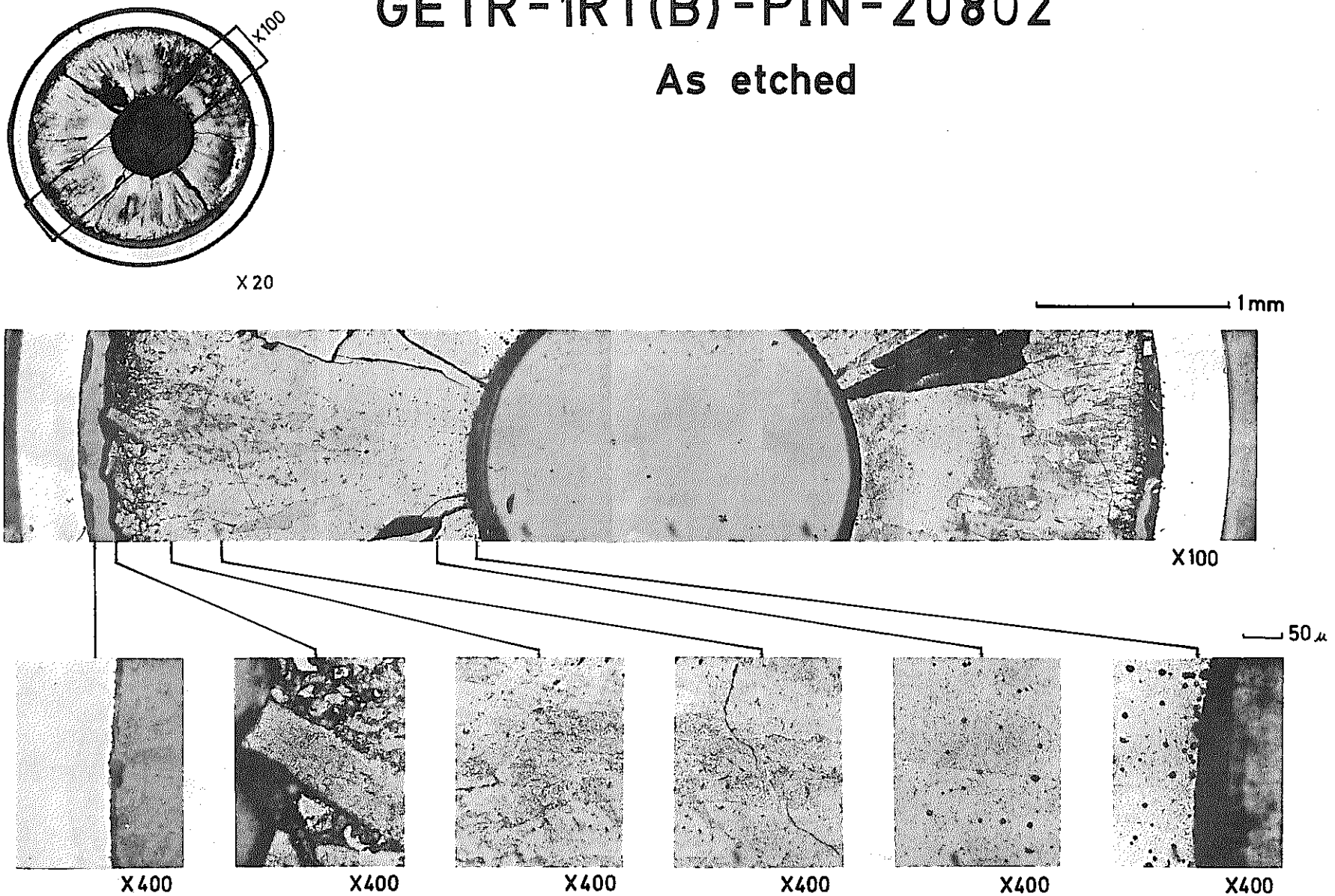

Photograph 17. Metallographic photograph, Specimen 20802

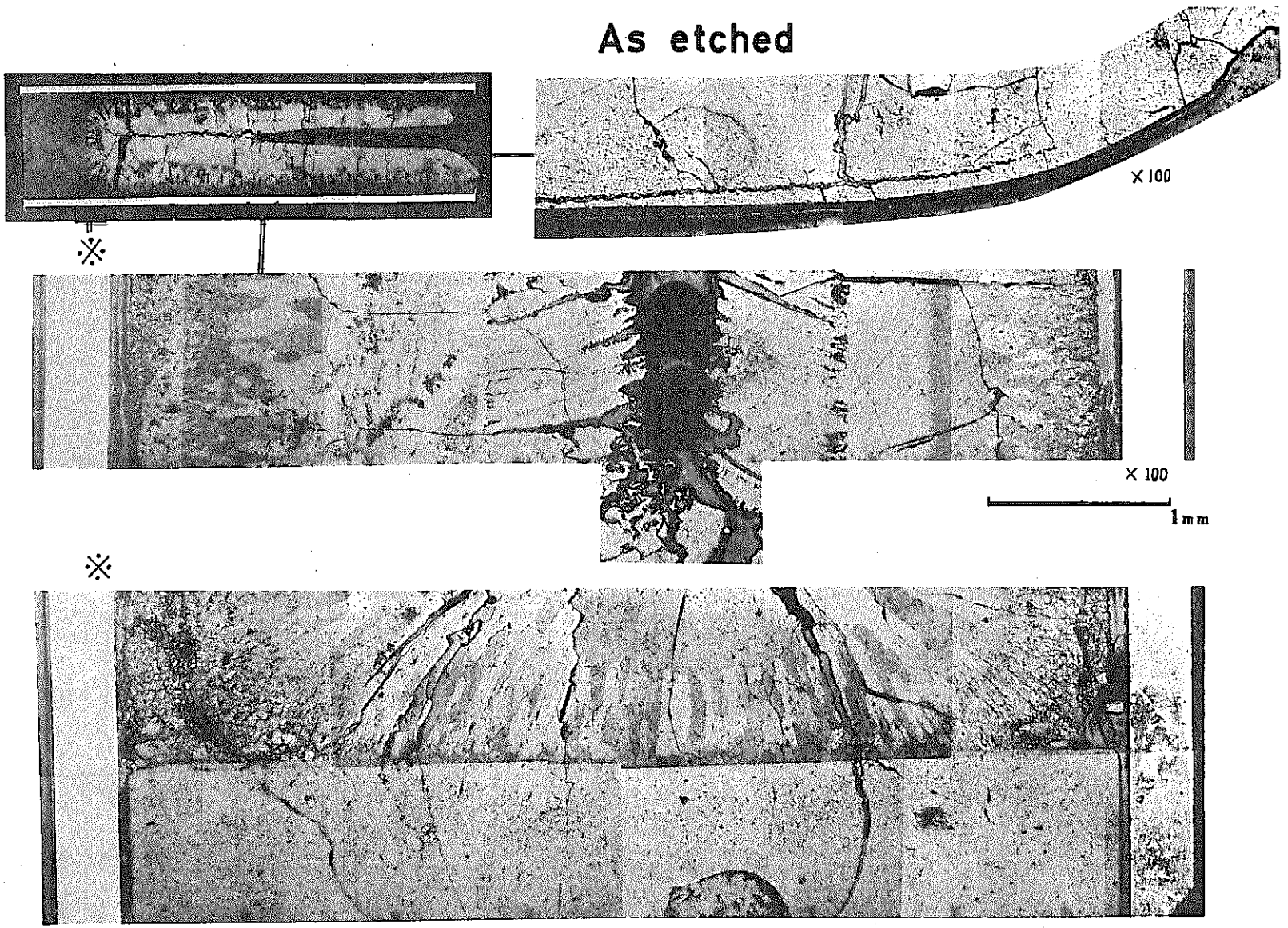

Photograph 18. Metallographic photograph, Specimen 20803

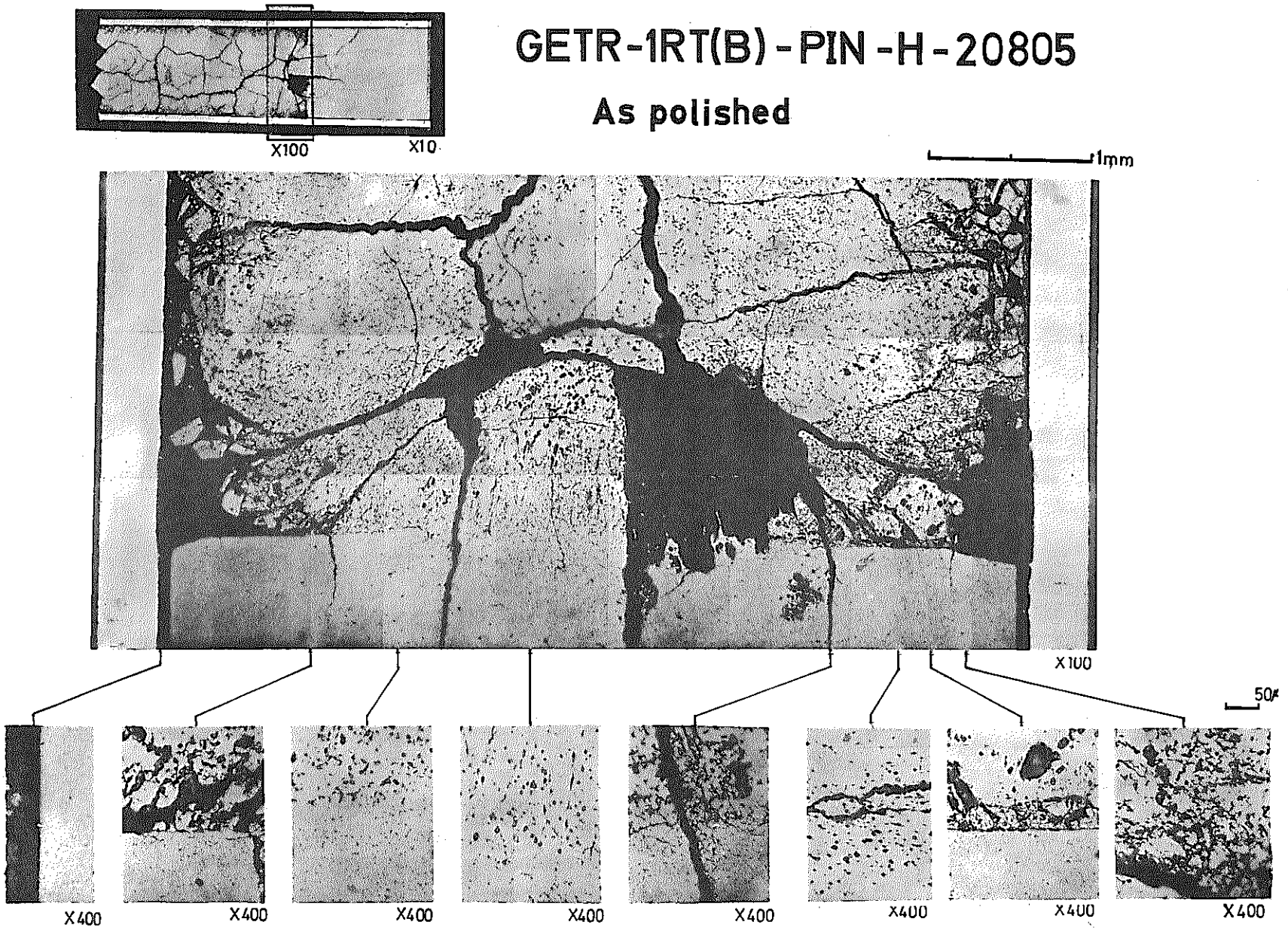

Photograph 19. Metallographic photograph, Specimen 20805

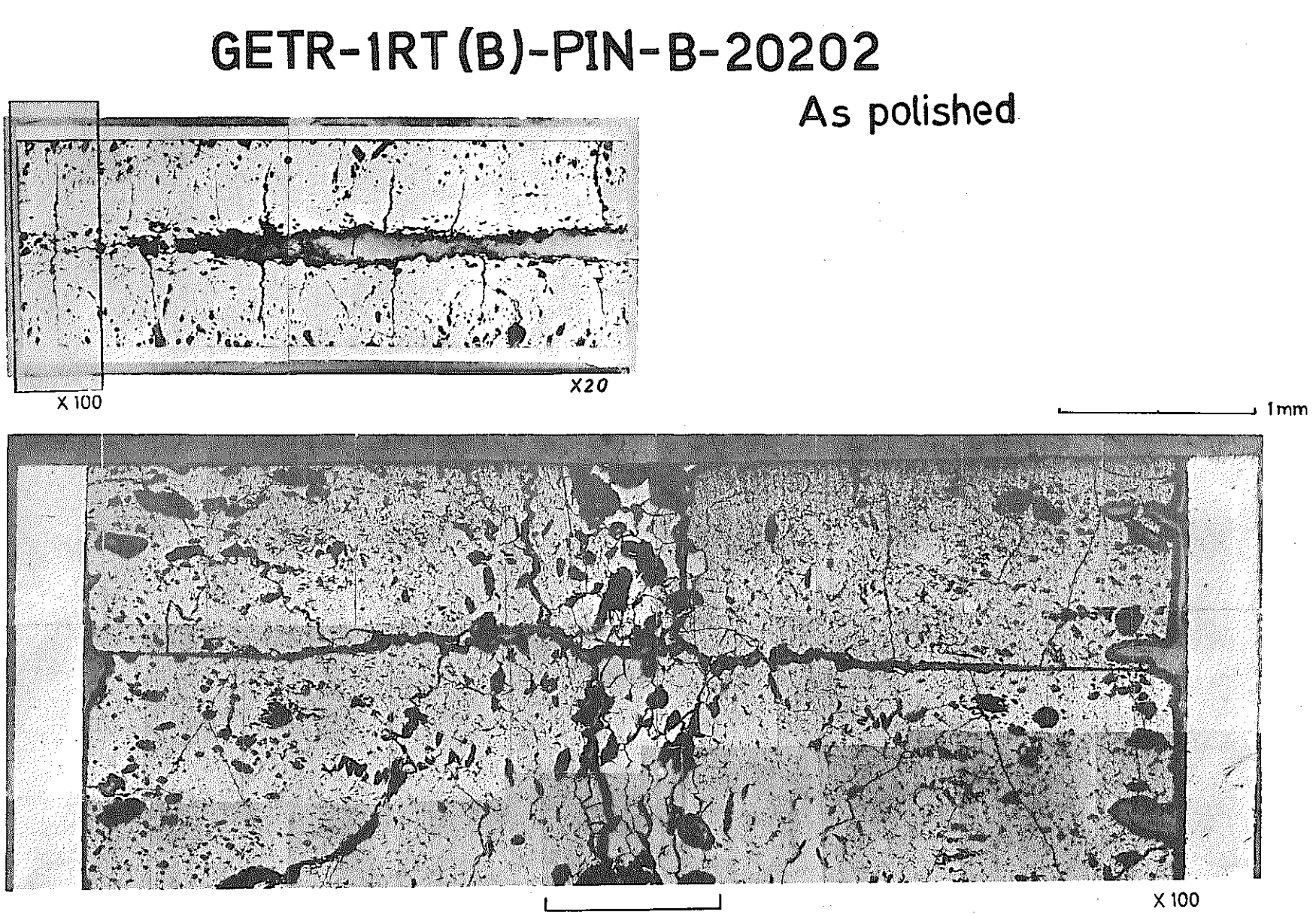

Photograph 20. Metallographic photograph, Specimen 20202

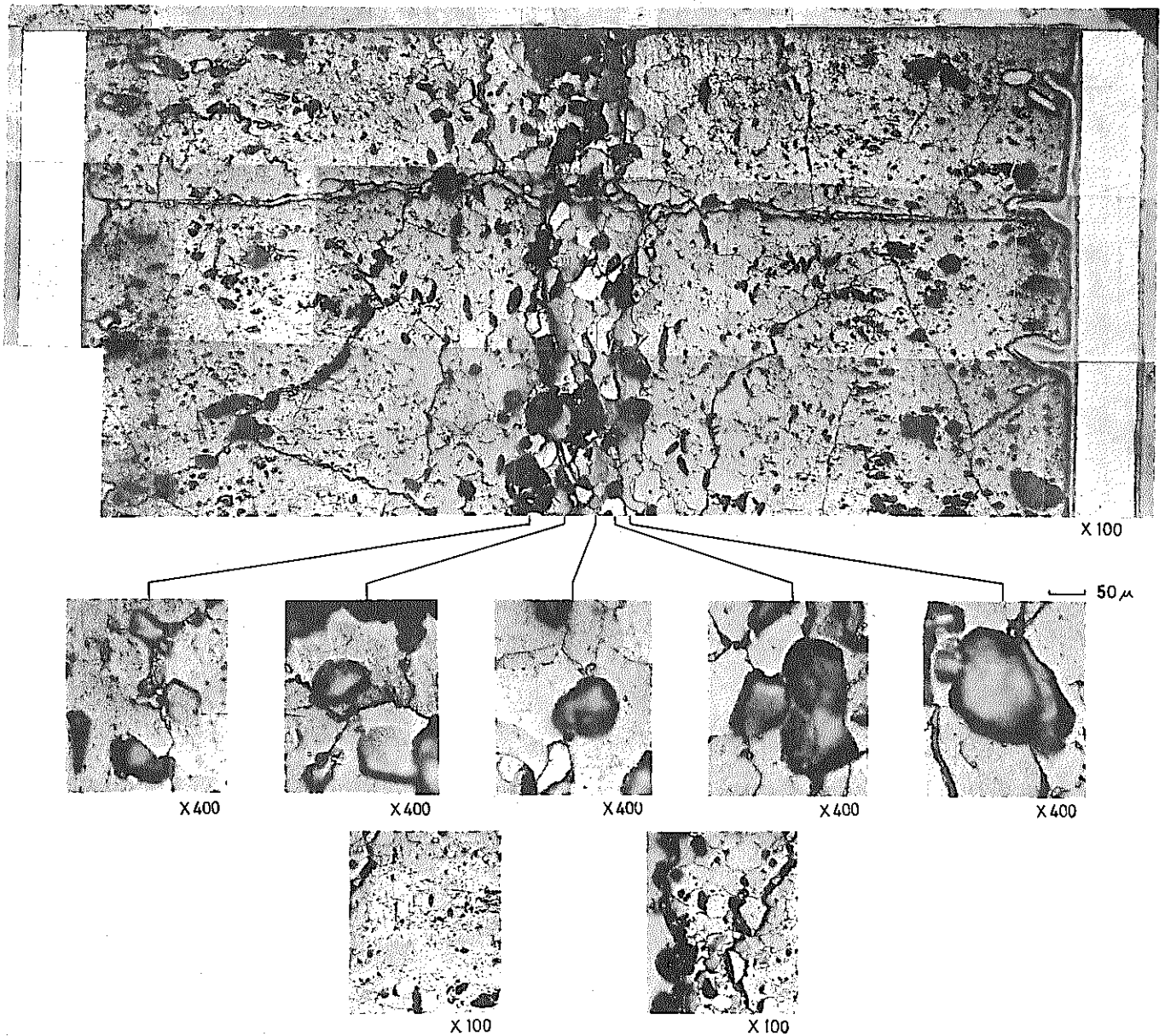

Photograph 21. Metallographic photograph, Specimen 20202

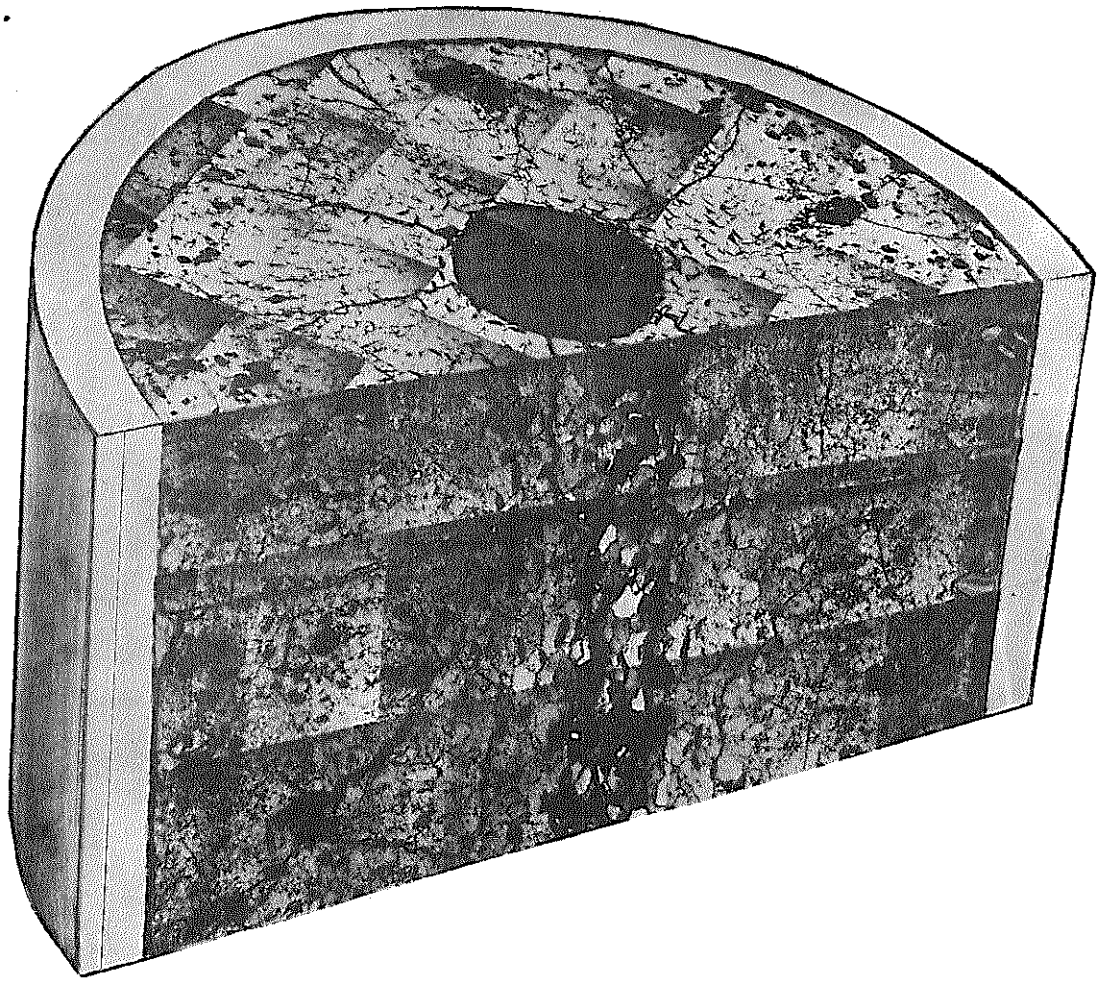

PHTOMICROGRAPH OF CROSS - SECTION (AS ETCHED)

Photograph 22. Stereogram, Specimen 20202

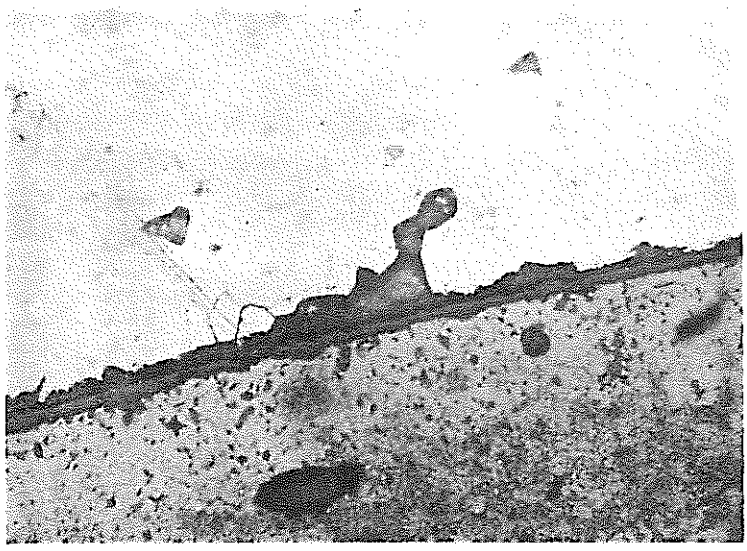

As polished 50 μ

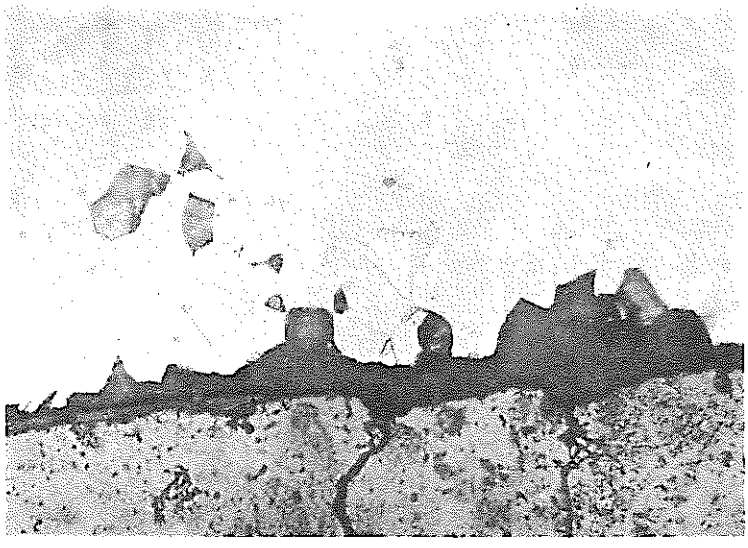

As polished 50 μ

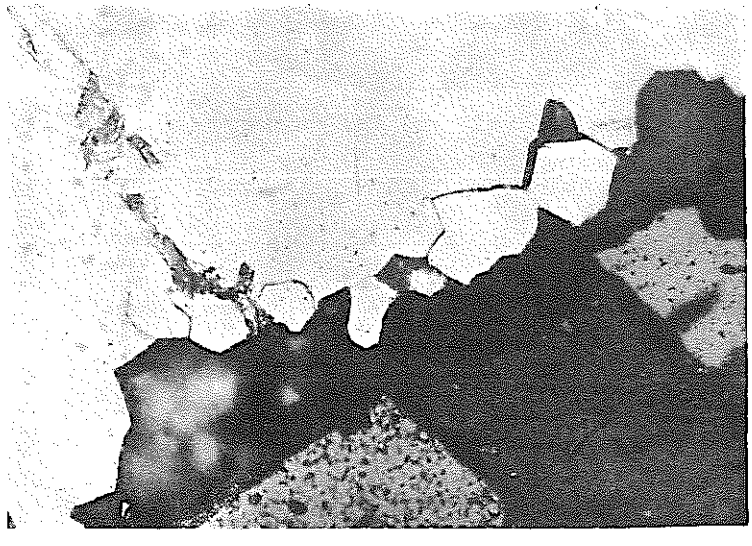

As polished 50 μ

Photograph 23. Damage to inner surface of cladding tube Pin-E-20502

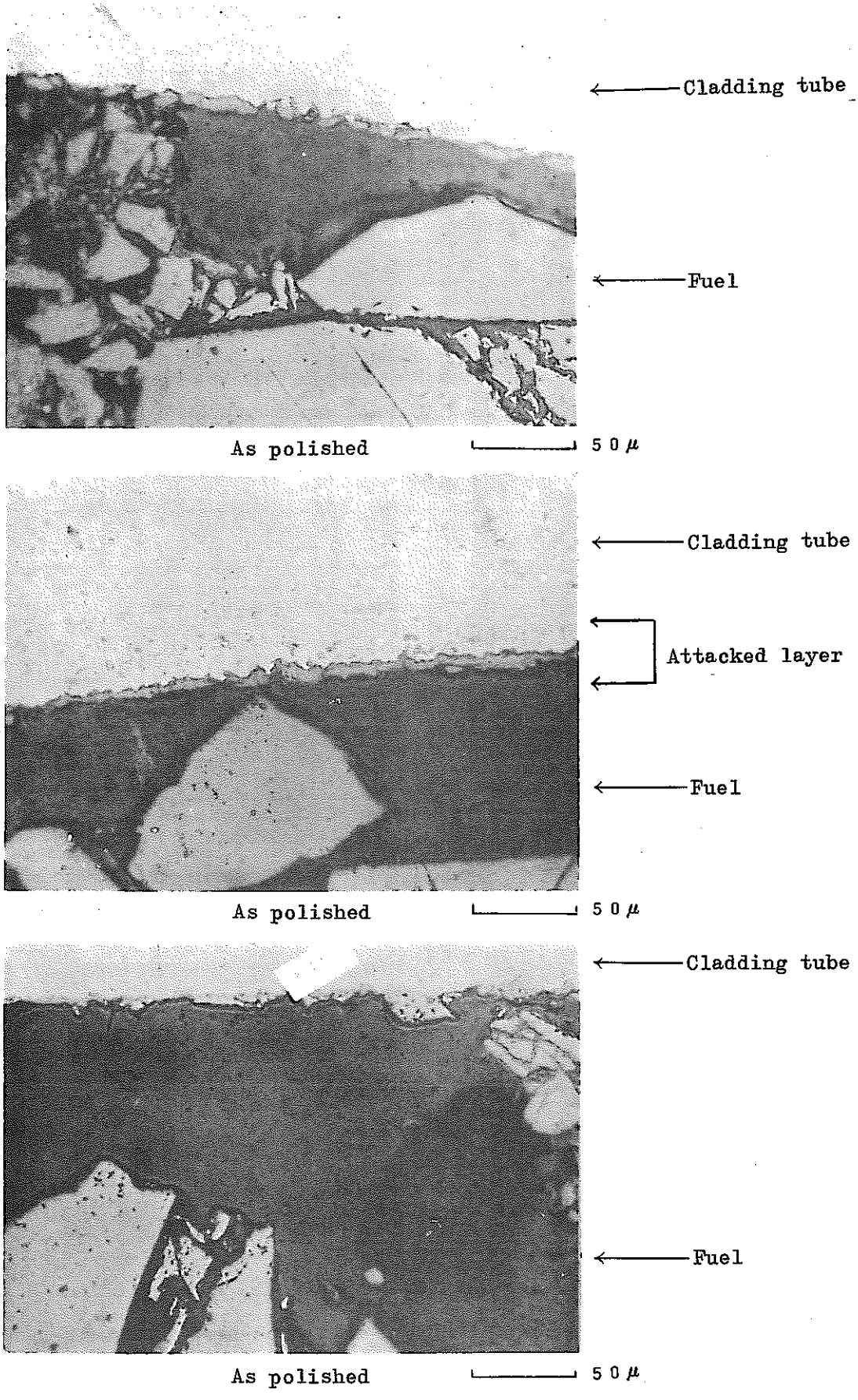

Photograph 24. Damage to inner surface of cladding tube Pin G 20702

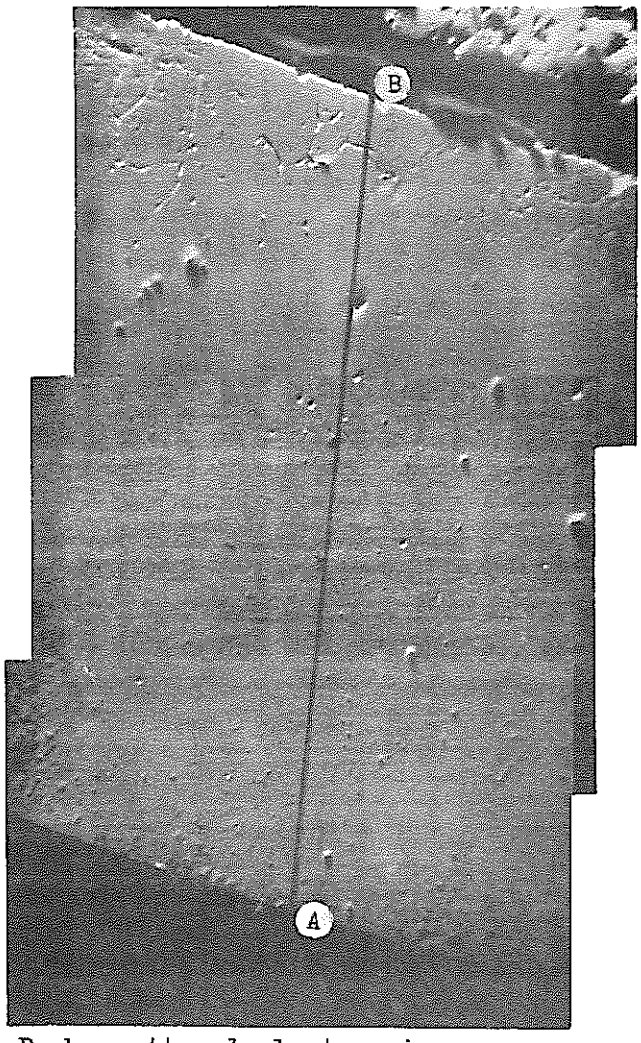

Back scattered electron image × 300 of the area where line analysis was performed (A → B).

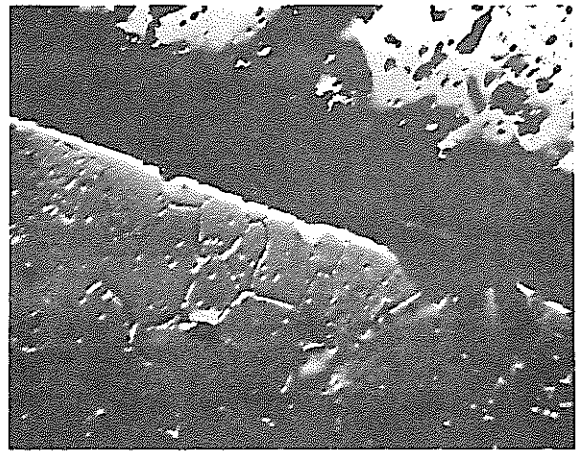

Back scattered electron image × 500

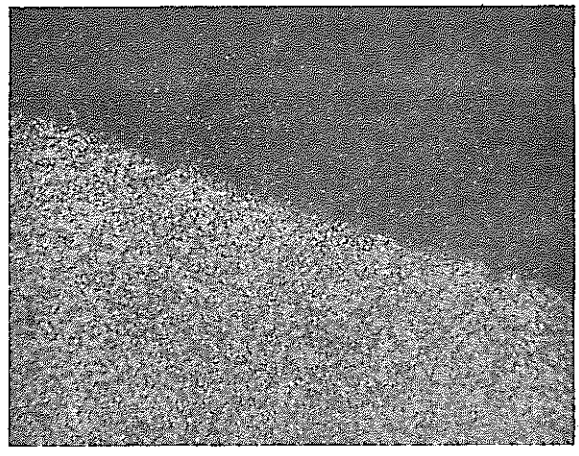

Fe X-ray display × 500

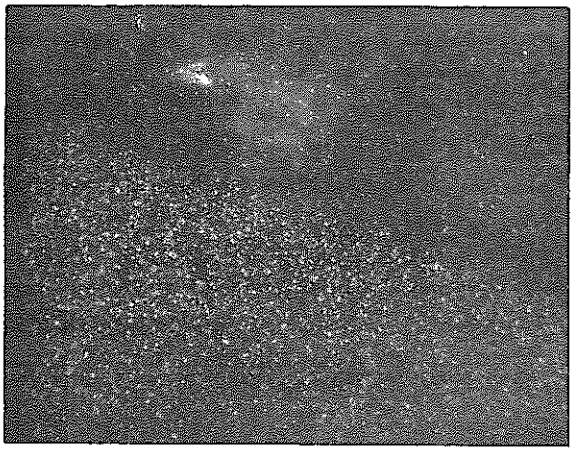

Cr X-ray display × 500

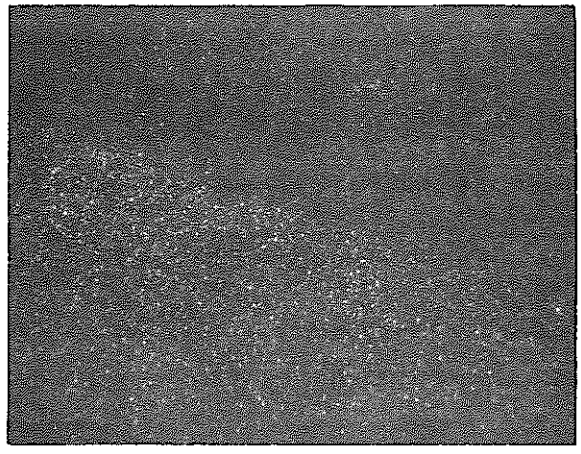

Ni X-ray display × 500

Photograph 25. Plane analysis of Specimen 20102
(Gap region between fuel and cladding tube)

Mo X-ray display × 500

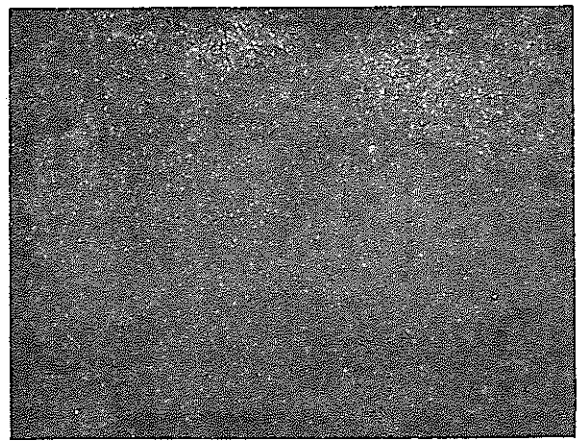

U X-ray display × 500

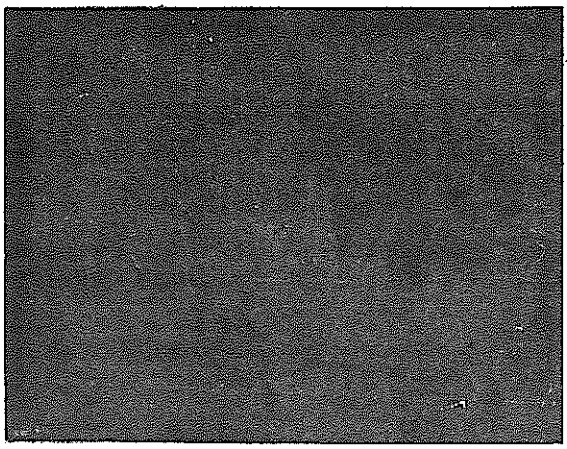

Pu X-ray display × 500

Photograph 25. Plane analysis of Specimen 20102
(Gap region between fuel and cladding tube)

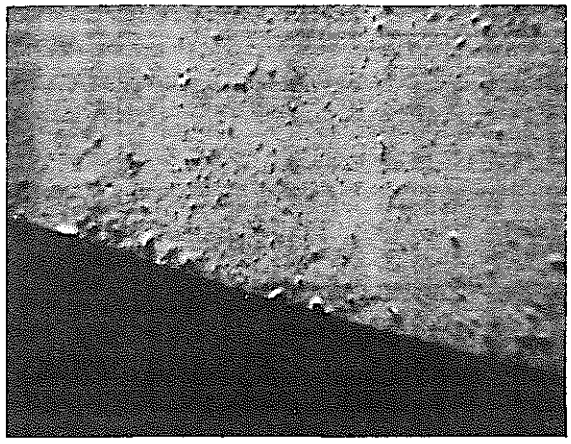

Back scattered electron image × 500

Fe X-ray display × 500

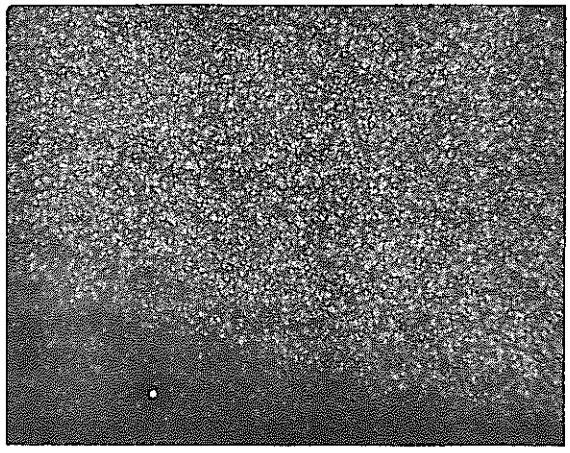

Cr X-ray display × 500

Ni X-ray display × 500

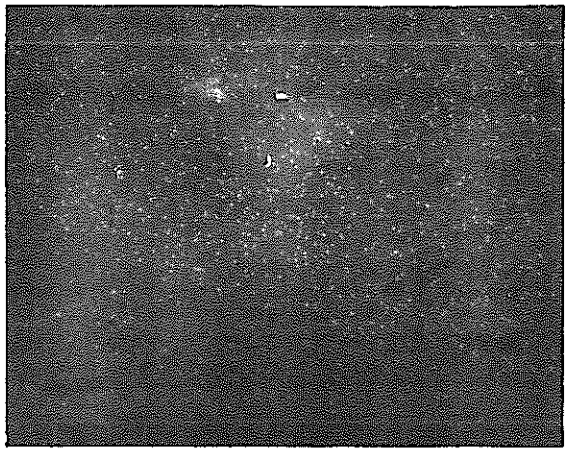

Mo X-ray display × 500

Photograph 26. Plane analysis of Specimen 20102 (Outer surface of cladding tube)

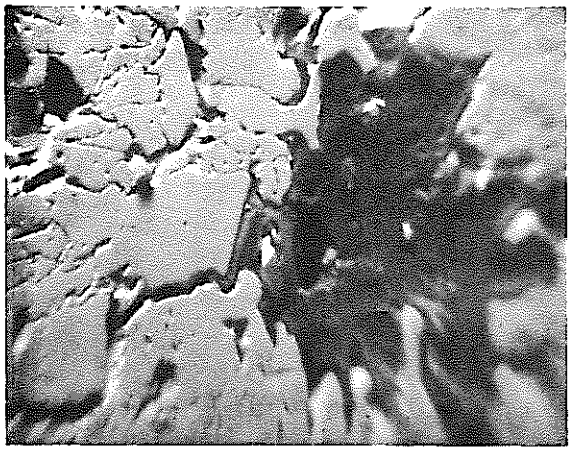

Back scattered electron image × 100

Back scattered electron image × 300

U X-ray display × 300

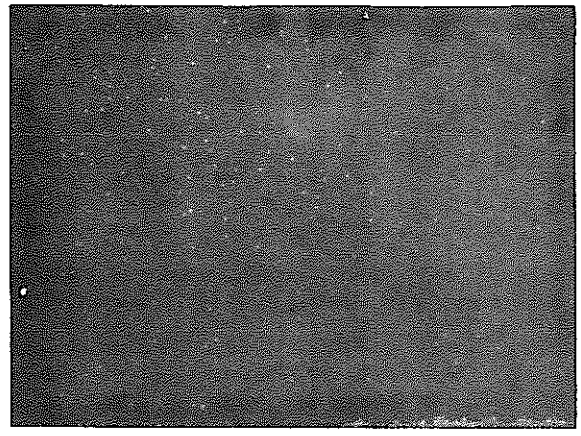

Pu X-ray display × 300

Photograph 27. Plane analysis of Specimen 20102
(Central part of fuel)

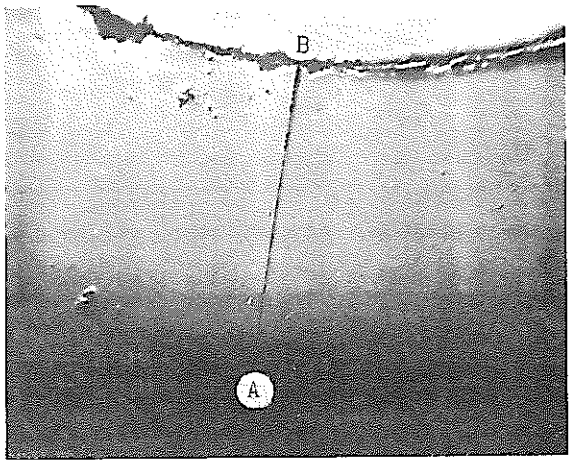

Back scattered electron image × 100
of the area where line analysis was performed (A → B).

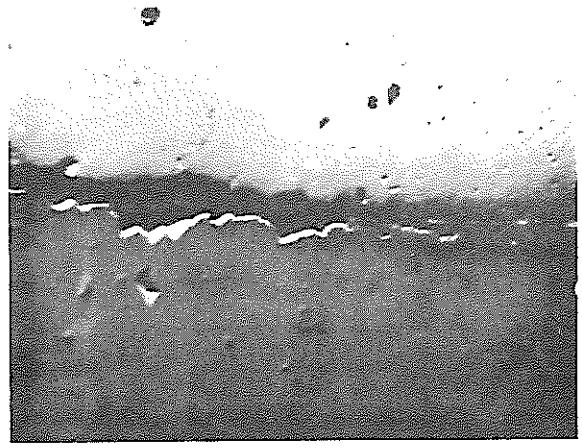

Back scattered electron image × 300

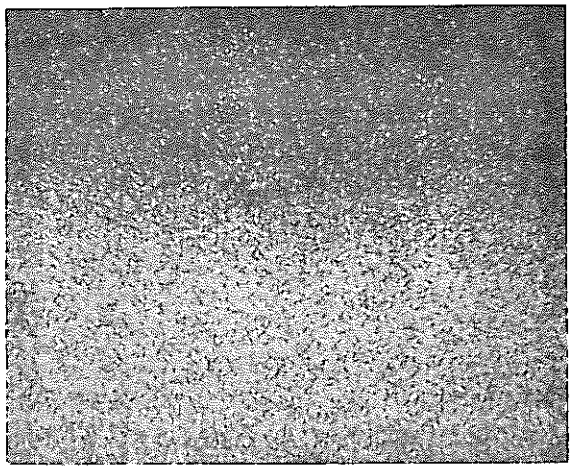

Fe X-ray display × 300

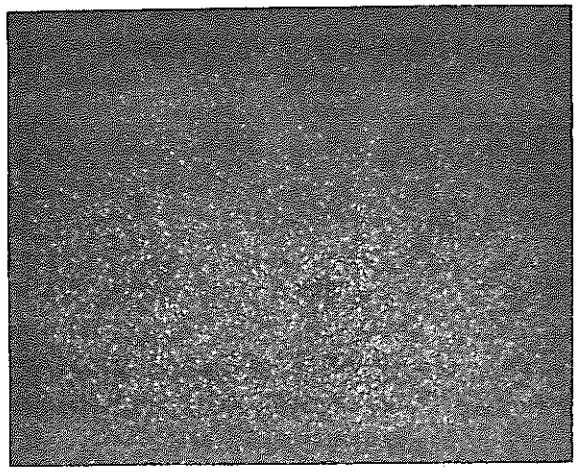

Cr X-ray display × 300

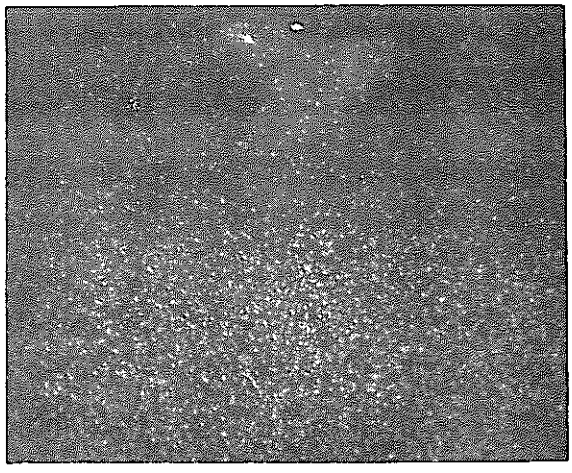

Ni X-ray display × 300

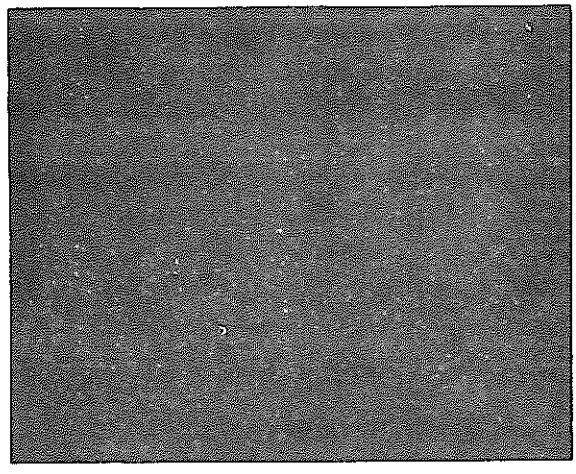

Mo X-ray display × 300

Photograph 28. Plane analysis of Specimen 20502
(Gap region between fuel and cladding tube)

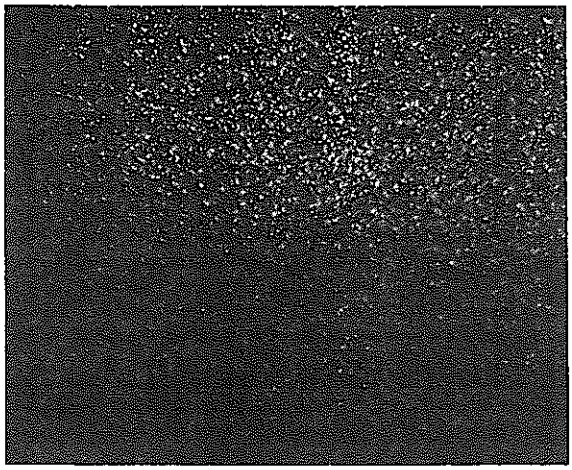

U X-ray display ×300

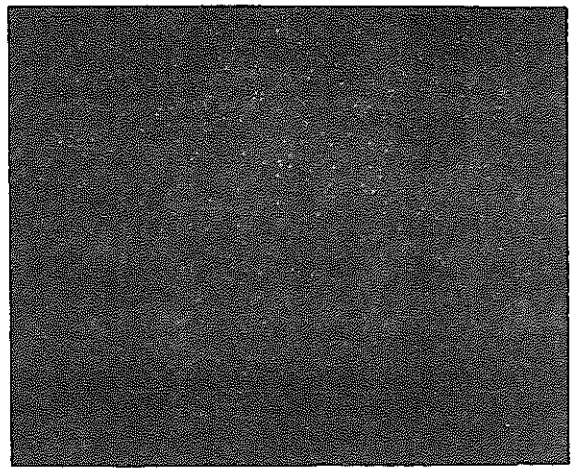

Pu X-ray display ×300

Photograph 28. Plane analysis of Specimen 20502
(Gap region between fuel and cladding tube)

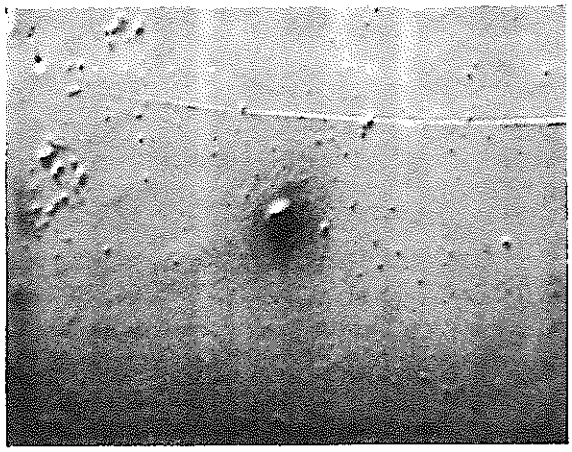

Back scattered electron image × 500

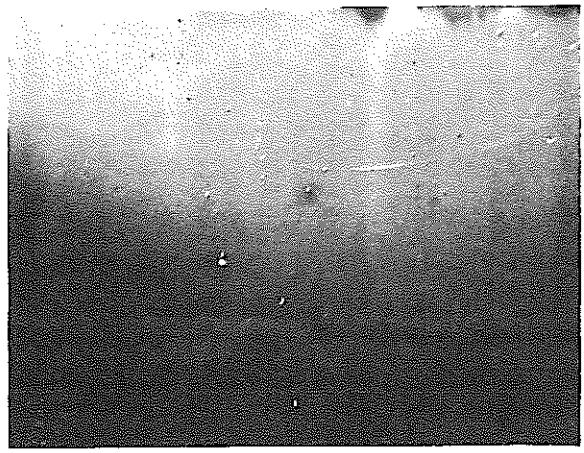

Back scattered electron image × 100

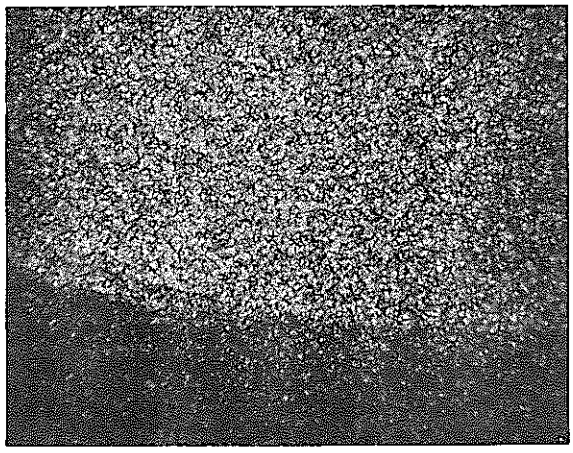

Fe X-ray display × 100

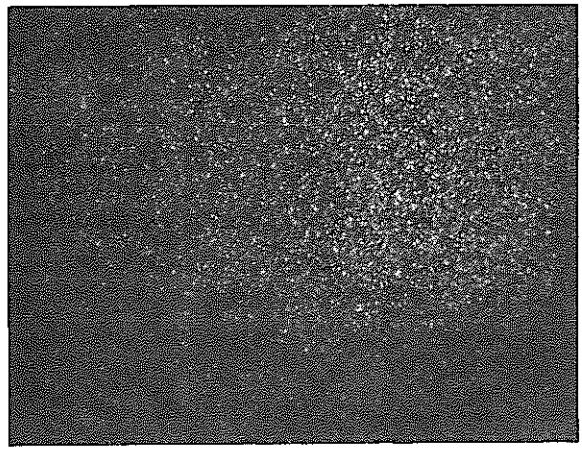

Cr X-ray display × 100

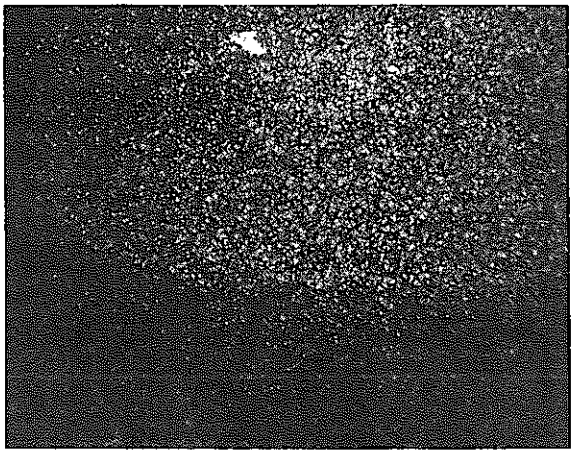

Ni X-ray display × 100

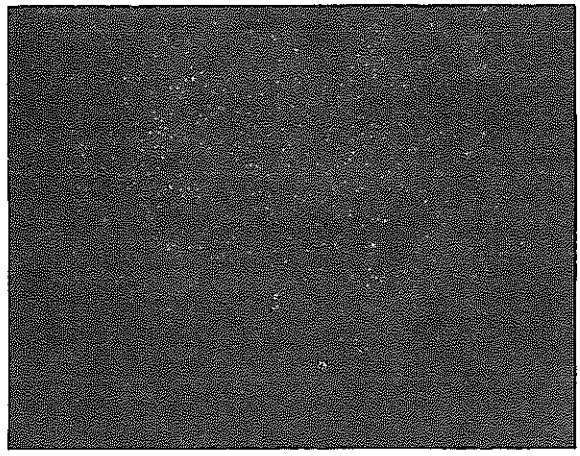

Mo X-ray display × 100

Photograph 29. Plane analysis of Specimen 20502
(Outer surface of cladding tube)

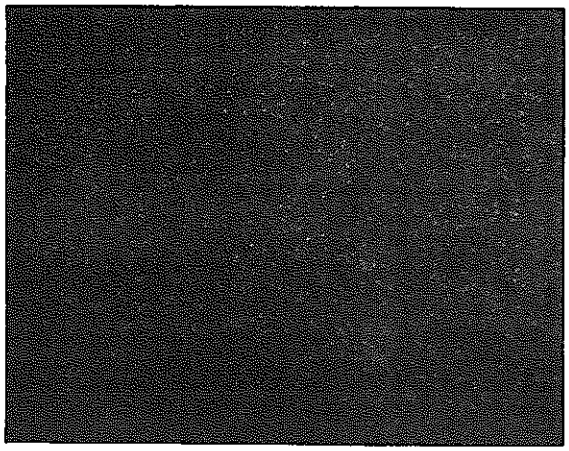

U X-ray display × 100

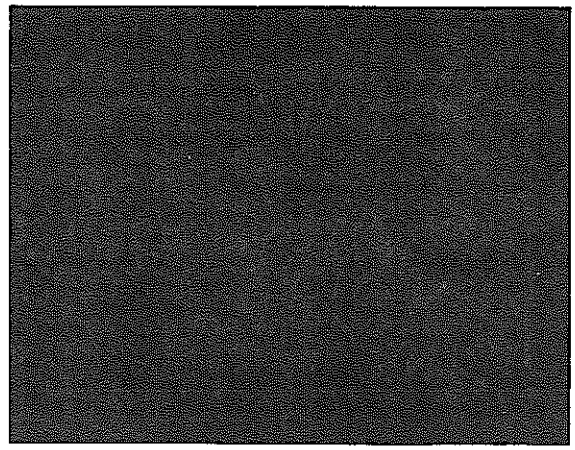

Pu X-ray display × 100

Photograph 29. Plane analysis of Specimen 20502
(Outer surface of cladding tube)

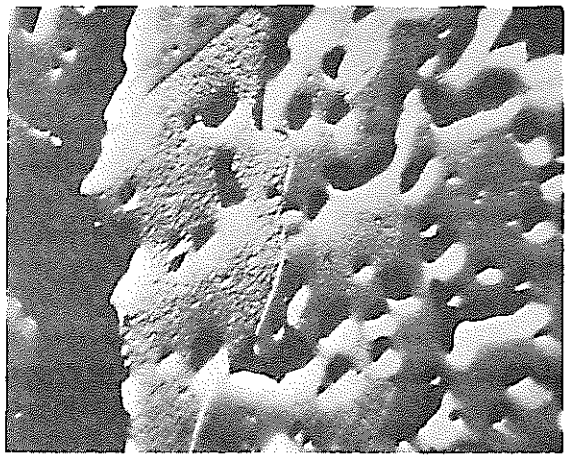

Back scattered electron image × 300

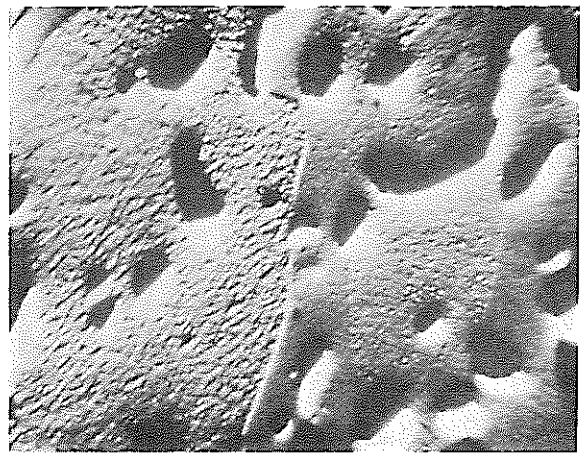

Back scattered electron image × 500

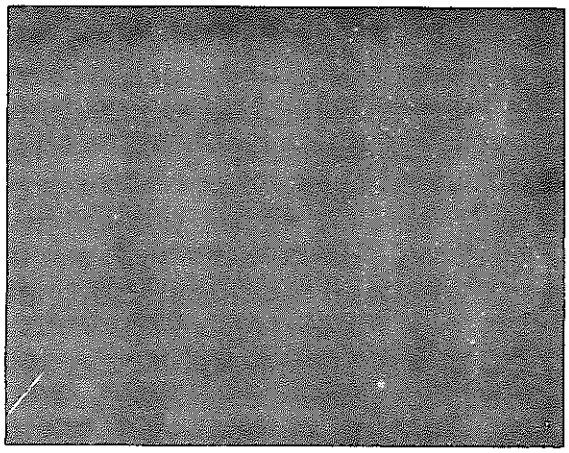

U X-ray display × 500

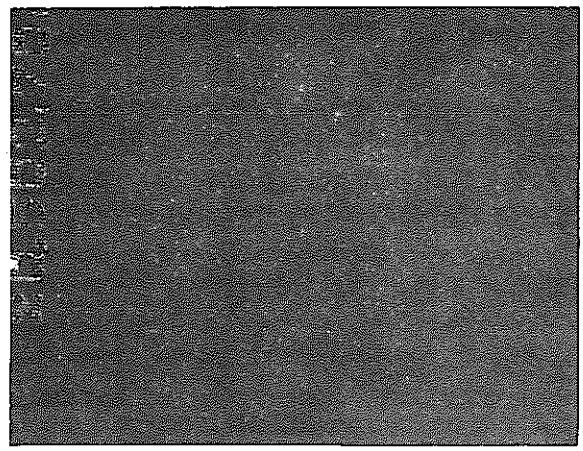

Pu X-ray display × 500

Photograph 30. Plane analysis of Specimen 20502
(Central part of fuel)

31-(1)

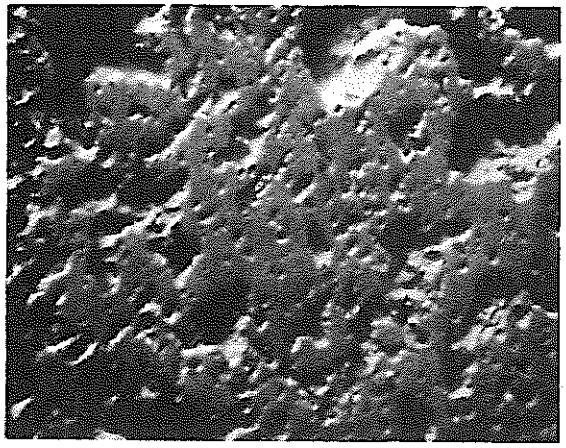

Back scattered electron image × 500

31-(2)

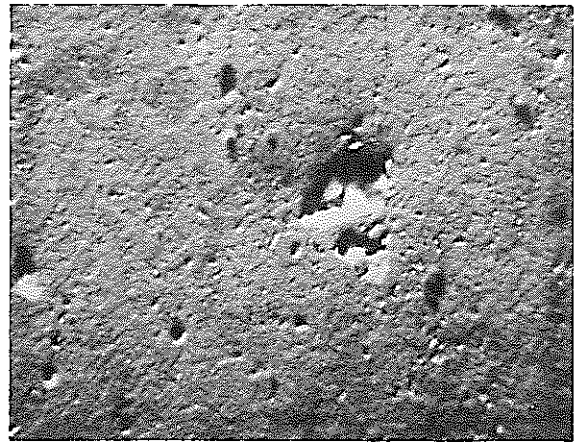

Back scattered electron image × 500

31-(1) Specimen 20102

31-(2) Specimen 20502

Photograph 31. Back scattered electron image of fuel surface